INTRACELLULAR pH REGULATION IN MICROVASCULAR ENDOTHELIAL CELLS

by

JOSÉ D. ROJAS, B.A.S.

A DISSERTATION

IN

PHYSIOLOGY

Submitted to the Graduate Faculty of
Texas Tech University Health Sciences Center
in Partial Fulfillment of the Requirements
for the Degree of

DOCTOR OF PHILOSOPHY

Advisory Committee

Raul Martínez-Zaguilán
Sandor Györke
Alan Neely
Thomas Pressley
Donald Wesson

Accepted

Dean of the Graduate School of Biomedical Sciences
Texas Tech University Health Sciences Center

May, 2000

ACKNOWLEDGMENTS

I would like to thank those who have inspired me to complete this endeavor. I dedicate this work to the two people without whom this would not have been possible. First, in loving memory of my father Pedro Canales Rojas who I knew for too short a period, but whose integrity I hope to emulate. Secondly, to my mother Dolores Casas Rojas who, although she received no formal education, has taught me the most important lessons of my life and merits this degree far more than I do. I only hope that I can be as much a positive force in my children's lives as she has been in mine.

Mom always told me that my family would always be by my side. I thank God daily for my brothers (Ramon and Jesus) and my sister (María). You three are my rock, my strength, my life. I have been fortunate to be blessed with many things, yet the most precious gifts I have received in life are my children. James, Kathryn, and Joshua I love you more than words can ever say and I am proud of you. My accomplishments in this world will quickly wane from memory, yet the three of you have given my life true meaning. I must also thank my first true love, Andréa, you taught me that persistence pays.

I am deeply indebted to my mentor Dr. Raul Martínez-Zaguilán, if not for your friendship and guidance I would not be here today. I can never repay you for what you have given me, but I will always hold you dear in my heart. I would also thank the members of my committee (Drs. Sandor Györke, Alan Neely, Tom Pressley, and Donald Wesson) for their assistance, patience, and guidance. I would be remiss if I did not also

acknowledge the individuals in our laboratory who have supported me with their friendship, knowledge, and technical expertise throughout the years (Cathy Hudson, Gloria Martinez, and Geraldine Tasby). Lastly to the "Boys of Physiology" (Lee Gervitz, Andy Lovering, Defeng Luo, and Shankar Sanka) you brightened my days, taught me to laugh again, and have made this fun. I will forever remember how we laughed at the "Andyisms"and how we always kept the "color television" turned on. I do not know why fate brought such an unlikely group of individuals together, yet I am thankful for my new family.

Technical and Financial Support

I also gratefully acknowledge the technical assistance of Hesham N. Attaya, Amanda Bezner, Christian Busch, Defeng Luo, and Demet Nalbant. This work has been supported by grants to RMZ from AHA (National) 9750558N, ACS RPG-00-035-01CNE, and from the Texas Higher Education Coordinating Board Advanced Technology Program (ATP) #010674-034.

TABLE OF CONTENTS

ABSTRACT

Many advances in vascular biology are a result of the use of cultured endothelial cells as a model. This model system has shown that endothelial cells synthesize and secrete various substances involved in regulating blood flow. There can be considerable heterogeneity in the properties and function of endothelial cells. These heterogeneities are a result of the tissue of origin and whether they are from macro- or microcirculation. Nitric oxide, a vasoactive substance synthesized by endothelial cells, has been shown to activate other second messenger systems in both a calcium-dependent and -independent fashion. There is a substantial body of work on intracellular calcium $[Ca^{2+}]^{in}$ regulation in endothelial cells. Similarly, it is known that intracellular pH (pH^{in}) is important in signal transduction following hormonal stimulation, and in regulating many physiological processes including cell growth, secretion, contraction, and invasion/migration. Significant work has been done on pH^{in} regulation in macrovascular endothelial cells; however, there remains a large gap in the knowledge of pH^{in} regulation in microvascular endothelial cells. Since there have been reported differences in $[Ca^{2+}]^{in}$ regulation and nitric oxide production in microvascular and macrovascular endothelial cells, one specific aim of this dissertation was to perform an in-depth study of pH^{in} regulation in microvascular endothelial cells from different vascular beds. Microvascular endothelial cells are intimately involved in the invasive process of angiogenesis and there have been reports of plasma membrane vacuolar-type ATPase (pmV-ATPase) in several invasive cell types. These observations led to the formulation of the hypothesis that pmV-ATPase

is required for invasion and was tested in this study. To our knowledge, this study is the first reported observation of pmV-ATPase as a pH^{in} regulatory mechanism in microvascular endothelial cells along with evidence that the mechanism is involved in the process of invasion. Diabetes affects the cardiovascular system with complications that include acidosis, abnormalities in blood flow regulation, and altered microvascular proliferation and angiogenesis. Part of this study examined pH^{in} regulation in microvascular endothelial cells from a model of spontaneous diabetes. As a result of this work we determined that diabetic cells have decreased pmV-ATPase activity. Along with decreased pmV-ATPase activity diabetic cells also exhibit decreased invasive potential and angiogenesis. Pharmacologic inhibition of pmV-ATPase activity in normal cells renders them as non-invasive as diabetic cells and unable to form capillary-like structures in an angiogenesis model. Finally, the study examines endothelial cells from lung microvasculature. This vascular bed is known to undergo extensive vascular remodeling with prolonged hypoxia. Since prolonged hypoxia results in acidosis, it was predicted that these cells would have a dynamic pH^{in} regulatory that allows them to cope with this situation. Moreover, because vascular remodeling is an invasive process, it was predicted that these endothelial cells would also express pmV-ATPase. In support of the hypothesis; immunocytochemical, fluorescence spectroscopy, and pharmacologic studies reveal pmV-ATPase as a major pH^{in} regulatory mechanism in these cells. In summary this work demonstrates the presence of pmV-ATPase in several microvascular beds and provides functional evidence for its role in the invasive process of vascular remodeling.

LIST OF FIGURES

CHAPTER 1

INTRODUCTION

Endothelial Cell Biology

Endothelial cells not only serve as a barrier to control vessel permeability to large molecules, they also regulate blood flow to tissues. Furchgott and Zawadzki (1980) demonstrated that aortic ring preparations denuded of endothelial cells were unable to respond with vasodilation on treatment with acetylcholine. This ultimately led to the identification of nitric oxide as endothelial derived relaxing factor. The endothelium also synthesizes and secretes other vasoactive substances that control blood flow (i.e., prostacyclin (PGI_2), endothelin). These substances elicit their affect on targets by activation of second messenger systems (i.e., $[Ca^{2+}]^{in}$, pH^{in}). Many of the advances in vascular biology have come as a result of the use of cultured endothelial cells. Techniques to isolate and culture endothelial cells have been well established (Garlanda and Dejana, 1997). The routine culture of endothelial cells isolated from macro- and microvessels has demonstrated that there are differences in characteristic markers as well as function in endothelial cells (Garlanda and Dejana, 1997); however, there remain many unanswered questions about microvascular endothelial cell function.

Angiogenesis

Angiogenesis is a normal physiologic process of microvascular endothelial cells (Hudlická et al.,1998). This process occurs in response to wounding and is important in tissue healing. It also is known to occur in muscle tissue as a response to endurance training (Hudlická et al.,1998). Angiogenesis has also been implicated in pathophysiologic conditions where its occurrence leads to detriment or its absence results in tissue loss (Hudlická et al.,1998). These conditions are exemplified in: (1) cancer tumors that when vascularized result in metastasis of the cancer; and (2) the peripheral vasculature in diabetes, where angiogenesis is decreased and results in poor wound healing and ischemia. There is currently much active research attempting to understand the key elements and regulation of this process (Folkman, 1995). Angiogenesis requires the invasion by microvascular endothelial cells into adjacent tissue. It also requires that these normally quiescent cells begin to proliferate. Cultured microvascular endothelial cells are a good experimental paradigm to study these processes and the role of second messenger systems in the processes. In vitro models of angiogenesis have utilized three-dimensional gels of extracellular matrix proteins (i.e., Matrigel®) to study the process of invasion (Folkman and Haudenschild, 1980). Endothelial cells plated in Matrigel® readily invade this matrix and form capillary-like networks in as little as twelve hours (Grant et al., 1990). In other cell types invasion and proliferation have been shown to involve changes in pH^{in} (Gillies et al., 1992). It is interesting that plasma membrane vacuolar-type H^+- ATPase (pmV-ATPase) has been observed as a dynamic pH^{in}

regulatory mechanism in cells such as macrophages, osteoclasts and tumor cells (Bidani and Brown, 1989; Vaananen et al., 1990; Martínez-Zaguilán et al., 1993). These cells along with microvascular endothelial cells share a common invasive phenotype.

Hypotheses

These observation were the impetus that drove the initiation of this project. From reviews of the literature it was decided that a characterization of pH^{in} regulation in microvascular endothelial cells was warranted. There were three hypothesis formulated to be tested in this study.

1. The similarities in the invasive profile of the above mentioned cells led to the hypothesis that pmV-ATPase is required for invasion in microvascular endothelial cells.

2. A specific complication of diabetes that involves the cardiovascular system is peripheral angiopathy/decreased angiogenesis characterized by poor wound healing. It is hypothesized that, if pmV-ATPase is required for the invasion observed in angiogenesis, normal microvascular endothelial cells would exhibit this activity and cells with decreased invasive potential/angiogenesis would exhibit decreased or absent pmV-ATPase activity.

3. The invasion in angiogenesis occurs in specific regions of the cell. If pmV-ATPase were involved in this invasion then it is hypothesized that proton gradients would exist in a polarized cell (i.e., a cell polarized to invade/migrate) with the invading (leading) edge of the cell being more alkaline than the lagging edge.

Testing these hypotheses resulted in the submission of three manuscripts describing the results of these studies. They will be presented and discussed in Chapters II, III, and IV. Chapter II is a characterization of the invasiveness of microvascular and macrovascular endothelial cells. Since angiogenesis is a process of microvascular endothelial cells, it is hypothesized that microvascular endothelial cells will express pmV-ATPase activity while macrovascular endothelial cells will not. The absence of pmV-ATPase activity in macrovascular endothelial cells should cause them to be less invasive, and conversely inhibition of pmV-ATPase activity in microvascular endothelial cells should block invasion. Chapter III is a comparison of pH^{in} regulation in microvascular endothelial cells from spontaneously diabetic animals and age-matched normal animals. The observation that angiopathies/decreased peripheral angiogenesis are common vascular complications of diabetes suggests that microvascular endothelial cells from diabetics are less invasive. If pmV-ATPase is required for invasion, decreased invasion in diabetic cells could be a result of decreased pmV-ATPase activity. Acidosis is a common occurrence in diabetes; therefore, it is possible that these cells would have altered pH^{in} regulation. If pmV-ATPase is decreased in diabetes, the inhibition of pmV-ATPase in normal cells should result in invasion characteristics and pH^{in} regulation similar to diabetic cells. Finally, Chapter IV examines pH^{in} in a different vascular bed that is also known to undergo vascular remodeling. If pmV-ATPase is important for invasion/vascular remodeling, then it should be observed in all vascular beds that actively undergo vascular remodeling. Before presenting these results I will discuss a few salient points of pH^{in} regulation and provide a brief overview of some of the experimental

methods employed. Chapter V will summarize the significance of the findings in these manuscripts and discuss possible mechanisms for the role of pmV-ATPase in invasion/migration.

Intracellular pH Regulation

One specific aim of this study is to expand the current knowledge of pH^{in} regulation in microvascular endothelial cells. As stated previously, it is well accepted that differences exist between endothelial cells from macro- and microcirculation (Kumar et al., 1987; Garlanda and Dejana, 1997; Stevens et al., 1997; Geiger et al., 1997). A substantial body of work exists on pH^{in} regulation in macrovascular endothelial cells; however, to our knowledge there have only been three studies done on pH^{in} regulation in microvascular endothelial cells (Hsu et al., 1996; Cutaia et al., 1997). These studies were done in microvascular endothelial cells from brain and lung (porcine and human, respectively). In these studies and those performed on macrovascular endothelial cells (various tissues and species) the Na^+/H^+-exchanger has been shown to be an important mechanism for pH^{in} regulation (Escobales et al., 1990; Schmid et al., 1992; Ziegelstein et al., 1992; Cutaia and Parks, 1994; Hsu et al., 1996). There are various isoforms of this exchanger distributed throughout all tissues and it is generally believed to accomplish housekeeping pH^{in} regulation (Roos and Boron, 1981). This exchanger is a secondary transporter that utilizes the sodium gradient that exists across the cell membrane and causes intracellular alkalinization. All isoforms are inhibited to varying degree by amiloride and its derivatives (Roos and Boron, 1980; Gillies et al., 1992).

Cells can also utilize HCO_3^- transport mechanisms to regulate pH^{in}. There are various HCO_3^- transport mechanisms present to varying degree in tissues. There have been described Na^+ -dependent and -independent, as well as Cl^- -dependent and -independent mechanisms (Roos and Boron, 1980; Sanchez-Armass et al., 1994). These transporters couple the transport of HCO_3^- to other ions in either a symport or antiport manner. Some of these mechanisms lead to intracellular alkalinization, while others cause acidification; however regardless of the mechanism all are blocked by anion transport inhibitors like the stilbene derivatives (Roos and Boron; 1980; Jentsch et al., 1988; Gillies and Martínez-Zaguilán, 1991). In endothelial cells from macro- and microvasculature there have been reports of Na^+-dependent HCO_3^-/Cl^- exchange (Hsu et al., 1996); Na^+-independent HCO_3^-/Cl^- exchange (Jentsch et al., 1988; Ziegelstein et al., 1992); and the electrogenic Na^+/HCO_3^- symporter (Jentsch et al., 1988).

Some cells also utilize proton pumps as pH^{in} regulatory mechanisms. Three classes of proton pumps have been described. These are the mitochondrial (F-type), those regulated by a phosphorylated intermediate (P-type), and the vacuolar (V-type) proton pumps (Forgac, 1989). These pumps can be distinguished by pharmacologic inhibition (Forgac, 1999; Mendlein and Sachs, 1990). P-type ATPases are inhibited by SCH 28080, ouabain, and vanadate which have no effect on V-type ATPases. Conversely, V-type ATPases are inhibited by bafilomycin, concanamycin, and to a less specific degree 7-chloro-4-dinitrobenz-2-oxa-1,3-diazole [NBD-Cl] (Bowman et al., 1988; Forgac, 1999) which have no effect on P-type ATPases. The vacuolar H^+-ATPase is a multimeric holoenzyme (M_R ~ 750 kDa) that has two domains, V_o and V_1. The V_o domain is

membrane bound and has a molecular mass of ca. 250 kDa. This domain is proposed to function in proton translocation and has been shown to have associated proteins that are not part of the integral membrane protein (Nelson and Klionsky, 1996; Forgac, 1989). It consists of at least four subunits with proposed composition of $100_1 38_1 19_1 17_6$. The V_1 domain has a relative mass of ca. 500 kDa and consists of five subunits $73_3 58_3 40_1 34_1 33_1$ This domain contains the ATP binding site and the catalytic sector of the holoenzyme (Nelson and Klionsky, 1996; Forgac, 1989). To date there have been no reports of plasma membrane proton pumps as a pH^{in} regulatory mechanism in endothelial cells.

Experimental Methods

Cell Culture

The hypothesis in this study was tested using the cell culture paradigm. Microvascular endothelial cells were obtained from vascular beds of different origin. Human lung microvascular endothelial cells were purchased from Clonetics (San Diego, CA.). Rat aortic (macrovascular) endothelial cells were purchased from VEC Technologies (Rensselaer, NY). Rat microvascular endothelial cells from diabetic and age-matched normal animals were a generous gift of Dr. Cynthia Meininger (Texas A&M University, College Station, TX). Endothelial origin was determined by positive staining for Factor VIII and by the uptake of modified low-density lipoprotein. Cells exhibited the typical cobblestone morphology in culture and were used from passage 5-15. Cells were maintained in DMEM supplemented with 10% fetal bovine serum (FBS), 2 mM L-glutamine, 0.4 mM L-arginine, 5 mM D-glucose, 20 U/ml heparin, 1 mM sodium

pyruvate, 100 U/ml penicillin, 100 μg/ml streptomycin, and 0.2 μg/ml amphotericin B (Gibco, Grand Island, NY). Cells were passaged weekly and plated at various densities and conditions for experiments. These conditions will be described in subsequent chapters.

Fluorescent pH Indicators

Intracellular pH has been measured by various techniques including micro-electrodes, nuclear magnetic resonance, and fluorescence (Martínez-Zaguilán, 1992). Of these techniques fluorescence provides the least physiologic disturbance and best temporal response. Although fluorescent indicators prove to be a powerful technique for measuring pH^{in} (some systems will allow for 2 msec sampling rates with high spatial resolution) they are not without drawbacks. When using fluorescent ion indicators to monitor pH^{in}, it is important to know whether or not the indicator compartmentalizes. Compartmentalization of dyes could lead to errors in pH^{in} estimation. Similarly, it is important to have an idea of the pH range to be seen by the indicator. This will allow for better selection of indicators to match experimental needs. In order to have optimum sensitivity, the pK_a of the fluorphore must be within the range of pH being measured (Martínez-Zaguilán, 1992). In measuring cytosolic pH, with perturbation, pH can range from 6.0 to 8.5; thus, the ideal fluorphore will have a pK_a of ca. 7.4. Ideally, the fluorphore will be a ratiometric probe with a good dynamic range in its ion-sensitive wavelengths. It should also possess a clear ion-insensitive point that will allow for assessment of dye concentration/dye leakage and quenching artifacts.

Unfortunately, simply because a dye has ideal characteristics does not warrantee that it will be problem free. This was the case in this study. Most ion indicators come in the acetoxymethylester (AM) form which renders them cell permeant. Once in the cell. non-specific esterases will cleave the dye into the free acid form and trap it within the cell. There is no guarantee that cells will readily take up a dye. Some cells will not load well with indicators. In these studies we employ the pH indicators 2', 7'-bis(2-caroxyethyl)-5(and-6)carboxyfluorescein (BCECF) and carboxy-seminaphtorhodafluor (SNARF-1). Both dyes are available in the AM form and have reported pK_a`s of 7.0 and 7.4, respectively (Martínez-Zaguilán, 1992). BCECF is a dual excitation single emission dye. Typically it is excited at 500 nm (its ion-sensitive wavelength) and 440 nm (its iso-excitation/ion-insenstive wavelength) with emission captured at 529 nm (Fig. 1.1A). Thus the ratio of 500/440 is an indicator of pH, that increases with increasing pH.

BCECF is not the best dye because the ion-insensitive point is not a true iso-excitation point, but given that drawback it can be used adequately to monitor pH. One distinct advantage is that the quantum yield of BCECF is high. SNARF-1 is a dual emission, single excitation dye. When excited at 534 nm, SNARF-1 has ion-sensitive wavelengths at 644 and 584 nm that increase and decrease, respectively, with increasing pH (Fig. 1.1B). It also has a true isoemissive point at 610 nm. The ratio of 644/584 is used to monitor pH and increases with increasing pH. SNARF is the dye that we prefer using for that reason; however, we were unable to obtain an appreciable signal when we attempted to load lung microvascular endothelial cells with SNARF. These cells, however, readily loaded with BCECF.

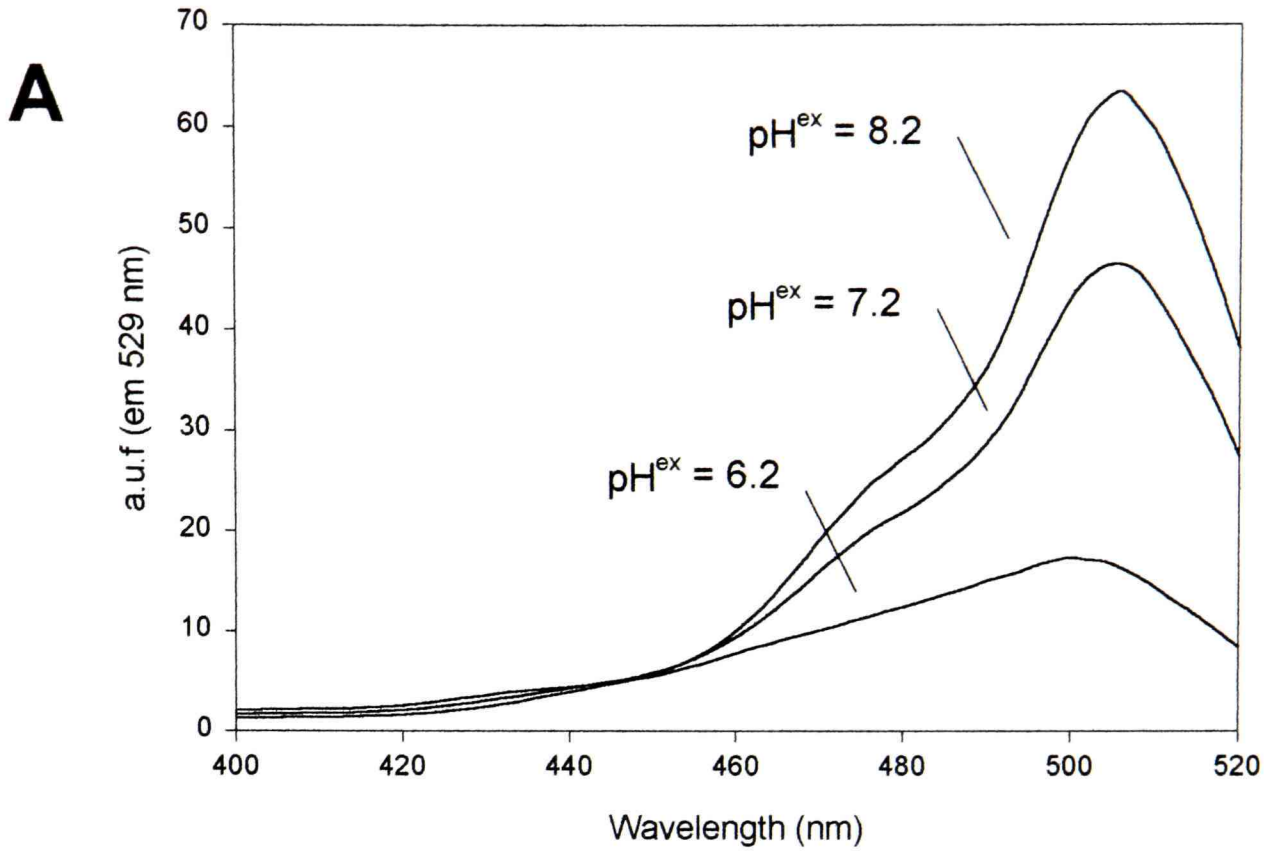

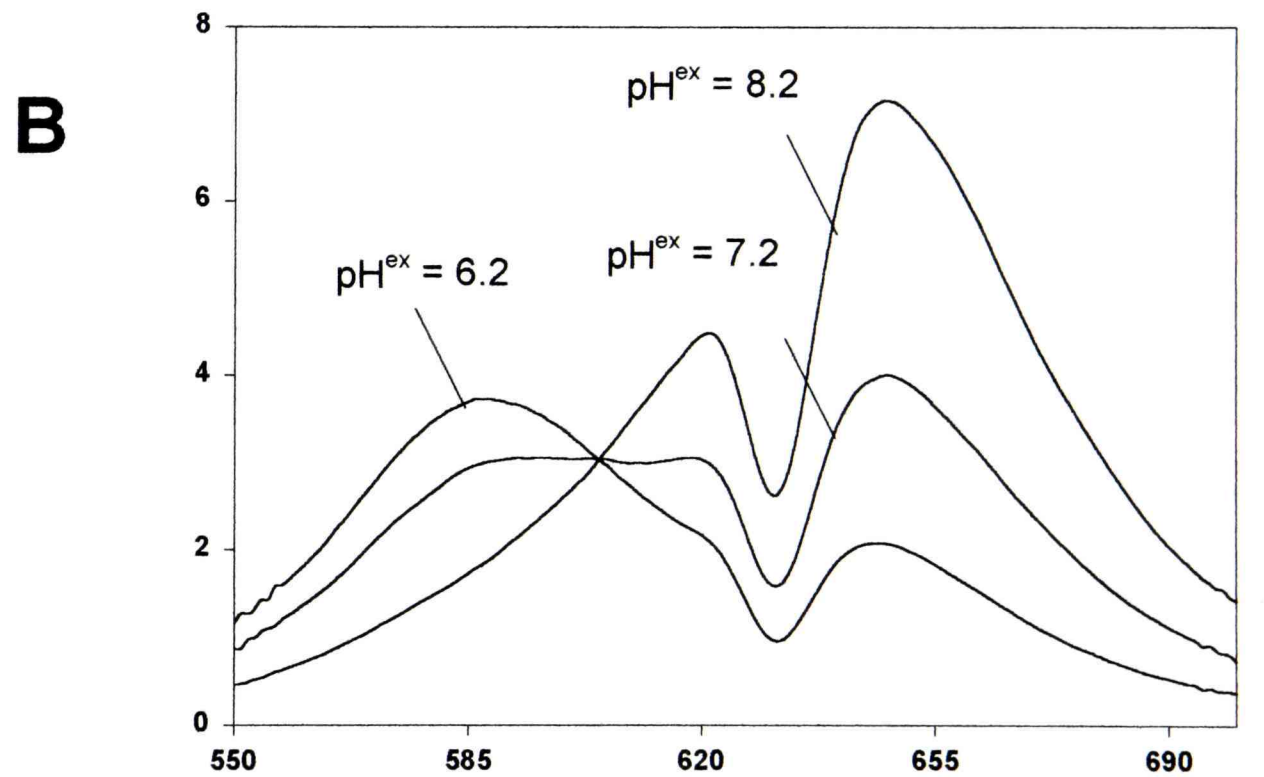

Figure 1.1 Spectra of BCECF and SNARF-1. (A) BCECF free acid (2 μM) in High K^+-buffer (146 mM KCl, 20 mM NaCl, 10 mM HEPES, 10 mM MES, and 10 mM Bicine) pH^{ex} 6.2. The pH is increased by addition of 3 μl/ml 1 M NaOH. Spectra at pH of 6.2, 7.2, and 8.2 are shown. (B) SNARF-1 free acid (2 μM) treated as in (A).

We monitored pH^{in} in cell populations with fluorescence spectroscopy as previously described (Martínez-Zaguilán et al., 1991). Briefly, cells were loaded with either 2 μM BCECF-AM or 7 μM SNARF-AM for thirty minutes at 37°C / 5% CO_2, then subsequently washed and the cells allowed to hydrolyze the dye for thirty minutes. Fluorescence studies were performed at 37°C with an SLM 8100-DMX spectrofluorometer equipped for perfusion. Data was acquired in the continuous acquisition mode with total acquisition time taking less than 0.5 secs. Thus studies in cell populations provide the average response of many cells with relatively fast temporal resolution that allows us to better interpret the responses observed at the single cell level.

Perturbation of pH^{in}

In these studies we used various paradigms to study intracellular pH^{in} regulation. If one considers the pH^{in} regulatory mechanisms are available to cells, predictions can be made about cell behavior on exposure to ion substitution or acid loading experiments. In cells that exhibit the Na^+/H^+ exchanger as a pH^{in} regulatory mechanism, substituting Na^+ with N-methyl-glucamine extracellularly results in acidification (Roos and Boron, 1981; Gillies et al., 1992). Recovery from this acidification in a nominally HCO_3^- -free buffer suggests the presence of other pH^{in} regulatory mechanisms (i.e., proton pumps). In a similar fashion, the acute addition of HCO_3^- results in either acidification or alkalinization of a cell depending on the type of HCO_3^- transporting mechanism present. Utilization of these maneuvers, in the presence and absence of inhibitors of the different pH^{in} regulatory mechanisms, is useful in determining the regulatory systems available to the cell.

Another paradigm involves the NH_4Cl prepulse technique (Roos and Boron, 1981). In this paradigm, a known amount of NH_4Cl added to the exterior of cells. The NH_4Cl dissociates in solution and yields ionic species that are relatively impermeant to the cell membrane. The NH_4^+ will also dissociate in solution and yield NH_3 and H^+ ($pK_a = 8.9$). If the pH of the extracellular solution is below the pK_a, the reaction is driven towards the production of NH_3. The NH_3 is membrane permeable. Once in the cell it can scavenge any cytosolic H^+ and results in intracellular alkalinzation that is sustained until removal of the NH_4Cl. Upon removal, the cell rapidly acidifies below baseline pH^{in} and the subsequent recovery is a result of all pH^{in} regulatory mechanisms available to the cell. Classically this maneuver has been interpreted in two ways. One method simply involves analysis of pH^{in} change over some period of time (Martínez-Zaguilán et al., 1993). A time period is selected during which the rate of recovery is fairly linear. The delta pH at specific intervals is plotted against time and the slope of this relationship is interpreted as quantified the rate of recovery.

One caveat to utilizing dpH/dt as a method of comparing pH^{in} recoveries in different cell types is that although the rates of recovery may be different these may just be attributed to differences in the cells' ability to resist pH^{in} change (buffering capacity). To minimize this potential for error of interpretation, the apparent buffering capacity (β_i) for cells is estimated. Since ammonia is readily permeable to the cell it is assumed that equilibrium is reached during the pre-pulse. The pH^{ex} is known and pH^{in} is determined experimentally, thus the amount of ammonia that is inside the cell can be calculated by (Roos and Boron, 1981):

$$\Delta [NH_3]^i = [NH_3]^o \times \frac{10^{(pK - pH^{in})}}{1 + 10^{(pK - pH^{ex})}}. \qquad \text{Equation [1.1]}$$

The β_i (mM H^+/pH unit) is given by (Roos and Boron, 1981):

$$\beta_{i\,(apparent)} = \frac{\Delta [NH_3]^i}{\Delta pH}, \qquad \text{Equation [1.2]}$$

with ΔpH being the change in pH^{in} from the plateau after the NH_4Cl load and the nadir pH^{in} after NH_4Cl removal. Thus, if cells have similar β_i and different dpH/dt the interpretation would be that rates of recovery are different because of differences in pH^{in} regulatory mechanisms. This type of analysis has given rise to comparing recoveries expressed as proton fluxes (J_{H^+}). Proton fluxes (mM H^+/min) are given by:

$$J_{H^+} = \beta_{i\,(apparent)} \times dpH/dt. \qquad \text{Equation [1.3]}$$

A criticism of this analysis is that flux measurements by definition are a rate of flow per specific area, and as such the surface area should be known/expressed. In our experiments this criticism is minimized by keeping the same number of cells attached to a specific area constant. Interpretation of data in this fashion was no different than when we estimated cell number/area and estimated the volume of cells.

Statistical Analysis

Data are expressed as mean ± SE. Data were analyzed by paired *t*-tests or by *ANOVA* when more than one group was compared. Statistical significance was assigned at P values of < 0.05.

Confocal/Spectral Imaging Microscopy

To test the hypothesis that pmV-ATPase at the migrating/invading edge of endothelial cells would result in pH gradients across the cell, we employed line scanning confocal microscopy and spectral imaging microscopy in SNARF-1 loaded cells. Cells were loaded with SNARF-1 as described for populations. Both of these techniques allow for high temporal and spatial resolution of SNARF in distinct regions of microvascular endothelial cells. Confocal microscopy was performed with a Bio-Rad 1024 confocal microscopy (Chu et al., 1995; Opas, 1997). Endothelial cell polarization is determined by morphology and the cell is aligned so that the "x"-axis extends from leading to lagging edge of the cell. A single point is selected on the "y"-axis and the laser can scan the entire length of the cell (leading to lagging edge) in 2 msecs. Specific regions of interest are selected along the line so that data is collected from the leading and lagging edge of the cell. SNARF-1 is excited with the 488 nm line of a 25 mW argon laser and the emission collected at 584 nm (570/32) and 644 nm (640/40) with two separate photomultiplier tubes.

Spectral imaging microscopy allows for measurement of ions in single cells, and in discrete subcellular regions with high spatial and spectral resolution (Martínez-Zaguilán et al., 1996a). The spectral imaging microscope constitutes the following elements: a fluorescence inverted microscope (Olympus IX-70 with a 60x objective, N.A. 1.4), a 6.7 eyepiece used to image the cell through the side port of the microscope onto the input slit of a grating monochromator (Chromex 250 IS/SM spectrograph, Albuquerque NM) and the diffracted fluorescence spectra is collected using a cooled charged coupled device (CCD) camera (Photometrics, Mod CH350, Tucson, AZ) equipped with a 512x512 element (27 μm^2/pixel) imaging chip (Fig. 1.2). The full spectral output of the cell can be obtained within a time frame of as little as 2 msec. Data were collected from 12 discrete regions (tracks) of the cell and data values from adjacent pixels of the CCD are summed (binned) to obtain a higher signal/noise ratio. The optical filters were as follows: 488 nm narrow bandpass filter; 550 long bandpass dichroic (Omega Optical, Brattleboro, VT).

In Vitro Angiogenesis

Endothelial cells seeded into three dimensional gels of Matrigel® have been utilized as an in vitro model of angiogenesis. Matrigel® (Becton Dickinson, Bridgeport, NJ) is isolated from the Engelbreth-Holm-Swarm mouse sarcoma. It is rich in extracellular matrix proteins (laminin, collagen IV, entactin, heparan sulfate proteoglycan) and also contains growth factors, matrix metalloproteinases, and other components (Baatout, 1997). This model system closely mimics the structure,

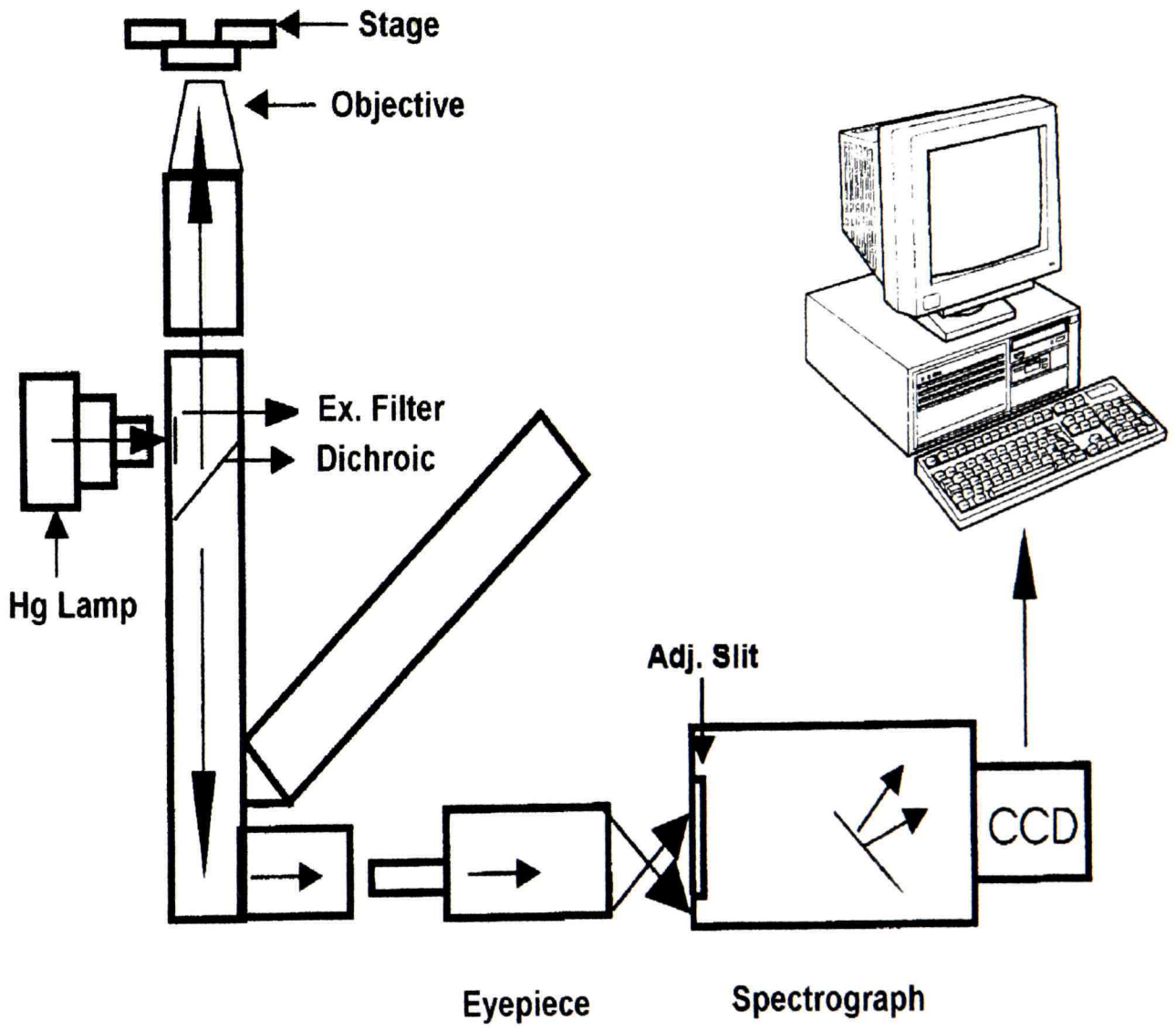

Figure 1.2 Schematic of spectral imaging microscope. Hg lamp (mercury lamp); Ex. Filter (excitation filter); CCD camera (cool charge-coupled device); Adj. Slit (adjustable slit).

composition, physical properties, and functional characteristics of the basement membrane in vivo. It is known to promote the differentiation of endothelial cells such that they invade the ECM and form capillary-like structures in as little as twelve hours (Grant et al., 1990). In these experiments, cells are passaged by trypsinization and seeded at densities of 1×10^5 in Matrigel® and incubated at 37°C/5% CO_2 with DMEM for 24 hours.

Invasion Assay

HTS Fluoroblok™ inserts (Becton Dickinson) coated with Matrigel® were used to evaluate invasion. These inserts are 10 μm polycarbonate filters that are impregnated with dyes that block fluorescence. Microvascular endothelial cells are loaded with 5 μM Calcein-AM and seeded onto the inserts and incubated at 37°C/5% CO_2 for 24 hours. At this time point the inserts are taken to the stage of the confocal microscope and the bottom of the inserts are imaged with a 20x objective. Calcein is excited with the 488 nm line of a 25 mW argon laser and emission measured at 515 nm. Images of the top and bottom of the inserts are obtained, cells are visually counted, and percent invasion determined.

CHAPTER II

PLASMALEMMAL VACUOLAR TYPE H^+-ATPASES ARE IMPORTANT FOR MIGRATION/INVASION AND MAINTAIN OF pH GRADIENTS IN MICROVASCULAR ENDOTHELIAL CELLS[1]

Abstract

It is paradoxical that angiogenesis normally occurs in an acidic environment that is not permissive for growth. We hypothesize that microvascular endothelial cells must exhibit plasmalemmal vacuolar type H^+-ATPase (pmV-ATPase) as a unique intracellular pH (pH^{in}) regulatory system to cope with acid loads. We show by immunocytochemistry that these cells express pmV-ATPase at the leading edge, in addition to its well-known distribution in acidic organelles. Studies of pH^{in} in cell populations by fluorescence spectroscopy, and in single cells by line scanning confocal/spectral imaging microscopy, indicated that these cells recover from acid loads in the absence of Na^+ and HCO_3^-. These pH^{in} recoveries were suppressed by V-H^+-ATPase inhibitors. The presence of pmV-ATPase at the leading edge allows these cells to maintain a higher pH^{in} in the

---

[1] Forthcoming

J.D. Rojas[a], M.J.C. Hendrix[b], S.C. Sanka[a], G.M. Martinez[a], E.A. Seftor[b], C. J. Meininger[c], G. Wu[d], D.E. Wesson[a,e], and R. Martínez-Zaguilán[a,f].

Departments of [a]Physiology, [e]Internal Medicine, and [f]Southwest Cancer Center, Texas Tech University Health Sciences Center, Lubbock, Texas; Departments of [c]Physiology and [d]Animal Science, Texas A&M University, College Station, Texas; and [b]Department of Anatomy and Cell Biology and The University of Iowa Cancer Center, University of Iowa College of Medicine, Iowa City, Iowa.

leading than at the lagging edge. Invasion/migration assays indicated that growth of microvascular endothelial cells under acidic conditions exacerbated invasive/migratory behavior. Inhibition of pmV-ATPase suppressed migration/invasion. These data indicate that pmV-ATPase expression in the leading edge of microvascular endothelial cells is relevant for pH^{in} regulation and invasion/migration of these cells through extracellular matrix.

Introduction

Endothelial cells are uniquely positioned within vessels of the macro- and microcirculation. Macrovascular endothelial cells play an important role in regulating blood vessel tone and blood flow through both direct and indirect effects on adjacent vascular smooth muscle cells (Gerritsen, 1996; Mehta, 1995; Cines et al., 1998). A similar role has been ascribed for endothelial cells in the microcirculation (Lüscher et al., 1991). Endothelial cells synthesize and secrete a number of growth factors, hormones, and other factors that are involved in regulating blood flow and blood pressure in both macro- and microcirculation (Lüscher et al., 1991). They also secrete proteolytic enzymes necessary for invasion into the extracellular matrix (ECM), a necessary step in vascular remodeling (Moscatelli et al., 1986). It is known that microvascular endothelial cells respond to growth factors and will degrade extracellular matrix to form a new capillary network (Folkman and Haudenschild, 1980; Kalebic et al., 1983; Folkman, 1997). Thus, endothelial cells have both paracrine and autocrine roles in the macro- and microcirculation.

It is known that changes in intracellular pH (pH^{in}) are important in signal transduction mechanisms following hormonal stimulation (Gillies et al., 1992). Moreover, changes in pH^{in} are important in regulating many physiological processes including cell growth, secretion, contraction, and invasion/migration (Gillies et al., 1992: Roos and Boron, 1981). These processes are important in the formation of new blood vessels, i.e., angiogenesis, and in vascular remodeling (Folkman and Haudenschild, 1980: Kalebic et al., 1983; Folkman, 1997).

The regulation of pH^{in} in most eukaryotic cells is mediated by the Na^+/H^+ exchanger and HCO_3^--dependent transporting mechanisms (Roos and Boron, 1981; Gillies and Martínez-Zaguilán, 1991; Escobales et al., 1990; Ziegelstein et al., 1992; Hsu et al., 1996; Cutaia et al., 1997; Jentsch et al., 1988). The Na^+/H^+ exchanger utilizes the Na^+ gradient that exists across the plasma membrane and extrudes protons from the cell resulting in intracellular alkalinization (Roos and Boron, 1981). This mechanism is pharmacologically inhibited by amiloride and its derivatives (Roos and Boron, 1981; Gillies and Martínez-Zaguilán, 1991; Escobales et al., 1990; Ziegelstein et al., 1992; Hsu et al., 1996; Cutaia et al., 1997). The various HCO_3^- transport mechanisms include Na^+ -dependent and -independent Cl^-/HCO_3^- exchange, Cl^- -independent Na^+/HCO_3^- cotransport, and Cl^- channel mediated HCO_3^- transport (Roos and Boron, 1981; Ziegelstein et al., 1992; Jentsch et al., 1988). These mechanisms distribute HCO_3^- by coupling its transport to other ions. As such, some mechanisms acidify while others cause intracellular alkalinization. All are inhibited by stilbene disulfonate derivatives (Roos and Boron, 1981; Gillies and Martínez-Zaguilán, 1991; Jentsch et al., 1988).

Some specialized and highly invasive cells (metastatic cells, macrophages, neutrophils, and osteoclasts) also utilize plasma membrane V-H^+-ATPase (pmV-ATPases) to regulate pH^{in} (Martínez-Zaguilán et al., 1993; Bidani and Brown, 1990; Nanda et al., 1992; Vaananen et al., 1990). These ATPases are distinguished from other proton pumps by their pharmacologic inhibition (Bowman et al., 1988; Mendlein and Sachs, 1990; Forgac, 1999). The other two types of proton pumps found in cells are the mitochondrial or F-type and the P-type proton pumps (Bowman et al., 1988; Mendlein and Sachs, 1990; Forgac, 1999). The F- and P-type pumps are inhibited by oligomycin and SCH 28080, respectively, and these drugs have no effect on the V-type pump (Mendlein and Sachs, 1990). The V-type pump is inhibited by bafilomycin A_1, concanamycin, and to a less specific degree by 7-chloro-4-dinitrobenz-2-oxa-1,3-diazole [NBD-Cl] (Bowman et al., 1988; Forgac, 1999).

It is known that microvascular endothelial cells, like tumor cells, are exposed to a hypoxic and acidic environment (Vaupel, 1996; McCoy et al., 1996). These conditions are not favorable for growth and cell survival. We have previously shown that pmV-ATPase expression in highly invasive metastatic tumor cells provides a dynamic pH^{in} regulatory mechanism for these cells (Martínez-Zaguilán et al., 1993). The similarity between metastatic cells and angiogenic microvascular endothelial cells in regards to invasion of adjacent tissue by the invading cell led us to hypothesize that micro- but not macrovascular endothelial cells express pmV-ATPase as a dynamic pH^{in} regulatory mechanism that allows them to cope with acidic environments. Furthermore, we hypothesize that microvascular endothelial cells employ this pump's activity for

invasion/migration. We also hypothesize that the presence of pmV-ATPase at the leading edge in microvascular endothelial cells allows them to maintain a higher pH^{in} in the leading than in the lagging edge, thus creating a pH gradient favorable for invasion/migration.

Results and Discussion

Microvascular endothelial cells are capable of invading/migrating through extracellular matrices. Since migration and invasion through extracellular matrix proteins are important elements in angiogenesis, we evaluated if endothelial cells would penetrate through an artificial basement membrane. We have successfully used this in vitro membrane invasion culture system (MICS) assay to evaluate the invasive/migratory characteristics of tumor cells (Hendrix et al., 1987; Sheng et al., 1996). Our data indicated that the degree of migration/invasion of microvascular endothelial cells through an artificial basement membrane constituted of extracellular matrix proteins is higher than that observed in macrovascular endothelial cells (Figs. 2.1A & 2.1B).

Growth of microvascular endothelial cells at acidic pH enhances their invasive/migratory capabilities. We have previously shown that growing both poorly and highly invasive human melanoma cells under mildly acidic conditions (i.e., $pH^{ex} = 6.8$). enhances their migration/invasive potential (Martínez-Zaguilán et al., 1996c). We therefore investigated if growth of microvascular endothelial cells for 7 days at $pH^{ex} =$ 6.8. would alter their migration/invasion characteristics. There are no effects on cell

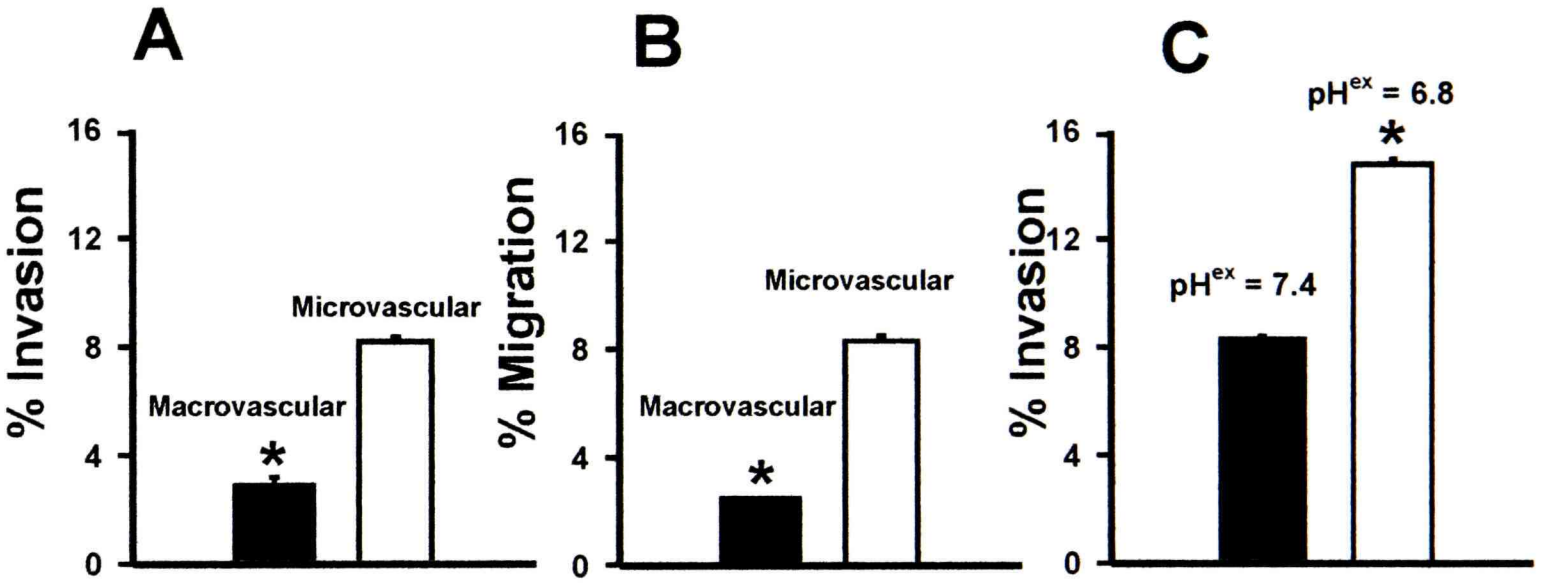

Figure 2.1 Comparison of invasive potential of microvascular and macrovascular endothelial cells. (A) INVASION. Cells were plated onto an Matrigel®-coated polycarbonate filter (10 μm pores) in a modified Boyden chamber as described in "Experimental Procedures" (Hendrix et al., 1987; Sheng et al., 1996). Each experiment was repeated at least 3 times. Data are expressed as S.E.M. (n = 18) * $P < 0.05$ paired *t*-test, microvascular compared to macrovascular. (B) MIGRATION. Cells were handled as in (A), except that filters were soaked in 0.1% BSA (no Matrigel®) and incubated for 6 hours. Data are expressed as S.E.M. (n = 18). * $P < 0.05$ Microvascular compared to macrovascular. (C) INVASION. Endothelial cells were grown at pH^{ex} 7.4 or pH^{ex} 6.8. Conditioned cells grown at the indicated pH^{ex} were subsequently plated onto modified Boyden chambers as described in (A) and their invasion properties were assayed. Data are expressed as S.E.M. (n = 18). * $P < 0.05$ pH^{ex} 6.8 compared to 7.4.

viability by growing cells under these conditions, as compared to control cells grown at $pH^{ex} = 7.4$. Subsequently, cells were transferred to the MICS assay to evaluate the effect of acidic pH^{ex} on invasion/migration. As controls for these experiments we employ microvascular endothelial cells grown at $pH^{ex} = 7.4$. Our data indicate that growth of microvascular endothelial cells under acidic conditions ($pH^{ex} = 6.8$) enhanced their invasiveness, when compared to control cells grown at $pH^{ex} = 7.4$ (Fig 2.1C).

Microvascular endothelial cells exhibit a bafilomycin sensitive invasiveness. In order to determine the mechanism involved in the observed invasiveness we utilized HTS FluoroBlok™ (10 μm pores; Becton Dickinson, Franklin Lakes, NJ) inserts coated with Matrigel® to compare the invasiveness of microvascular endothelial cells in the presence or absence of bafilomycin. The FluoroBlok™ inserts are impregnated with dyes that block fluorescence, as such when viewed from the bottom of the insert fluorescence is only see when cells have migrated through the insert. Calcein-AM loaded cells were seeded on Matrigel® coated inserts as described in "Experimental Procedures". At twenty-four hours, confocal microscopy analysis revealed that fluorescently labeled cells had invaded the membrane (Fig.2.2A). Cell counts in random fields above and below the insert demonstrated that 20 ± 3% of cells had invaded the membrane (Fig. 2.2C). Treatment with 20 nM bafilomycin completely blocked this invasion (Fig. 2.2B and C).

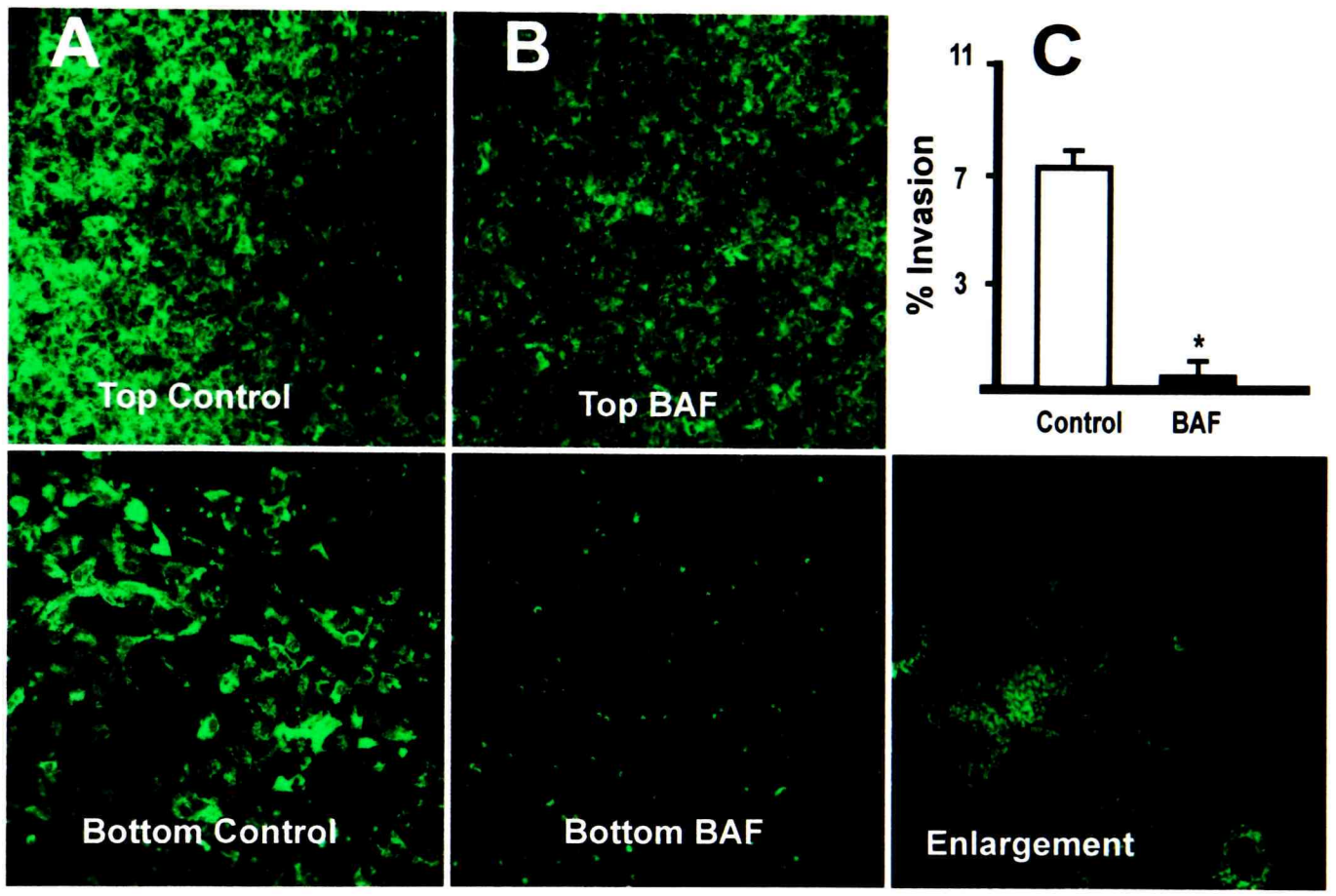

Figure 2.2 Invasive profile of microvascular endothelial cells in the presence and absence of bafilomycin. (A) Cells were loaded with 5 μM Calcein-AM, plated onto 10 μm FluoroBlok™ inserts coated with Matrigel® and incubated for 24 hrs. Insets were visualized by confocal microscopy (20x; Ex = 488 nm; Em = 515 nm). The images were captured from either the top or the bottom of the insert in untreated cells. (B) In parallel experiments to those shown in (A) cells were treated with 20 nM bafilomycin (BAF). (C) Quantification of invasion from experiments done in (A) and (B) was accomplished with visual counts of multiple fields and using Eqn. 2.2. Data are expressed as S.E.M. (n = 7). $^{*}P < 0.05$ when compared to untreated control. Enlargement: Representative area from bottom of FluoroBlok™ insert taken at 20x and enlarged three times.

Wounding of microvascular endothelial cells grown on a monolayer reveals leading edge of the cells. Vascular remodeling following a lesion involves migration of endothelial cells outwardly from the injured area to repair the lesion. Taking advantage of this characteristic, scrapping off a 300 μm region in a confluent monolayer of endothelial cells results in cells migrating towards the damaged region to repair it (Selden and Schwartz, 1979). This orderly cellular movement of all cells adjacent to the lesion occurs immediately, so that after 10 min a clear leading edge is easily distinguishable. Allowed to continue healing, it is observed that the wound will be completely occupied in ca. twenty-four hours. To quantify this migration we stained wounded monolayers with FITC-phalloidin after 18 hours of recovery as described in "Experimental Procedures". This approach allows us to measure the healing/migration that occurs at this time-point as a function of wound distance. We observed that the average wound distance at 18 hours was 69 ± 21 μm (n = 3; Figs. 2.3A & 2.3C). Treatment of wounded monolayers with 20 nM bafilomycin A_1 resulted in wound distance of 215 ± 47 μm (Figs. 2.3B and 2.3C), while amiloride and DIDS had no effect (data not shown). As a negative control, wounded monolayers treated with 1 μM cytochalasin D showed an average distance of 260 ± 25 μm (Fig. 2.3C). Cytochalasin D disrupts the actin cytoskeleton thus prevents migration of cells. These data indicate that a bafilomycin sensitive component is involved in migration of microvascular endothelial cells.

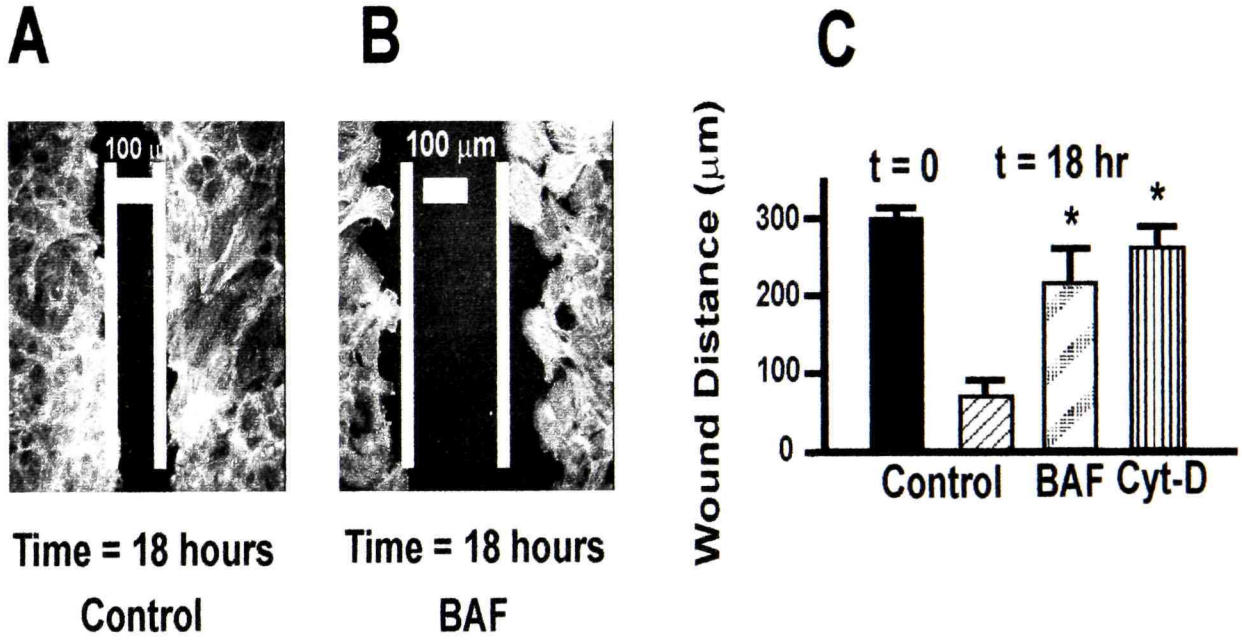

Figure 2.3 Pharmacologic inhibition of endothelial cell migration in wounded monolayers. (A) Cells grown on cover slips to confluency (pH^{ex} 7.4), were wounded, allowed to recover, then fixed, permeabilized, and stained with FITC-phalloidin. Cells were allowed to recover for 18 hours in the absence (control; A) or presence of 20 nM bafilomycin (BAF; B), or 1 μM cytochalasin D (Cyt-D; C). Images were obtained with confocal microscopy (20x). (C) Migration was assessed as described in "Experimental Procdure" and the average wound distance was determined for control, bafilomycin, or cytochalasin D treated cells. Data are expressed as S.E.M. (n = 5). $P < 0.05$ when compared by one-way *ANOVA* to control (18 hrs).

Immunocytochemistry reveals pmV-ATPases in microvascular endothelial cells.

Shown in Fig. 2.4A are paraformaldehyde-fixed and permeabilized microvascular endothelial cells that were stained with MaB-60 to visualize V-H^+-ATPases secondarily stained with Texas-Red, and fluorescein-conjugated phalloidin (FITC-phalloidin) which binds to F-actin to delineate the morphology of the cells. Confocal microscopy images of five randomly selected areas per coverslip from five independent experiments were analyzed. Simultaneously acquired images of FITC-phalloidin (cytoskeleton) and. Texas-Red (V-H^+-ATPase) revealed a plasma membrane distribution of V-H^+-ATPase (Fig. 2.4A, arrows). Sectional images (XYZ series) were collected and each section was analyzed on a pixel by pixel basis utilizing LaserSharp software (Bio-Rad) to assess colocalization of FITC-phalloidin and Texas-Red at the plasma membrane Colocalization of V-H^+- ATPase and actin filaments is shown in white. Consistent with the presence of V-H^+-ATPases in intracellular organelles, intracellular compartments are loaded with proton pumps. Similar observations were made using MaB-69 (data not shown). Parallel experiments, with secondary antibody only, did not show any labeling in intracellular compartments or at the plasma membrane (data not shown). These data indicate that V-ATPase is located at the plasma membrane in microvascular endothelial cells.

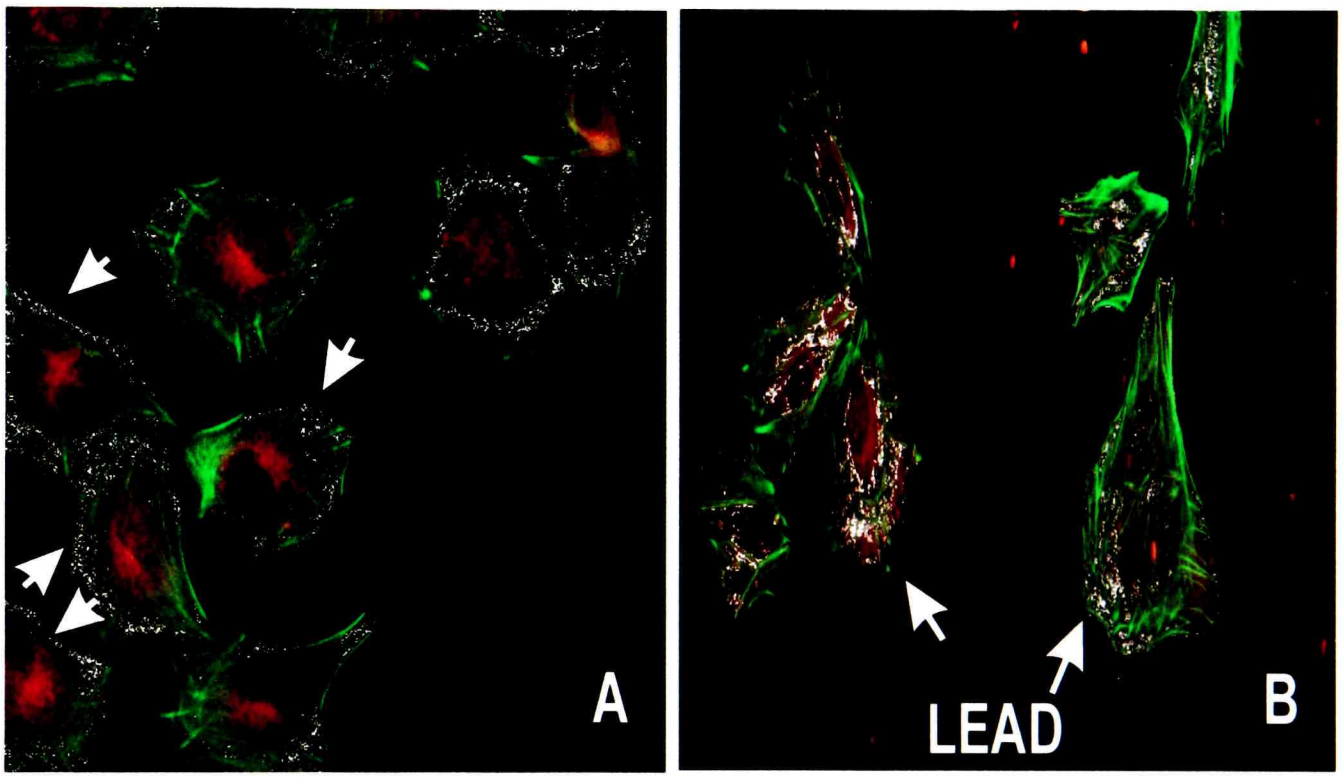

Figure 2.4 Immunocytochemical evidence of pmV-ATPase at the leading edge of microvascular endothelial cells. (A) MaB to 60 kDa subunit of V-ATPase and secondary antibody are shown in red. Cytoskeleton was defined with FITC-phalloidin. Simultaneous images of FITC and Texas Red obtained with a Bio-Rad 1024 MRC confocal microscope. (Ex = 488 and 568 nm; Em = 515 and 585 nm). Colocalization of red and green were assessed on a pixel by pixel basis using LaserSharp image software (BioRad, Hercules, CA) and are indicated in white. Plasma membrane distribution of colocalization is shown with arrows. (B) Cells were handled as described in (A). MaB for ezrin and secondary antibody shown in red. Red/green colocalization determined as described in (A). Arrows show that ezrin protein is more abundant at the leading (LEAD) than at the lagging edge of the cell.

V-ATPase is localized at the leading edge of microvascular endothelial cells.

During the course of our experiments we noticed that some cells exhibit preferential localization of the pump at the migrating edge as determined from morphology. Our understanding of the events involved in migration/motility in different cell models has been enhanced by the identification of markers for leading edge of a cell, such as myosin-I and ezrin proteins (Buss et al., 1998). Monoclonal antibodies to these proteins are commercially available. Ezrin is a protein that links the plasma membrane to the actin-based cytoskeleton (Buss et al., 1998). It has been located in high concentrations at the leading edge of extending pseudopodia in several cell types (Buss et al., 1998). We have evaluated the usefulness of ezrin as a marker for leading edge in microvascular endothelial cells while using a secondary antibody conjugated with Texas-Red. FITC-phalloidin was used to label actin filaments (green). Notice that ezrin localizes at higher concentrations in the leading (LEAD) of the cell (Fig. 2.4B). The image shown in Fig. 2.4B corresponds to one out of 25 sectional images (XYZ series) that were analyzed on a pixel by pixel basis utilizing LaserSharp software (Bio-Rad) to assess co-localization of FITC-phalloidin and Texas-Red at the plasma membrane. The white dots indicate areas of co-localization of ezrin and actin cytoskeleton. These data indicate that ezrin proteins are highly localized to one edge of cells and that they do co-localize with actin bundles. The region of high localization coincides with the leading edge as determined by morphology. We have also employed ezrin staining and MaB-60 in wounded monolayers

and concluded that both localize preferentially at the leading/ migratory edge. Thus from morphological and biochemical analysis we have identified that V-H^+-ATPase is present at the leading edge of migrating cells.

Steady-state pH^{in} is more alkaline in micro- than in macrovascular endothelial cells in the absence of HCO_3^-. The pH^{in} regulation of endothelial cells is thought to be regulated by the Na^+/H^+-exchanger and HCO_3^- transport systems (Escobales et al., 1990; Jentsch et al., 1988). To evaluate pH^{in} regulation, endothelial cells were perfused with media containing Na^+ and HCO_3 . Under these conditions all pH^{in} regulatory mechanisms work in concert to maintain steady-state pH^{in} (Gillies et al., 1992). We determined that at a $pH^{ex} = 7.15$, the pH^{in} was similar between microvascular (7.171 ± 0.053; $n = 5$) and macrovascular (7.188 ± 0.006; $n = 5$) endothelial cells. To evaluate the contribution of HCO_3^- transport mechanism in the regulation of pH^{in}, we performed experiments in a HCO_3 -free media. Under these conditions, the steady-state pH^{in} values in micro- and macrovascular endothelial cells were 7.156 ± 0.018 ($n=5$) and 7.052 ± 0.017 ($n = 5$), respectively at a $pH^{ex} = 7.15$. These data indicate that in the absence of HCO_3 , the pH^{in} values are significantly higher in micro- than in macrovascular endothelial cells ($P < 0.05$). Because it is possible that difference in pH^{in} in the presence or absence of HCO_3 might exist at other pH values, we performed these type of experiments in micro- and macrovascular endothelial cells at various pH values (6.5, 7.0, 7.15, 7.4 and 7.7). Our data indicated that the pH^{in} values of microvascular endothelial cells are unaffected by HCO_3 , whereas the pH^{in} values of macrovascular endothelial cells are ca. 0.15 pH unit higher in the presence than in the absence of HCO_3 throughout the entire pH curve (i.e.

pH^{ex} = 6.5 - 7.7). These data suggest that pH^{in} regulation is accomplished via distinct mechanisms in micro- and macrovascular endothelial cells.

Acid loading experiments allow the identification of a Na^+-and HCO_3^--independent pH^{in} recovery. To address the nature of the differences in the mechanisms of pH^{in} regulation between micro- and macrovascular endothelial cells, we selected conditions where the two main pH^{in} regulatory mechanisms should be dormant. Thus, acid loading experiments utilizing the NH_4Cl pre-pulse technique (Roos and Boron, 1981) were used to evaluate the characteristics of the pH^{in} recoveries in the absence of Na^+ and HCO_3^-. Our expectations were that such maneuver could reveal a novel Na^+- and HCO_3^--independent pH^{in} regulatory mechanism (Martínez-Zaguilán et al., 1993). Cells loaded with SNARF-1 were perfused with CPB, until steady-state pH^{in} was achieved. The addition of 25 mM NH_4Cl causes a rapid intracellular alkalinization (Fig. 2.5A), while the acute removal of NH_4Cl reverses the situation and causes a rapid acidification in both micro- and macrovascular endothelial cells. In the absence of Na^+ and HCO_3^-, macrovascular endothelial cells do not recover from acidification (dpH/dt = 0.001 ± 0.005, J_H^+ = 0.01 ± 0.1; n = 6). Interestingly, microvascular endothelial cells did recover from this acid load (dpH/dt = 0.038 ± 0.004 ; J_H^+ = 1.38 ± 0.15; n= 34; Figs. 2.5A and 2.5B). During the course of these experiments, we noticed that the H^+ buffering capacities (β_i) are significantly higher in micro- than in macrovascular endothelial cells: β_i = 36.7 ± 1.08 and β_i = 30.9 ± 1.37 ($P < 0.05$). To determine if the recovery in

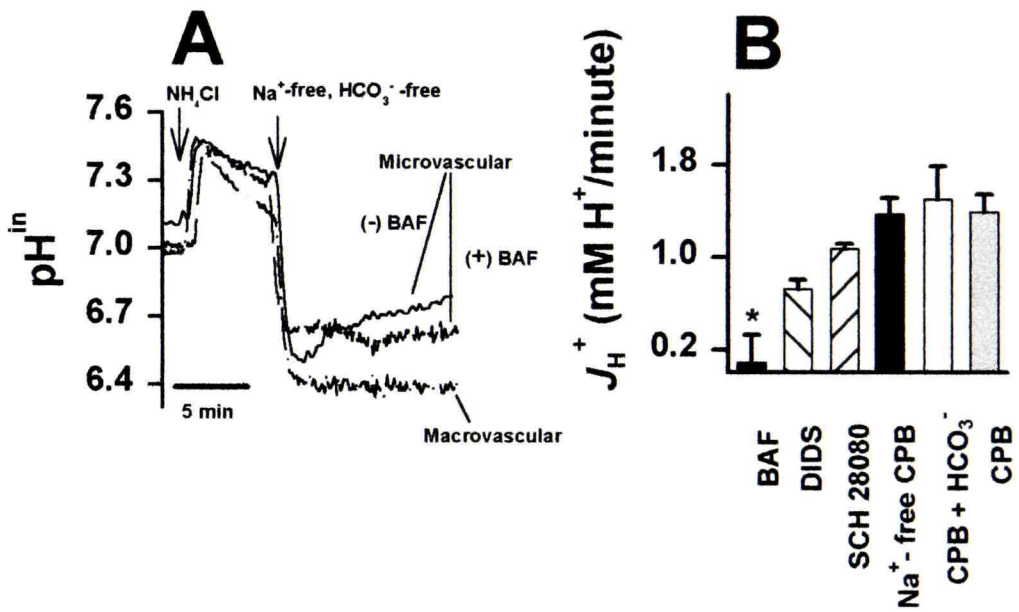

Figure 2.5 Characterization of pH^{in} regulation in microvascular and macrovascular endothelial cells. (A). Cells were loaded with 7.5 μM SNARF-1, superfused with CPB, then superfusate was exchanged with NH_4Cl at the time indicated by the first arrow. Subsequently, NH_4Cl was removed with Na^+- and HCO_3^--free CPB. In parallel experiments, microvascular endothelial cells were superfused with (+) 50 nM BAF. Data are representative of 34 and 6 experiments for micro- and macrovascular endothelial cells, respectively. (B). Cells were handled as described for (A). At the second arrow in (A), the superfusate was exchanged with Na^+- and HCO_3^--free CPB containing DIDS = 100 μM (n = 3); SCH 28080 = 5 μM (n = 5); or BAF = 50 nM (n = 6). The pH^{in} recoveries (J_H^+) were determined from experiments similar to those shown in (A). The J_H^+ values are the product of dpH/dt and β_i as described previously (Martínez-Zaguilán et al., 1993). Data are expressed as SEM. * $P < 0.05$ compared by one-way *ANOVA*, J_H^+ compared to those in Na^+- and HCO_3^-- free media.

microvascular endothelial cells could be attributed to V-H^+-ATPase, we performed experiments with NH_4Cl in a Na^+- and HCO_3^--free buffer, in the presence of V-H^+-ATPase inhibitors, i.e., bafilomycin and NBD-Cl^-. This resulted in suppression of the pH^{in} recovery (Fig. 2.5A and 2.5B). P-type H^+-ATPase inhibitors such as SCH 28080, had no effect on the pH^{in} recovery (Fig. 2.5B). Nevertheless that these experiments were performed in the absence of Na^+ and HCO_3^-, to further demonstrate that neither Na^+/H^- exchanger nor HCO_3^- based H^+-transporting mechanisms were involved in the pH^{in} recoveries, we performed experiments with 5-(N,N-hexamethylene)-amiloride (HMA) and 4,4' diisothiocyanato stilbene-2,2' disulfonic acid (DIDS) in the absence of Na^+- and HCO_3^- (Fig. 2.5B). These drugs are blockers of Na^+/H^+ exchanger and anion transport, respectively. These data indicated that HMA did not alter the kinetics of pH^{in} recovery observed in a Na^+- and HCO_3^--free buffer (data not shown). However, DIDS has a tendency to decrease the Na^+ and HCO_3^- - independent recoveries although not significantly (cf Fig. 2.5B).

Microvascular endothelial cells exhibit Na^+/H^+ exchange and HCO_3^--based H^+-transporting mechanisms. To evaluate the relevance of these ubiquitous pH^{in} regulatory systems in microvascular endothelial cells, we performed acid loading experiments in the presence of Na^+ and HCO_3^-. The removal of NH_4Cl in the presence of Na^+ and HCO_3 resulted in a rapid acidification followed by pH^{in} recovery. The magnitude of the pH^{in} recoveries were similar to those observed in media containing Na^+ and lacking HCO_3^- (cf. Fig. 2.5B). In the presence of Na^+ and HCO_3 macrovascular endothelial cells acidified in a similar fashion and had similar fluxes to microvascular endothelial cells (dpH/dt = 0.02

$\pm$ 0.006; J_{H}^{+} = 1.44 $\pm$ 0.34; n = 3). Altogether, these data indicate that both micro- and macrovascular endothelial cells exhibit the ubiquitous Na^+- and HCO_3^- -dependent pH^{in} regulatory mechanisms. Importantly, microvascular endothelial cells also exhibit an additional Na^+- and HCO_3^- -independent pH^{in} regulatory system that allows them to better cope with acid loads (cf. Figs. 2.5A and 2.5B).

Acute acidification elicited by Na^+ removal or HCO_3^- addition corroborates a Na^+- and HCO_3^-- independent pH^{in} regulatory mechanism in microvascular endothelial cells. It has been shown that cell types that exhibit the Na^+/H^+ exchanger as a major pH^{in} regulatory system respond to acute Na^+ removal (in the absence of HCO_3^-) with either a rapid or a slow decrease in pH^{in} (Escobales et al., 1990; Ziegelstein et al., 1992). In the absence of Na^+ and HCO_3^-, most cells do not recover from this acidification (Martínez-Zaguilán et al., 1993). This is the case for macrovascular endothelial cells that respond to Na^+ removal with a slow acidification (Δ pH^{in} = 0.28 $\pm$ 0.03 pH unit; $t_{1/2}$ of acidification = 163 secs $\pm$ 30; n = 3; Fig. 2.6A). Interestingly, Na^+ removal in microvascular endothelial cells resulted in an acidification (ΔpH^{in} = 0.17 $\pm$ 0.03 pH unit, n = 11) followed by a rapid recovery to baseline (Fig. 2.6A). This recovery occurred in a HCO_3^--free buffer and was unaffected by preincubation with DIDS (Fig. 2.6B). Importantly, the pH^{in} recovery in a Na^+- and HCO_3^--free buffer was suppressed by V-H^+-ATPase inhibitors (Fig. 2.6B). As an alternative approach to elicit an acute acidification, we perfused cells with a HCO_3^- containing media. In certain cell types, the acute addition of HCO_3^- causes an abrupt decrease in pH^{in} (Gillies and Martínez-Zaguilán, 1991). The

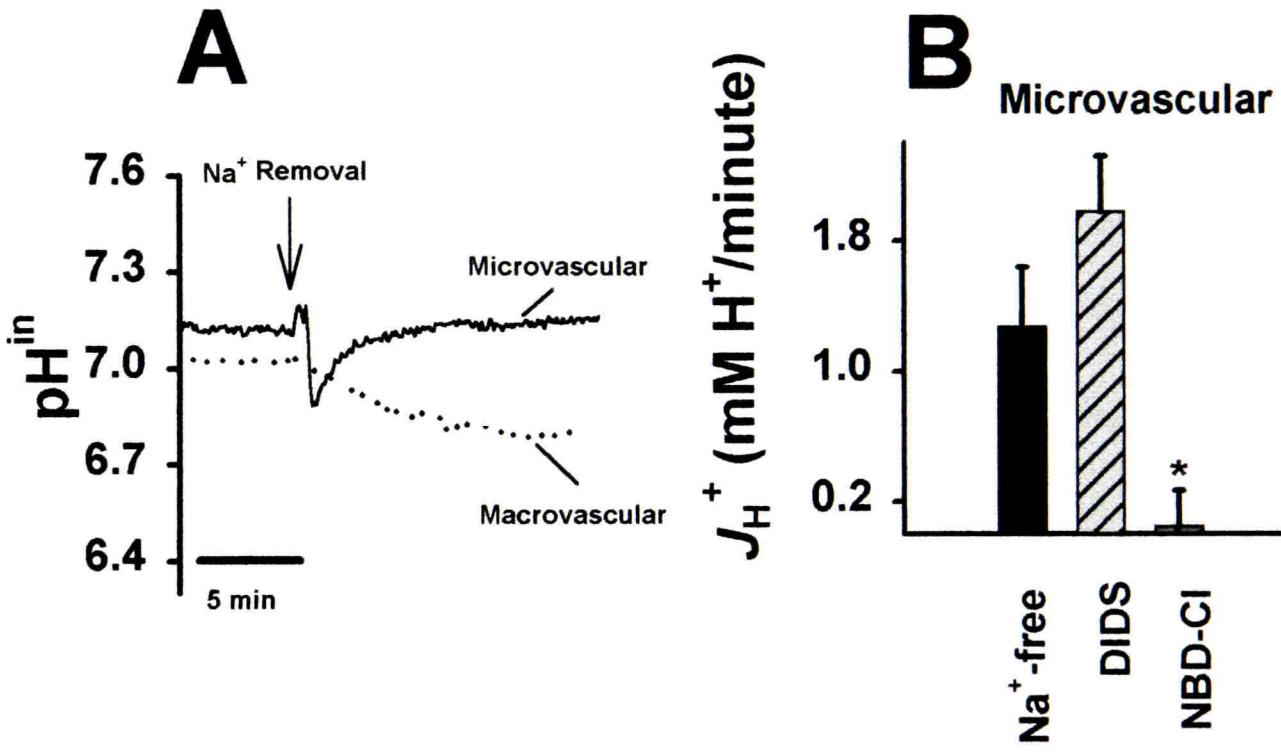

Figure 2.6 Differential effects of sodium removal in microvascular and macrovascular endothelial cells. (A). Microvascular (solid line) and macrovascular (dotted lines) endothelial cells were handled as in (Fig 2.5A), except that at the arrow, perfusate was changed to CPB with 110 mM N-methyl-glucamine substituted for Na^+. Data are representative of 11 and 5 experiments for micro- and macrovascular endothelial cells, respectively. (B) The pH^{in} recoveries (J_H^+) were estimated during the first 5 min from experiments similar to those shown in (A), except that Na^+-free CPB also contained 100 μM (n = 3) DIDS or 2 μM (n = 6) NBD-Cl. Data are expressed as SEM. * $P < 0.05$ by one-way *ANOVA* compared to Na^+- free media.

acute addition of HCO_3 resulted in a rapid acidification (ΔpH^{in} = 0.21 ± 0.02 pH unit, n = 8) followed by a rapid recovery to baseline in microvascular endothelial cells, while macrovascular endothelial cells respond with rapid decreases in pH^{in} followed by a recovery that is ca. 0.1 pH unit above baseline. The recovery of pH^{in} to baseline (microvascular) or above baseline (macrovascular) could be due to HCO_3 transport, since the media contained Na^+ and HCO_3. To address this, we preincubated both cell types with 100 μM DIDS. The recovery from acidification was unaffected by DIDS, suggesting a HCO_3^- independent recovery mechanism (data not shown). In microvascular endothelial cell the pH^{in} recovery was unaffected by either SCH 28080 (an H^+/K^+-ATPase inhibitor) or oligomycin (a F_0/F_1-ATPase inhibitor), but was completely inhibited by V-H^+-ATPase inhibitors (data not shown). These data suggest that the V-H^+-ATPase was responsible for the pH^{in} recovery from an acid load induced by HCO_3 addition in microvascular endothelial cells and that Na^+/H^+ exchange is the likely mechanism in macrovascular endothelial cells.

Confocal microscopy allows the study of pH^{in} in leading and lagging edge of the cell with unsurpassed time resolution. Our experiments in cell populations (i.e., invasion assays and time resolved fluorescence spectroscopy of cells loaded with SNARF-1) suggested that pmV-ATPase is present in micro- but not macrovascular endothelial cells. These studies also indicated that microvascular endothelial cells are more invasive than macrovascular endothelial cells. We then focused on microvascular endothelial cells to further understand the mechanisms underlying their distinct pH^{in} regulation. These

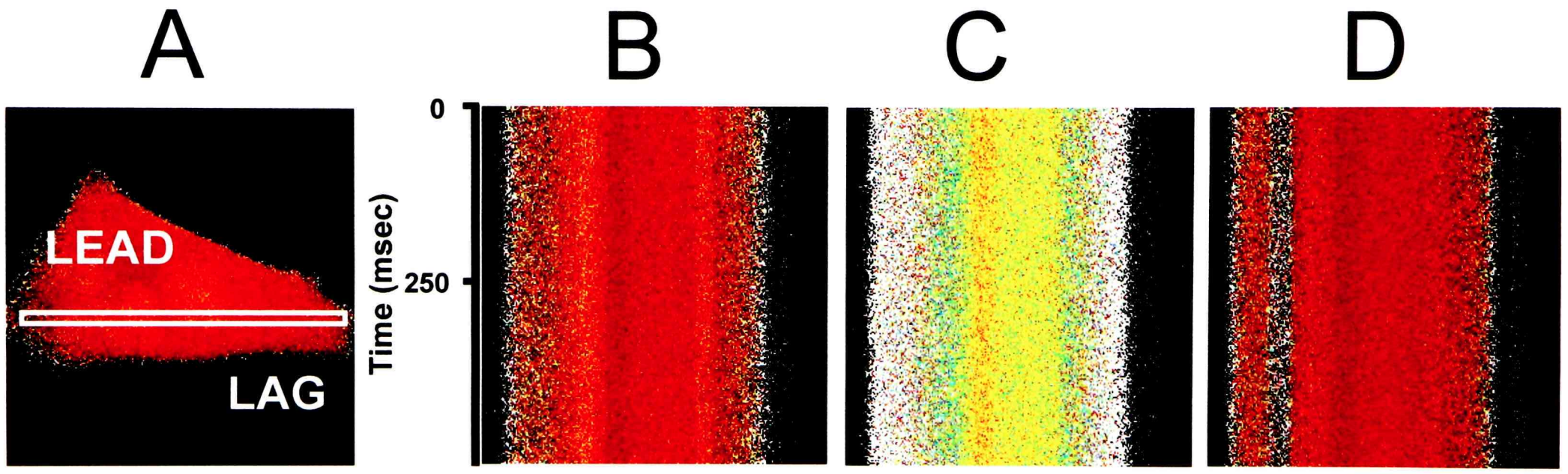

Figure 2.7 Confocal line scan images of a microvascular endothelial cells reveal pH^{in} gradients. Cells were grown on round glass coverslips (25 mm) to sub-confluence and loaded with SNARF-1, as described for cell populations. Cells were transferred to the microscope stage and maintained at 37°C. (A) Ratio image of a single cell. Leading (LEAD) and lagging (LAG) edge of the cell were determined by morphology. The white box indicates the region from which the line scan was obtained. (B) Line scan of region identified in (A) while cell was superfused with CPB. (C) Perfusate was changed to 25 mM NH_4Cl. (D) Perfusate was changed to Na^+ and HCO_3^- -free CPB.

studies were performed at the single cell level and in discrete subcellular regions involved in cell motility such as the leading edge of the cell. The immunocytochemical evidence of pmV-ATPase at the leading edge of the cell prompted us to hypothesize that the preferential localization of pmV-ATPase in the leading edge of the cell might result in cells exhibiting a distinct pH^{in} gradient from leading to lagging edge of the cell (cf. Fig. 2.4). Confocal/spectral imaging microscopy of cells loaded with SNARF-1, a ratiometric pH indicator allowed us to evaluate pH^{in} from leading to lagging edge with a high spatial, temporal, and spectral resolution (Opas et al., 1997; Martínez-Zaguilán et al., 1996a). We employed line scanning confocal microscopy to evaluate pH^{in} with high temporal resolution. Cells were loaded with SNARF-1 and its emission at the pH sensitive wavelengths was captured and ratio images were obtained. The white line across the ratio image of a cell visualized with a 60 x objective (N.A. 1.4) shows the region studied from leading (LEAD) to lagging (LAG) edge (Fig. 2.7A). During line scan, the laser is moved back and forth along the single point of Y axis and the resulting 2-D image shows the X axis of the cell and time is the Y axis. Since SNARF-1 is a ratiometric dye, differences in color denote difference in ratio and therefore differences in pH. Notice that there are distinct pH domains along the X axis (i.e., leading to lagging edge; left to right Fig. 2.7B). Because the images were obtained using ratio mode, it is unexpected that such pH^{in} differences are due to different dye concentration across the cell, since ratio should correct for this (Haugland, 1993). Addition of NH_4Cl elicits cytosolic alkalinization (Fig. 2.7C) and its removal 5 min thereafter decreases pH^{in} (Fig. 2.7D) that is followed by recovery towards basal (data not shown). Note that the presence of pH

gradients is more remarkable at alkaline (i.e., following NH_4Cl treatment) than at acidic pH (i.e., following NH_4Cl removal). Ratio values were obtained from defined regions of interest (leading and lagging edge) of the cell throughout the experiment and converted to pH^{in} using in situ parameters obtained at the end of each experiment. These data indicate that at steady-state the mean pH^{in} is higher in the leading than in the lagging edge (Figs. 2.8A and 2.8B). During the course of these experiments using rapid acquisition time the magnitude of pH^{in} changes being ca. 0.26 pH unit larger in the lagging than in the leading edge (Fig. 2.8C). These findings are novel in that they suggest that the presence of pmV-ATPase at the plasma membrane in microvascular endothelial cells confers these cells the ability to maintain pH^{in} values more alkaline in the leading than in the lagging edge of the cell. This also allows cells to maintain a higher H^+ buffering capacity in the leading than in the lagging edge of the cell.

Spectral imaging microscopy shows that leading edge exhibits a more alkaline pH^{in} than lagging edge. To eliminate any bias in our interpretation of the data regarding differences in pH^{in} (that could be due to differences in dye concentration and/or intracellular environment that may be distinct at the leading [LEAD] or the lagging [LAG] edge of the cell), we performed spectral imaging experiments in SNARF-1 loaded cells. The rationale of using this approach is that it allows to monitor the full spectral output of the pH indicator from leading to lagging edge of the cell. Under these conditions, the spectral properties of SNARF-1 (i.e., relative distance of the ion-sensitive spectral shoulders) are only sensitive to H^+ concentration and unaffected by dye

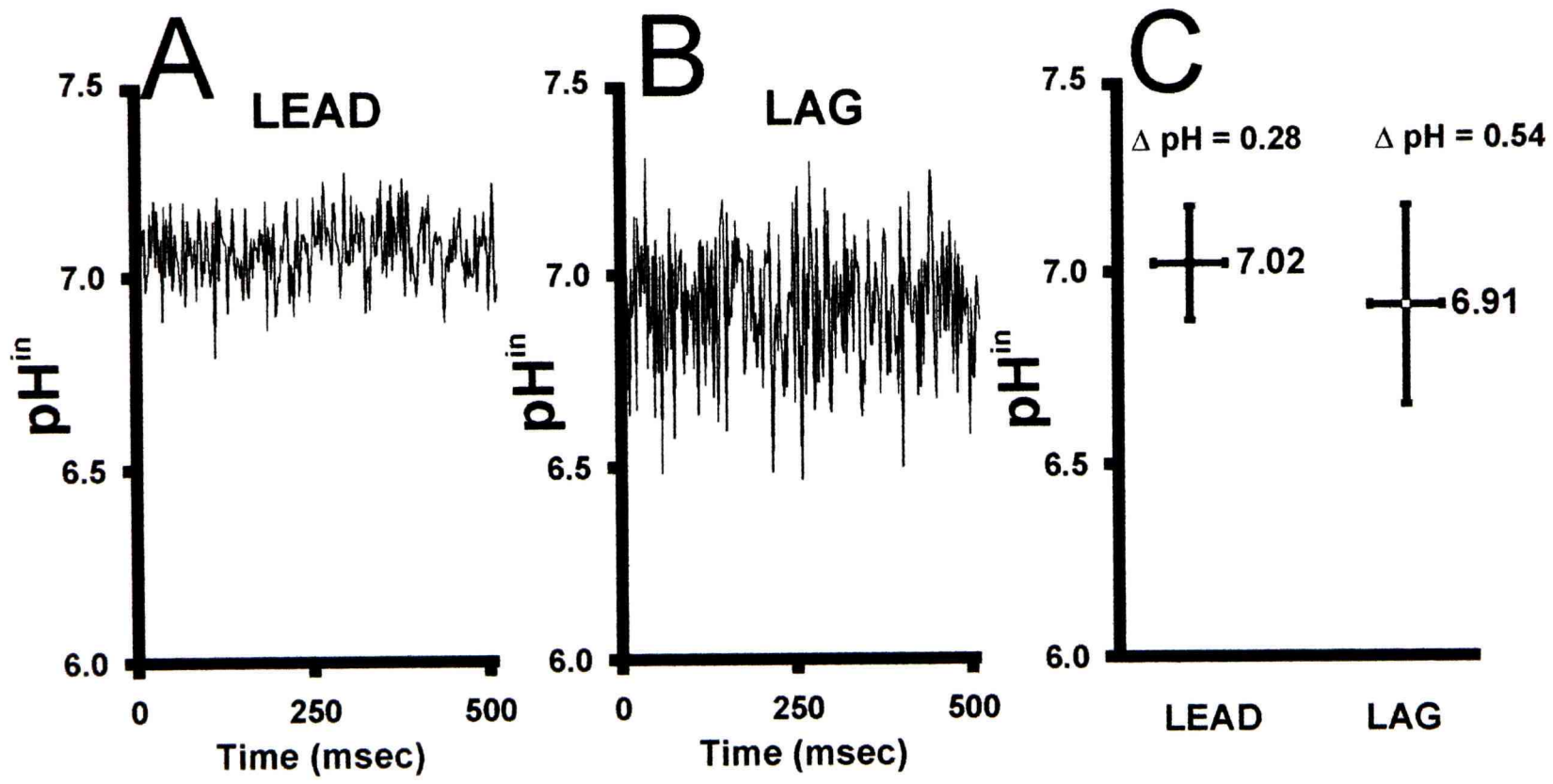

Figure 2.8 Selected regions from a confocal line scan demonstrate that the leading edge of the cell is more alkaline than the lagging edge. Regions of interest were selected from Fig 2.7A at the (A) leading and (B) lagging edge of the cell and ratio values obtained at 2 msec sampling rates. These figures show the pH^{in} values at steady-state. (C) Mean pH^{in} of the regions shown in (A) and (B), as well as the magnitude of pH^{in} oscillations. $^{*}P < 0.05$ compared by paired *t*-test leading vs lagging edge. Data are representative of 6 experiments

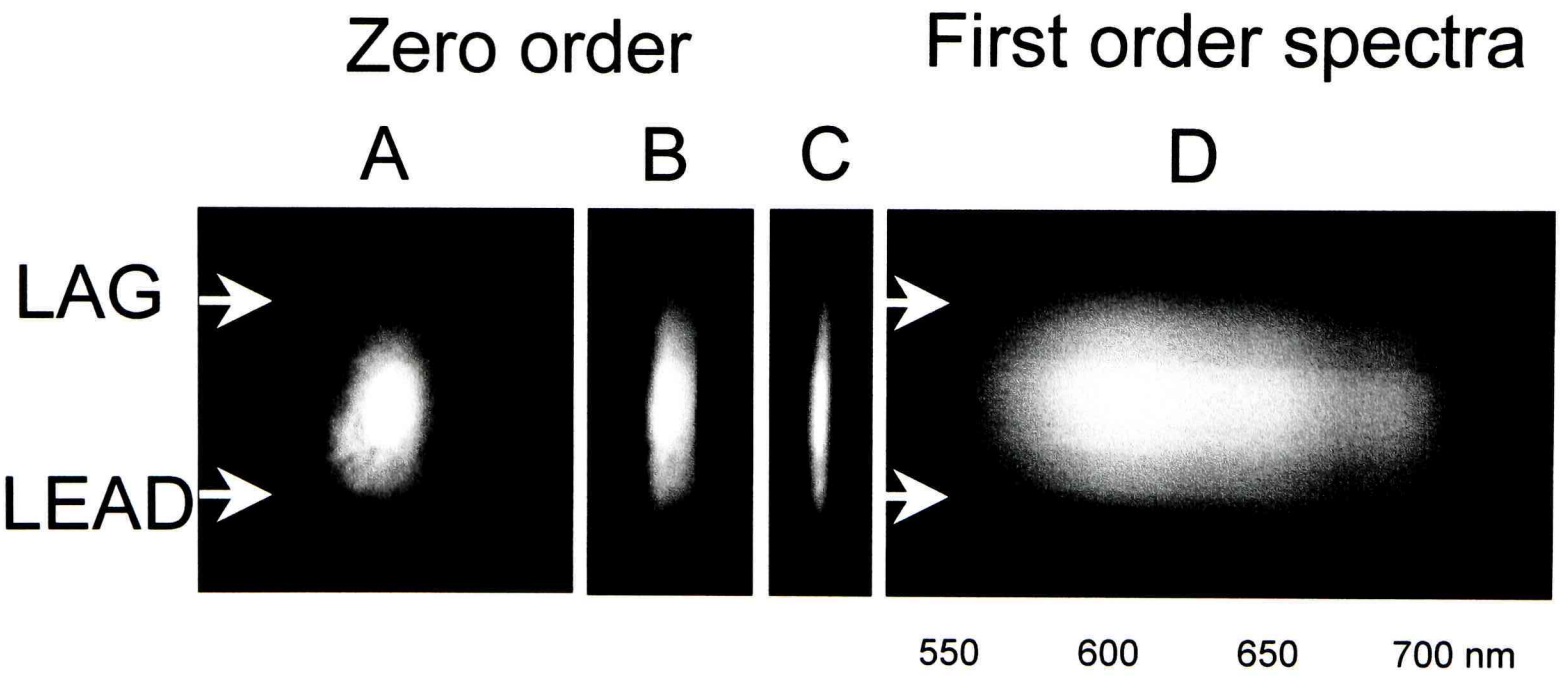

Figure 2.9 Spectral imaging microscopy allows for high spectral resolution of fluorescence data in discrete regions of a cell. Microvascular endothelial cells grown on glass coverslips to sub-confluence and loaded with SNARF-1. (A) A single cell is aligned onto the entrance slit (2.0 mm) of the spectragraph (see "Experimental Procedures") allowing identification of its leading and lagging edge. (B) Slit width is decreased (0.5 mm) to allow for increased spatial resolution and increased signal/noise ratio. (C) Final slit width is 0.2 mm. (D) Emission filters are removed and the fluorescence spectra are collected and de-convoluted from individual tracks.

Fig. 2.9A shows a cell aligned along the slit entrance of the spectragraph and that decreasing the slit width provides spatial information from the leading to lagging edge of the cell (cf. Fig. 2.9A, 2000 μm; Fig. 2.9B, 500 μm; Fig. 2.9C, 200 μm). Fig. 2.9D shows the first order spectra. For these experiments we binned 12 tracks (each corresponding to ca. 10 μm across the length of the cell (leading to lagging edge). Notice that although there are differences in dye concentration between leading and lagging edge (Y axis on the spectra; Fig. 2.10A), the spectral shape indicates that the pH^{in} is more alkaline in the leading than in the lagging edge by ca. 0.2 pH unit (cf. Fig. 2.10A).

Measurements of pH^{in} in discrete cellular regions allows study of pmV-ATPase in endothelial cells. Spectral imaging microscopy allows us to obtain both spatial and temporal information regarding pH^{in} changes (and thereby pmV-ATPase activity) in leading and lagging edge of the cell. Fig. 2.10B shows that the spectral properties of SNARF-1 followed the predicted behavior for this ratiometric dye: increases and decreases in the fluorescence signal at 644 and 584, respectively, as pH is increased by NH_4Cl treatment. The washout of NH_4Cl to elicit acidosis (indicated as Na^+ and HCO_3^- free), results in decrease and increase in the signals at 644 and 584 nm, respectively. The data shown in Fig. 2.10C were derived by measuring pH^{in} in the lagging (closed circles) and in the leading (open circles) regions of the cell. Acid loading experiments in the absence of Na^+ and HCO_3^-, indicated that the rate of pH^{in} recovery in the leading and lagging edge are distinct. The magnitude of the pH^{in} changes following NH_4Cl treatment and wash-out were larger in the lagging than in the leading edge, consistent with lower H^+

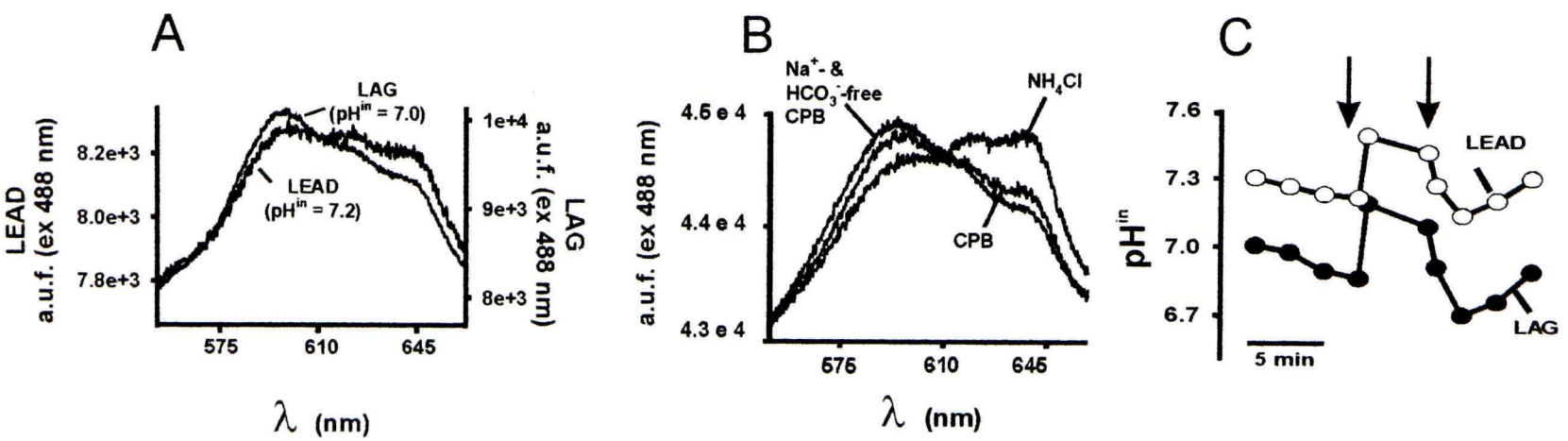

Figure 2.10 NH_4Cl experiments reveal differences in Na^+ - and HCO_3^- -independent recoveries in the leading and lagging edge of microvascular endothelial cells. (A) The emission spectra collected and recorded from two distinct tracks in the cell (LEAD and LAG; arrows) at steady-state pH. (B) Spectral pH^{in} changes of SNARF-1 from a single track with changes in superfusate: CPB (steady-state), NH_4Cl (alkalinization), Na^+-, and HCO_3^--free CPB (acidification). (C) Recovery from an acid load in Na^+-, & HCO_3^--free CPB. Spectra similar to those shown in (B) were collected from 12 different tracks at 50 msec sampling rates. For data presentation only information from the leading (LEAD) and lagging (LAG) edge are shown. At the first arrow, cells were superfused with CPB containing 25 mM NH_4Cl and at the time point indicated by the second arrow the superfusate was exchanged for Na^+ and HCO_3^- -free CPB.

buffering capacity in the lagging edge of the cell (56.1 ± 8.5 versus 45.6 ± 6.7 in leading and lagging edges, respectively). Consequently, the proton fluxes are faster in leading than lagging edge. Because a limiting factor in spectral imaging microscopy is time-resolution, we could not address whether the pH oscillations determined by line laser scanning confocal microscopy are also observable by this approach. Nevertheless, at least within the time frame of these experiments (i.e., 2-50 msec exposure), we are confident that pH^{in} values are more alkaline in the leading than in the lagging edge of the cells. Differences in pH^{in} regulation in the leading and lagging edge are predicted by flux ratio equations since the passive H^+ influx is ca. 45 and 56 times the passive efflux at the leading edge and lagging edge, respectively (assuming a ψ = -90 mV; and using the pH^{in} values shown in Fig 2.10C for leading and lagging edge, at a pH^{ex} = 7.4). This suggest that H^+ influx is larger in the lagging edge, consistent with a more dynamic pH^{in} regulatory system at the leading edge. Further support for a dynamic mechanism to maintain such a pH^{in} difference in leading and lagging edge is given by the fact that although the H^+ ion permeability is extremely high ($P_H = 10^{-3}$ cm/sec), the actual J_{H^+} across the plasma membrane is very low because of the low free [H^+] in the cytosol and in the extracellular environment (if we assume a pH^{ex} = 7.4). Under these conditions, the passive H^+ ion influx is ca. 0.02 pH unit/hr, yet the observed differences in pH^{in} between the leading and lagging edge are ca. 0.1 pH unit within the time frame of our experiments (i.e., 2 msec). Thus, it is unlikely that such differences in pH^{in} values from leading to lagging edge are due to simple H^+ diffusion. We interpret these data to suggest that pmV-ATPase at the leading edge is a dominant pH^{in} regulatory system that allows these pH^{in}

gradients to exist in microvascular endothelial cells. The validity of these estimations on pH^{in} values rely on the ability to fully collapse the pH^{in} gradients across all compartments. Because we have performed complete in situ titrations at discrete distances of the cell from leading to lagging edge (i.e., at ca.10 μm intervals) and have utilized in situ calibration parameters for each of these regions, this should minimize errors inherent to distinct dye concentration and intracellular environment (i.e., viscosity, protein binding, etc.) that may exist in these discrete cellular regions from leading to lagging edge. This type of calibration is needed because fluorescent ion indicators have been reported to exhibit distinct dissociation constants in distinct cell types (Gillies et al., 1990). From a number of in situ titrations similar to those shown in Fig. 2.11A, we determined that there are no significant differences in pK_a of the dye in any of the regions studied (Fig. 2.11B). Thus, these data indicate that the pH^{in} gradients were fully collapsed. There are however significant differences in the R_{max} and R_{min} (Fig. 2.11C). Because the full spectral output from leading to lagging edge of the cell is obtained within a time frame of 2-50 msec, we are confident that the distinct pH^{in} values observed in leading and lagging edge of the cell are due to distinct pH^{in} regulation in these regions.

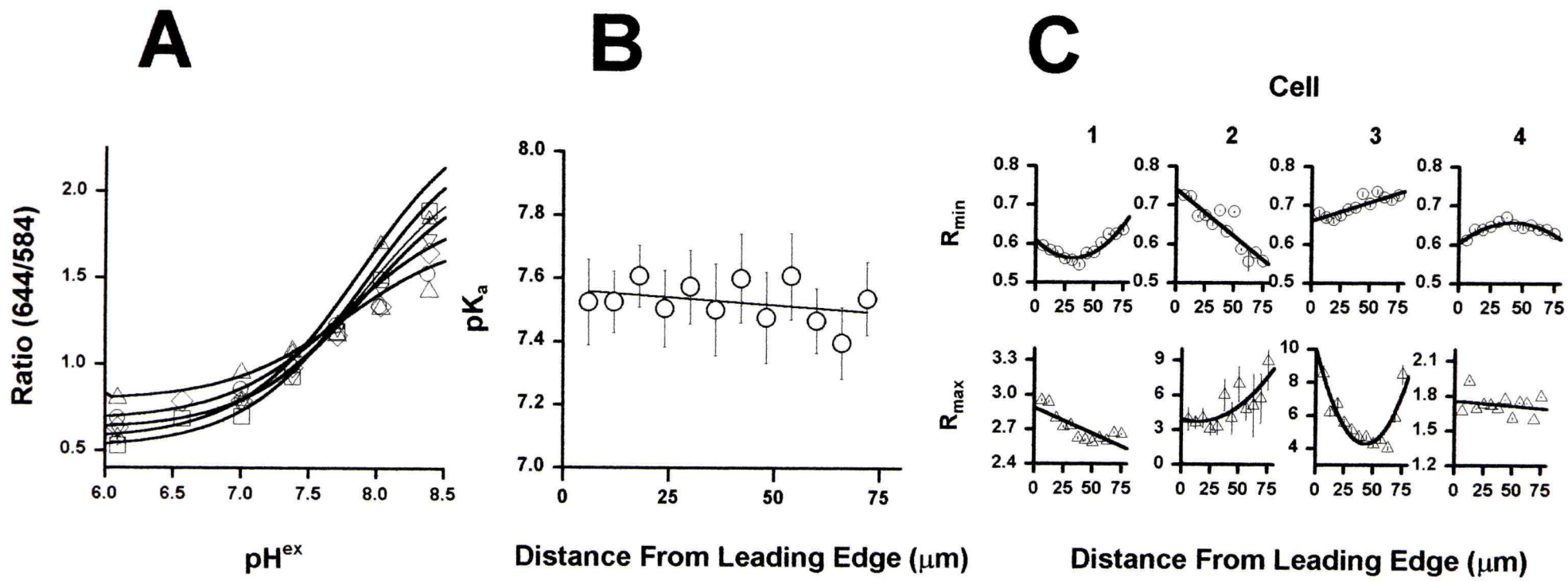

Figure 2.11 In situ calibrations of distinct subcellular compartments reveal differences in dye behavior and emphasize the importance calibrating dye in every region being tested. Cells were handled as described in Fig 2.10. (A) In situ titrations were performed with nigericin and valinomycin as described in "Experimental Procedures". The pH was increased with NaOH to obtain pH values shown on the X axis. SNARF-1 spectra were collected and the observed ratio values plotted. For data presentation, data from only 6 tracks are shown. Data were fit into Eqn 2.1, solved using nonlinear least squares analysis, and the values of pK_a (B), R_{min} (C), and R_{max} (C) were determined for each track. (B) pK_a from 12 tracks determined in (A) plotted as a function of distance from leading edge of cell. (C) R_{min} and R_{max} from 4 different cells. Data are plotted as a function of distance from leading edge. Note that pK_a is unchanged from leading to lagging edge. Similar behavior was observed for all cells studied. In contrast, the behavior of the R_{max} and R_{min} parameters is variable.

Conclusions

To our knowledge the relevance of pmV-ATPases for pH^{in} regulation and invasion/migration has not been reported in microvascular endothelial cells. Dynamic vascular remodeling during angiogenesis requires growth and invasion of endothelial cells into other tissues. However, the acidic extracellular environment that prevails in angiogenesis is not conducive for growth. Our studies indicate that pmV-ATPase helps them to cope with the acidic extracellular environment. This was demonstrated by pharmacological and ion substitution experiments. Our studies also indicated that microvascular endothelial cells exhibiting pmV-ATPase were more invasive/migratory than macrovascular endothelial cells that do not exhibit pmV-ATPase. Growth of microvascular endothelial cells under mildly acidic conditions, a condition which would activate pH^{in} regulatory mechanisms, exacerbated invasive/migratory behavior. Importantly, bafilomycin A_1, but not inhibitors of other pH^{in} regulatory mechanisms, suppressed migration/invasion of microvascular endothelial cells. The presence of V-H^+-ATPases at the plasma membrane in the leading edge of microvascular endothelial cells was demonstrated by immunocytochemistry. The unique distribution of pmV-ATPase resulted in distinct pH^{in} regulation in the leading and lagging edge of the cell. Altogether, these data indicate that pmV-ATPase expression in the leading edge of microvascular endothelial cells is relevant for pH^{in} regulation and invasion/migration of these cells

through extracellular matrix. pmV-ATPase has also been found in highly invasive tumors. Thus, pmV-ATPase could provide a target for pharmacological intervention in angiogenesis and cancer. Further studies are needed to identify biochemical pathways that regulate pmV-ATPase function in microvascular endothelial cells.

Experimental Procedures

Media, Buffers, and Chemicals

Dulbecco's modified Eagle's medium (DMEM) was supplemented with 10 or 20% fetal bovine serum (FBS), 2 mM L-glutamine, 0.4 mM L-arginine, 5 mM D-glucose, 20 U/ml heparin, 1 mM sodium pyruvate, 100 U/ml penicillin, 100 µg/ml streptomycin, and 0.2 µg/ml amphotericin B (Gibco, Grand Island, NY). Jokliks essential medium was supplemented with 60 mM taurine, 20 mM creatine, and 5 mM HEPES. This Jokliks medium is essentially Ca^{2+}-free. Cell Perfusion Buffer (CPB) consisted of 110 mM NaCl, 1 mM $MgSO_4$, 5.4 mM KCl, 1.5 mM $CaCl_2$, 0.44 mM KH_2PO_4, 0.35 mM NaH_2PO_4, 5 mM glucose, 2 mM L-glutamine, and 25 mM HEPES, pH = 7.15, unless otherwise noted. Na^+-free CPB consisted of all CPB ingredients, except those containing sodium. N-methyl-glucamine (110 mM) was substituted for NaCl. CPB solutions containing HCO_3 were continuously bubbled with 5% CO_2 at 37°C. The concentration of HCO_3^- in the buffer was determined as described earlier (Gillies and Martínez-Zaguilán, 1991). High K^+ buffer contained 146 mM KCl, 20 mM NaCl, 5 mM glucose, 2 mM glutamine, 10

mM HEPES, 10 mM MES, and 10 mM Bicine. The rationale for using these organic buffers was to allow for precise buffering across a wide pH ranging from 5.0-9.0 (Martínez-Zaguilán et al., 1996b).

Bafilomycin A_1 was obtained from Wako Chemicals (Richmond, VA), and SCH 28080 was a generous gift of Dr. A. Barnett (Schering, Bloomfield, NJ). The fluorescent dyes were obtained from Molecular Probes (Eugene, OR). All other chemicals were obtained from Sigma Chemical (St. Louis, MO), unless otherwise stated.

Isolation of Micro- and Macrovascular Endothelial Cells

Microvascular endothelial cells were isolated from small coronary vessels of adult Sprague Dawley rats obtained from the Animal Resources Division of the Health Protection Branch (Ontario, Canada). The protocols for isolation of the cells using the collagenase perfusion method, as well as the culture of these cells, have been described (Wu and Meininger, 1995). Microvascular endothelial cells were obtained free of smooth muscle cells and myocytes. Microvascular endothelial cells from three to four rats were pooled into one 60-mm gelatin-coated (1.5% gelatin in PBS) Petri dish and were cultured at 37°C under 10% CO_2 in DMEM with 20% FBS. Endothelial cell identity was confirmed as described earlier (Wu and Meininger, 1995). Aortic endothelial cells (macrovascular) were obtained in proliferating culture at fifth passage from VEC Technologies (Rensselaer, NY). Microvascular and macrovascular endothelial cells were passaged by trypsinization and subsequently grown at 5% CO_2 in DMEM supplemented with 10% FBS. For experiments, cells were plated as required for each study.

pH^{in} Measurements in Cell Populations

Intracellular pH was determined by the fluorescence of SNARF-1 (5-[and-6] carboxy-SNARF-1) as described previously (Martínez-Zaguilán et al., 1993). Briefly, two cover slips containing cells at confluency were loaded with 7.5 μM SNARF-1 in its acetoxymethyl (AM) ester form and incubated at 37°C in 5% CO_2 for 45 minutes. The cells were then rinsed and further incubated for 30 minutes to ensure complete ester hydrolysis/leakage of uncleaved dye. The two cover slips were placed back to back in a holder and perfused at a rate of 3 ml/min. The fluorescence of SNARF-1 was monitored with an SLM-8100/DMX spectrofluorometer equipped for sample perfusion. The sample temperature was maintained at 37°C by keeping both the water jacket and perfusion media at 37°C. Fluorescence was monitored in continuous acquisition mode by using an excitation wavelength of 534 nm and monitoring emissions at 584, 600, and 644 nm as described elsewhere (Martínez-Zaguilán et al., 1993). The fluorescence emission at 584 nm decreases and that at 644 nm increases, respectively, with increasing pH, as such the ratio of 644/584 was used to monitor pH changes. The 600 nm wavelength (iso-emission point) is used to evaluate the efficiency of loading, quenching or other artifacts. Fluorescence data were converted to ASCII format for data analysis.

In Situ Calibration of SNARF-1

In situ calibration curves were generated as described previously(Martínez-Zaguilán et al., 1993). Briefly, the cells attached to cover slips were perfused with a high K^+ buffer containing 2 μM valinomycin and 6.8 μM nigericin. The high K^+ is used to

approximate intracellular K^+ and nigericin sets the H^+ gradient equal to the K^+ gradient, with valinomycin completing the collapse of the K^+ gradient without significant effects on cell volume. The cells were then perfused with buffers ranging in pH^{ex} from 5.5 to 8.0 (at ca. 0.2 pH unit intervals). The ratio (R; 644/584) values of SNARF-1 at each pH^{ex} value were fitted into the following equation:

$$pH = pK_a + \log \frac{(R_{obs} - R_{min})}{(R_{max} - R_{obs})}, \qquad \text{Equation [2.1]}$$

where R_{obs} is the ratio observed at any given pH, R_{min} is the ratio observed when the dye is fully protonated, and R_{max} represents the ratio of fluorescence obtained when the dye is fully unprotonated. The equation is solved iteratively using nonlinear least squares analysis (MINSQ, MicroMath Scientific, Salt Lake City, UT) and yields the values of pK_a, R_{min}, and R_{max} for SNARF-1 in these cells. From these in situ calibration curves, the following parameters were obtained for SNARF-1 in microvascular endothelial cells (mean ± S.D.; n = 33): pK_a= 7.76 ± 0.076; R_{min} = 0.55 ± 0.004; and R_{max} = 2.49 ± 0.23. The in situ calibration parameters for SNARF-1 in macrovascular endothelial cells were as follows (mean ± S.D.; n = 33): pK_a= 7.69 ± 0.089; R_{min} = 0.435 ± 0.007; and R_{max} = 2.94 ± 0.28. These values were significantly different between cell types ($P < 0.05$). Intracellular pH values were then generated for each experiment by using equation [2.1] and their corresponding in situ calibration parameters with SigmaPlot version 5.0 (Jandel Scientific, San Rafael, CA).

pH^{in} Measurements Using Confocal Microscopy

SNARF-1 fluorescence was excited with 488 nm line of a 25 mW argon laser. A 610DRSP filter allows the collection of emission at 584 nm (570/32) and 644 nm (640/40) that were simultaneously captured by two separate photomultiplier tubes. Images of individual cells exhibiting a typical leading edge (i.e., lamellipodia) were obtained with a 60x Olympus objective (N.A. 1.4). To simplify the identification of the leading edge of the cells we induced a wound in cells grown at confluence using a forceps tip to scrape off cells. This maneuver consistently resulted in cells whose leading edge aligned along the wound and was easily observable under phase contrast and/or fluorescence microscopy. Data were collected from discrete regions of a single cell in the X-T mode. In the X-T mode data is only collected from a region along a single line on the Y-axis; thus sampling rate is increased to 2 msec per line.

pH^{in} Measurements Using Spectral Imaging Microscopy

This approach allows measurements of ions in single cells, and in discrete subcellular regions with high spatial and spectral resolution (Martínez-Zaguilán et al., 1996a). The spectral imaging microscope constituted of the following elements: a fluorescence inverted microscope (Olympus IX-70 with a 60x objective, N.A. 1.4). A 6.7 eyepiece was used to image the cell through the side port of the microscope onto the input slit of a grating monochromator (Chromex 250 IS/SM spectrograph, Albuquerque NM). The fluorescence signal emitted from a single cell loaded with SNARF-1 was focused

onto a monochromator (i.e., spectragraph), the light diffracted, and the full spectral output was collected using a cooled charged coupled device (CCD) camera (Photometrics, Mod CH350, Tucson, AZ) equipped with a 512x512 element (27 μm^2/pixel) imaging chip. The full spectral output of the cell can be obtained within a time frame of as little as 2 msec. Thus, spatial information was obtained along the length of the entrance slit and a single cell aligned along this slit so that spectra were acquired from unique subcellular locations (i.e. leading to lagging edge). Data were collected from 12 discrete regions (tracks) of the cell and binned to obtain a higher signal/noise ratio. The optical filters were as follows: 488 nm narrow bandpass filter; 550 long bandpass dichroic (Omega Optical, Brattleboro, VT).

Immunocytochemistry

Monoclonal antibodies to several subunits of V-type H^+-ATPase are available in our laboratory, or from commercial sources (e.g., 60 kDa, 69 kDa, and 100 kDa subunits; Molecular Probes, Eugene, OR). Cross reactivity and immunospecificity has been corroborated in our laboratory by Western blot analysis and we have observed that these antibodies recognize a single band at the appropriate molecular weight (data not shown). Monoclonal antibodies to well known markers of leading lamellae (ezrin) are also commercially available (Sigma Chemical, St Louis, MO). For immunocytochemistry,

cells are fixed with 4% paraformaldehyde for 15 min, washed with 25 mM Glycine, and then permeabilized with 0.1% Triton X-100. The cells are sequentially incubated with primary antibody, washed extensively, and then with Texas Red-labeled secondary (anti-mouse immunoglobulin G) antibody (Lynch et al., 1996).

Cell Invasion Assay

Endothelial cells were plated in the Membrane Invasion Culture System (MICS) assay to evaluate the degree of cell invasion through various extracellular matrix proteins (ECMs), as previously described (Hendrix et al., 1987; Sheng et al., 1996). Microvascular endothelial cells were grown to confluence in T-25 flasks in DMEM. At confluence the cells were loaded with 5 μM Calcein-AM for 30 minutes. Cells were then trypsinized, washed, and counted. To evaluate the degree of cell invasion through various extracellular matrix proteins (ECMs) in vitro, HTS FluoroBlok™ (Becton Dickinson, Bridgeport, NJ) inserts were briefly soaked in Matrigel®, seeded at densities of 1×10^5, and incubated at 37°C / 5% CO_2 for 24 hours in the presence or absence of 20 nM bafilomycin. HTS FluoroBlok™ inserts contain a 10 μm proprietary polyethylene terephthalate (PET) membrane impregnated with light absorbing dyes that will absorb visible light from 490-700 nm. The inserts were subsequently visualized and images of the bottom and top of the insert obtained with a 20x objective and a Bio-Rad 1024 MRC confocal microscope (Bio-Rad, Hercules, CA) by exciting the fluorophore with the 488 nm line of a 15 mW krypton/argon laser and collecting emission with a photomultiplier tube utilizing the T1/T2 series filter blocks which contain a OG515 emission filter. Five

images were obtained per insert of experiments done in triplicate. The images were subsequently analyzed and cells visually counted in defined areas. Percent invasion was corrected for proliferation and calculated by using the following equation:

$$\% \text{ Invasion } = \frac{\text{Total \# invading cells [lower well sample]} / \mu m^2}{\text{Total \# of cells seeded [upper well sample]} / \mu m^2} \times 100. \qquad \text{Equation [2.2]}$$

Cell Migration Assay

Migration was assessed in wounded confluent monolayers of microvascular endothelial cells. Cells are grown on 18 mm coverslips to confluence and subsequently wounded. The wound in this instance is inflicted by scratching the cover slip with an aluminum strip that induces a 300 μm gap (Selden and Schwartz, 1979). Cells were allowed to recover for 18 hours in the absence or presence of inhibitors and subsequently fixed, permeabilized, and incubated with FITC-phalloidin. Images of wounded monolayers were then obtained with a 20x objective and a Bio-Rad confocal microscope (ex 488; em OG515). Migration was assessed as wound distance at this time point from 3 randomly selected areas. We also evaluated unstimulated motility in MICS chambers containing polycarbonate filters, soaked overnight in 0.1 % bovine serum albumin as described elsewhere (Hendrix et al., 1987; Sheng et al., 1996). Measuring the ability of cells to migrate through 10 μm pores in the absence of matrix or chemoattractant(s) allows us to assess deformability and random mobility.

CHAPTER III

PLASMALEMMAL VACUOLAR TYPE H^+-ATPASE IS DECREASED IN ENDOTHELIAL CELLS FROM A DIABETIC MODEL[2]

In the previous manuscript we had demonstrated that microvascular endothelial cells exhibit pmV-ATPase. Its presence in migrating regions of the cell led to pH gradients across the cell and a more alkaline pH at the migrating/leading edge. Invasion assays revealed that microvascular endothelial cells were three-fold more invasive than macrovascular endothelial cells and treatment with bafilomycin blocked the invasion. We interpreted this data to support the hypothesis that pmV-ATPase was important for angiogenesis. It is known that a complication of diabetes is decreased wound healing and diminished angiogensis (Epstein and Sower, 1992). We hypothesized that since untreated diabetes results in acidosis, it is likely that acidosis continually occurs at the level of the microvasculature and that pH^{in} regulatory mechanisms either saturate or are altered by disease. If pmV-ATPase is altered and is required for invasion/angiogenesis this could be a possible explanation for the abnormalities observed in diabetes. In this study we

---

[2] Forthcoming

[a]José D. Rojas, [b]Cynthia J. Meininger, [c]Guoyao Wu, [a,d]Donald. E. Wesson and [a]Raul Martínez-Zaguilán

Departments of [a]Physiology and [d]Internal Medicine Texas Tech University Health Sciences Center; Lubbock, Texas, 79430; and Departments of [b]Physiology and [c]Animal Sciences Texas A&M University, College Station, Texas, 77843.

characterize pH^{in} regulation in diabetic cells and show that pmV-ATPase activity is essentially absent. Immunocytochemistry shows a decreased presence at the plasma membrane in these cells. In vitro angiogenesis models reveal that diabetic cells are unable to readily invade the extracellular matrix and that they are five-fold less invasive than normal cells.

Abstract

Complications of diabetes involve abnormalities in blood flow regulation, microvascular proliferation and angiogenesis. Because intracellular pH (pH^{in}) regulates cell growth, secretion, and cell motility/ migration, we examined if microvascular coronary endothelial (MCE) cells from the spontaneously diabetic BB rat (BBd) have altered pH^{in} regulation. Cells from BBd and non-diabetic (BBn) rats were grown on glass cover slips and were intracellularly loaded with the pH fluorescent indicator SNARF-1. The steady-state pH^{in} was similar in the BBd and BBn regardless of the HCO_3^- concentration. Acid loading experiments revealed similar levels of acidification in both cell types with BBn cells recovering faster than BBd in the presence of Na^+ and HCO_3^-. In the absence of Na^+ and HCO_3^- the rates of recovery again were faster in BBn than BBd. There were no differences in buffering capacity between BBn and BBd cells. In the absence of Na^+, proton fluxes (J_H^+) were two-fold faster in BBn than in BBd and were suppressed by V-H^+-ATPase inhibitors. Cells from BBn and BBd were tested for in vitro angiogenic potential and invasive potential and it was observed that BBn readily formed capillary-like structures whereas, BBd did not. Similarly BBn were more invasive than

BBd , and pmV-ATPase inhibition rendered BBn as non-invasive as BBd. The data suggest that a dysfunction of pmV-ATPase could be involved in the angiogenic abnormalities in diabetes.

Introduction

The endothelium plays an important role in blood flow regulation (Mehta, 1995; Gerritsen,1996; Cines et al., 1998). It is also involved in new blood vessel formation (i.e., angiogenesis) (Kalebic et al., 1983; Folkman, 1997). Angiogenesis is a complex process that includes proliferation and migration of microvascular endothelial cells, as well as invasion of the adjacent extracellular matrix by the endothelial cells (Kalebic et al., 1983; Folkman, 1997). It is known that intracellular pH(pH^{in}) is important for processes such as cell growth, secretion and invasion/ migration (Roos and Boron, 1981; Gilles et al., 1992). We have previously shown that plasma membrane V-H^+-ATPases (pmV-H^+-ATPases) are expressed in highly invasive and metastatic cells by providing a dynamic pH^{in} regulatory mechanism (Martínez-Zaguilán et al., 1993). The fact that highly invasive tumors are also highly vascularized (Folkman, 1995) lead us to hypothesize that pmV-H^+-ATPase activity is important for angiogenesis.

Diabetes is a disease that affects many organ systems, including the cardiovascular system (Epstein and Sowers, 1992; Servold, 1991). Long-term complications of diabetes include hypertension, abnormalities in blood flow distribution, and abnormal blood vessel formation (Epstein and Sowers, 1992; Stehouwer and Schaper, 1996). The abnormal blood vessel formation can be seen as altered peripheral

circulation evidenced by poor wound healing and decreased circulation that can result in necrosis to the affected tissue, ultimately requiring amputation (Epstein and Sowers, 1992; Stehouwer and Schaper, 1996; Servold, 1991). Altered blood flow regulation appears to be the result of altered angiogenesis . There is evidence of thickening of the capillary basement membrane and blockage of small vessels from abnormal luminal thickening (Beisswenger and Spiro., 1973; Zannini, 1974). Another complication of diabetes is altered metabolism that results in acidosis. It is possible that this condition is exacerbated at the level of the microvasculature and as such, affects the endothelial cells ability to function normally. It is also possible that the endothelial cells in diabetes have altered pH^{in} regulation. It has been shown that platelets (Salles et al., 1991) erythrocytes (Koren et al., 1997), leukocytes (Ng et al., 1992), and fibroblasts (Davies et al.,1992) in patients with diabetes exhibit increased Na^+/H^+ exchange activity. There has also been reported a genetic association between the susceptibility to diabetes in increased Na^+/H^+ exchange (Morahan et al., 1994).

The regulation of pH^{in} in most eukaryotic cells is mediated by the Na^+/H^+ exchanger and HCO_3^--dependent transporting mechanisms (Roos and Boron, 1981; Gillies et al., 1992). It has been suggested that the Na^+/H^+ exchanger and HCO_3^--transporting mechanisms accomplish housekeeping pH^{in} regulation in endothelial cells across a broad range of pH (Jentsch et al., 1988; Escobales et al., 1990; Schnid et al., 1992; Ziegelstein et al., 1992; Cutaia and Parks, 1994). Some specialized and, as noted above, highly invasive cells [metastatic cells (Martínez-Zaguilán et al., 1993), macrophage (Bidani et al., 1989), neutrophils (Nanda et al., 1992), and osteoclasts

(Vaananen et al., 1990)] also utilize pmV-ATPases to regulate pH^{in}. These ATPases are distinguished from other proton pumps by their pharmacologic inhibition (Bowman et al., 1988; Mendlein and Sachs, 1990). The F- and P-type H^+ pumps are inhibited by oligomycin and SCH 28080, respectively, and these drugs have no effect on the V-type H^+ pump (Bowman et al., 1988; Mendlein and Sachs, 1990; Forgac, 1999). The V-type H^+ pump is inhibited by bafilomycin A_1, concanamycin, and 7-chloro-4-dinitrobenz-2-oxa-1,3-diazole (NBD-Cl) (Bowman et al., 1988; Mendlein and Sachs, 1990).

We have previously suggested that pm V-H^+-ATPases are important for the acquisition of a more invasive phenotype in tumor cells (Martínez-Zaguilán et al., 1993). The similarity in invasion of adjacent tissue by the invading cell in metastasis and angiogenesis led us to hypothesize that microvascular endothelial cells may exhibit a similar dynamic pH^{in} regulatory mechanism. If this V-H^+-ATPase activity is important for angiogenesis, then the observed differences in angiogenesis in diabetes could be the result of altered or absent pm V-ATPases. In this study we employed microvascular coronary endothelial cells from normal and spontaneously diabetic animals to determine if these cells exhibited differences in pH^{in} regulation, specifically in pm V-H^+-ATPase activity.

Materials and Methods

Media, Buffers, and Chemicals

Dulbecco's modified Eagle's medium (DMEM) was supplemented with 10 or 20% fetal bovine serum (FBS), 2 mM L-glutamine, 0.4 mM L-arginine, 5 mM D-glucose, 20 U/ml heparin, 1 mM sodium pyruvate, 100 U/ml penicillin, 100 μg/ml streptomycin, and 0.2 μg/ml amphotericin B (Gibco, Grand Island, NY). Jokliks essential medium was supplemented with 60 mM taurine, 20 mM creatine, and 5 mM HEPES. This Jokliks medium is essentially Ca^{2+}-free. Cell Perfusion Buffer (CPB) consisted of 110 mM NaCl, 1 mM $MgSO_4$, 5.4 mM KCl, 1.5 mM $CaCl_2$, 0.44 mM KH_2PO_4, 0.35 mM NaH_2PO_4, 5 mM glucose, 2 mM L-glutamine, and 25 mM HEPES, pH = 7.15, unless otherwise noted. Na^+-free CPB consisted of all CPB ingredients, except those containing sodium. N-methyl-glucamine (110 mM) was substituted for NaCl. CPB solutions containing HCO_3^- were continuously bubbled with 5% CO_2 at 37°C. The concentration of HCO_3^- in the buffer was determined as described earlier (Gillies and Martínez-Zaguilán, 1991). High K^+ buffer contained 146 mM KCl, 20 mM NaCl, 5 mM glucose, 2 mM glutamine, 10 mM HEPES, 10 mM MES, and 10 mM Bicine. The rationale for using these organic buffers was to allow for precise buffering across a wide pH ranging from 5.0-9.0 (Martínez-Zaguilán et al., 1996b).

Bafilomycin A_1 was obtained from Wako Chemicals (Richmond, VA), and SCH 28080 was a generous gift of Dr. A. Barnett (Schering, Bloomfield, NJ). The fluorescent dyes were obtained from Molecular Probes (Eugene, OR). All other chemicals were obtained from Sigma Chemical (St. Louis, MO), unless otherwise stated.

Diabetic BB Rats

Diabetic BB (BBd) and age-matched, non-diabetes-prone BB (BBn) rats were obtained from the Animal Resources Division of Health Protection Branch (Ottawa, Ontario, Canada). Rats were housed in a light (12:12 h light/dark cycle)- and climate-controlled facility in stainless steel cages. Animals were fed ad libitum with laboratory rat chow (Hardland-Teklad, Bartonville, IL) and drinking water. Diabetic rats were maintained with daily subcutaneous injections of 2-4 U of Ultralente insulin (Eli Lilly, Indianapolis, IN) as previously described (Wu and Meininger, 1995). As in insulin dependent diabetes mellitius patients, the insulin treatment is necessary to prevent death of BBd rats (Wu and Meininger, 1995). BBd rats (95-110 days of age) 25-30 days post-onset of diabetes and age-matched BBn rats were used to prepare microvascular coronary endothelial cells. Urine glucose tests were performed twice daily (8 A.M. and 4 P.M.) in insulin-treated BBd rats using Chemstrip.uG (Wu and Meininger, 1995) and glucosuria was not detectable. Daily blood glucose tests were not performed because of the stress inflicted on the animals. Before the animals were sacrificed, blood was obtained from the tail vein of box-restrained unanesthetized and serum glucose concentrations were not statistically different in the BBd rats compared to BBn. The use of BB rats in this research was approved by Texas A&M University's Animal Care Committee.

Isolation of Microvascular Coronary Endothelial Cells

Microvascular coronary endothelial cells obtained from BB rats were isolated by collagenase perfusion as described previously (Wu and Meininger, 1995). Briefly, BBn and BBd rats weighing 200-300 g were given intraperitoneal injections of heparin, anesthetized, and the hearts surgically removed. The aorta was cannulated and perfused with Jokliks media that contained 0.1% dialyzed BSA and heparin (1 U/ml). After 10-min perfusion, collagenase (0.7 mg/ml) was introduced, and the perfusate was allowed to recirculate 30-40 minutes. Ventricles were cut from the hearts, minced, and placed in fresh collagenase-containing media and shaken in a water bath for 10 min. $CaCl_2$ (50 μM) was added to the minced tissue and digestion with collagenase continued for an additional 10 min. The cells were then dispersed, filtered, and diluted 1:4 with Jokliks modified media and 0.1% BSA, then allowed to settle to separate myocytes (which are heavier) from MCE cells. MCE cells were further purified by sequential filtration through a series of nylon screens obtaining a preparation free from smooth muscle cells and myocytes. Endothelial identity was confirmed by the uptake of modified low-density lipoprotein.

Culture of MCE Cells

MCE cells from three to four rats were pooled into one 60-mm Petri dish. MCE cells were cultured at 37°C under 5% CO_2 in DMEM with 20% FBS. After the cells reached confluency, they were passaged by trypsinization in Dulbeco's phosphate buffered saline containing 0.25% trypsin and 0.02% EDTA. The cells were subsequently

cultured in DMEM supplemented with 10% FBS. For fluorescence studies of pH^{in} with SNARF-1, the cells were inoculated onto 60 mm Petri dishes containing 9× 22-mm cover slips coated with 1.5% gelatin at densities of 1×10^5 cells/dish in the above noted medium until the cells reached confluency. Cells used for experiments were from passages 5-20.

Fluorescence Measurements

Intracellular pH was determined by the fluorescence of SNARF-1 (5-[and-6] carboxy-SNARF-1) as described previously (Martínez-Zaguilán et al., 1991). The dye is membrane permeable in the acetoxymethylester (AM) form, and once in the cell the dye is cleaved by cell esterases to produce the free acid form of the dye which is membrane impermeable. Two cover slips containing cells at confluency were placed into a 60 mm Petri dish with 3.0 ml CPB (pH^{ex} 7.15) and 7.5 μM SNARF-1-AM and incubated at 37°C in 5% CO_2 for 45 minutes on a rocker platform (Cole-Parmer, Vernon Hills, IL). The cells were then rinsed with excess CPB, and further incubated at the pH being studied for 30 minutes at 37°C in 5% CO_2 to ensure complete ester hydrolysis and leakage of uncleaved dye. The two cover slips were placed back to back in a holder perfusion device and perfused at a rate of 3 ml/min and the fluorescence of SNARF-1 was monitored with a SLM-8100/DMX spectrofluorometer (Spectronics Instruments, Rochester, NY) equipped for sample perfusion. The sample temperature was maintained at 37°C by keeping both the water jacket and perfusion media at 37°C. All measurements were performed using 4 nm-bandpass slits and an external rhodamine

standard as a reference. Fluorescence was monitored in continuous acquisition mode by using an excitation wavelength of 534 nm and monitoring emissions at 584, 600, 644 nm as described elsewhere (Martínez-Zaguilán et al., 1991). The fluorescence emission at 584 nm decreases and that at 644 nm increases, respectively, with increasing pH, as such the ratio of 644/584 was used to monitor pH changes. The 600 nm wavelength, which is insensitive to pH, is used to evaluate the efficiency of dye loading, quenching or other artifacts. Fluorescence data were converted to ASCII format for analyses.

Dye Calibration

In situ calibration curves were generated as described previously (Fig. 3.1; Martínez-Zaguilán et al., 1991). Briefly, the cells attached to cover slips were perfused with a high K^+ buffer (pH 5.5 to 8.0) containing 2 μM valinomycin and 6.8 μM nigericin. The high K^+ is used to approximate intracellular K^+ and nigericin sets the H^+ gradient equal to the K^+ gradient, with valinomycin completing the collapse of the K^+ gradient without significant effects on cell volume. The pH of the buffers was determined using a Beckman pH meter with a glass electrode (Corning Inc., Horseheads, NY) calibrated at 37°C with commercially available standard solutions (VWR Scientific, San Francisco, CA.) Using the ratio (644/584) of SNARF it was possible to determine the R values at each pH studied during in situ calibrations. The observed R values were fit into the following equation:

$$pH = pK_a + \log \frac{(R_{obs} - R_{min})}{(R_{max} - R_{obs})}, \qquad \text{Equation [3.1]}$$

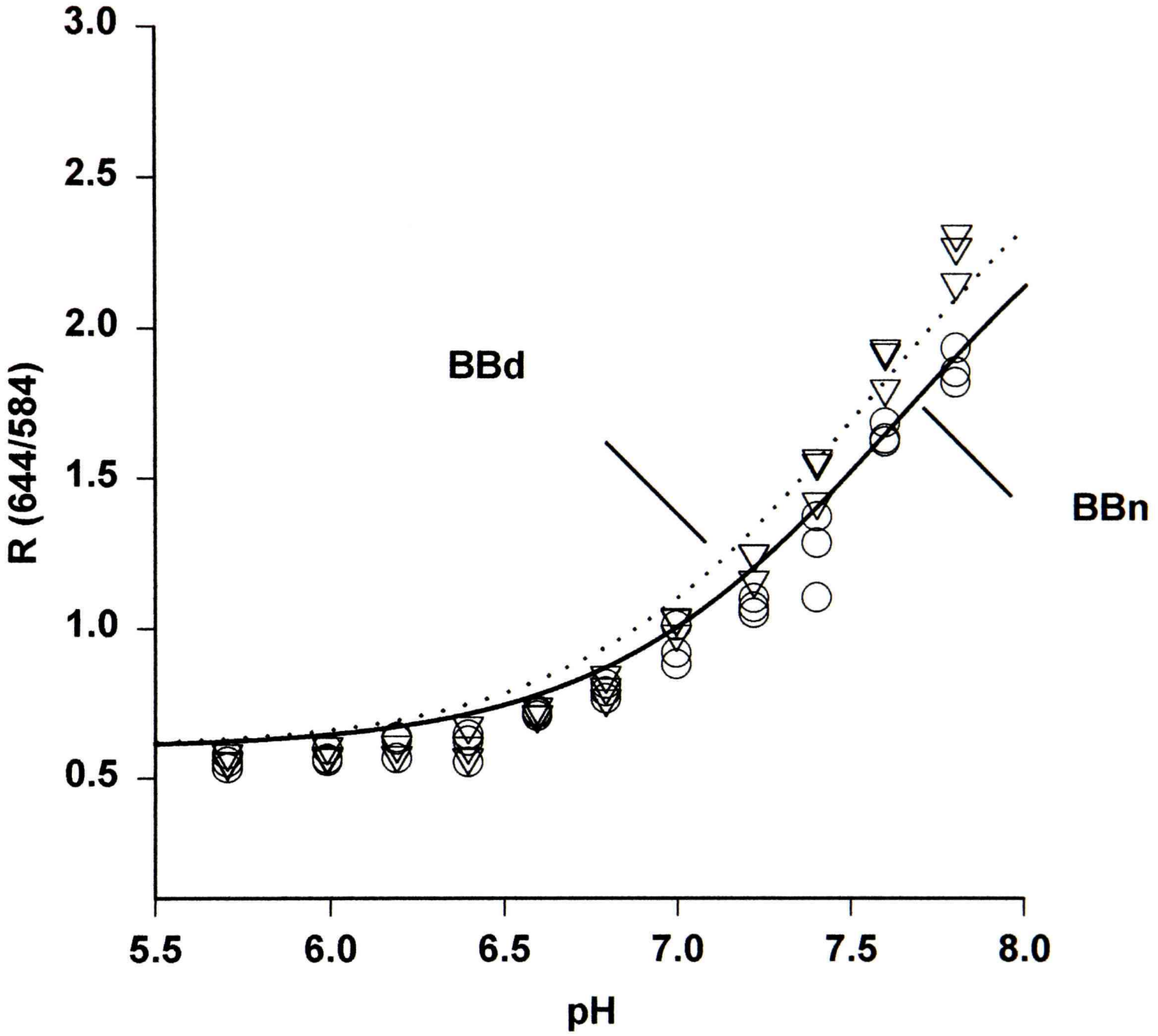

Figure 3.1 In situ calibration curves of normal and diabetic cells reveal the dye behaves similarly in both cell types. BBn (open circles) and BBd (open triangles) cells grown on cover slips were loaded with 7.5 μM SNARF as described in "Materials and Methods". Cells were then incubated in 2.0 μM valinomycin and 6.8 μM nigericin at pH^{ex} values from 5.5 to 8.0, setting $pH^{in} = pH^{ex}$. Fluorescence measurements were then obtained with SLM-8100/DMX spectrofluorometer to yield ratio values (644/584; ex = 534 nm) and equation [3.1] was iteratively solved using nonlinear least squares analysis to yield pK_a, R_{min}, and R_{max} for SNARF in BBn and BBd. Ratio values at each pH^{ex} are the result of 3 to 4 experiments.

where R_{obs} is the ratio observed at any given pH, R_{min} is the ratio observed when the dye is fully protonated, and R_{max} represents the ratio of fluorescence obtained when the dye is fully unprotonated. The equation is solved iteratively using nonlinear least squares analysis (MINSQ, MicroMath Scientific, Salt Lake City, UT) to obtain the values of pK_a, R_{min}, and R_{max} for SNARF-1 in these cells. From these in situ calibration curves, the following parameters were obtained for SNARF in MCEC: BBn $pK_a = 7.845 \pm 0.068$ (SD); $R_{min} = 0.5153 \pm 0.0041$; and $R_{max} = 2.836 \pm 0.231$; BBd $pK_a = 7.822 \pm 0.235$ (SD); $R_{min} = 0.517 \pm 0.0111$; and $R_{max} = 3.00 \pm 0.9859$. These values were not statistically different. These in situ calibration parameters were used to generate the pH^{in} values for each individual experiment by using equation [3.1] with SigmaPlot (Jandel Scientific, San Rafael, CA).

Immunocytochemistry

Monoclonal antibodies to several subunits of V-type H^+-ATPase are available in our laboratory, or from commercial sources (e.g., 60 kDa, 69 kDa, and 100 kDa subunits; Molecular Probes, Eugene, OR). Cross reactivity and immunospecificity has been corroborated in our laboratory by Western blot analysis and we have observed that these antibodies recognize a single band at the appropriate molecular weight (data not shown). For immunocytochemistry, cells are fixed with 4% paraformaldehyde for 15 min, washed with 25 mM Glycine, and then permeabilized with 0.1% Triton X-100. The cells are sequentially incubated with primary antibody, washed extensively, and then incubated with Texas Red-labeled secondary (anti-mouse immunoglobulin G) antibody. Cells were

subsequently incubated with fluorescein-conjugated phalloidin (FITC-phalloidin) which binds to F-actin to delineate the edges of the cells (Lynch et al., 1996). Confocal microscopy images of five randomly selected areas per coverslip from five independent experiments were analyzed. Simultaneously acquired images of FITC-phalloidin (cytoskeleton) and Texas-Red ($V\text{-}H^{+}$-ATPase) were collected and each section was analyzed on a pixel by pixel basis utilizing LaserSharp software (Bio-Rad) to assess colocalization of FITC-phalloidin and Texas-Red at the plasma membrane.

In Vitro Angiogenesis

Plating endothelial cells in Matrigel® has been used as a model to differentiate these cells and induce them to form capillary-like structures (Baatout, 1997). Microvascular endothelial cells from normal and diabetic animals were plated at densities of 1×10^5 in three dimensional gels of Matrigel® (1:1 with DMEM). They were incubated at 37°C and 5% CO_2 for 24 hours. At this time point they were imaged by phase contrast microscopy (IX-70 Olympus) with a 20x objective. Images were obtained with a CCD camera (Photometrics, Phoenix, AZ)

Invasion Assay

Microvascular endothelial cells were grown to confluence in T-25 flasks in DMEM. At confluence the cells were loaded with 5 μM Calcein-AM for 30 minutes. Cells were then trypsinized, washed, and counted. To evaluate the degree of cell invasion through various extracellular matrix proteins (ECMs) in vitro, HTS

FluoroBlok™ (Becton Dickinson, Bridgeport, NJ) inserts were briefly soaked in Matrigel®, seeded at densities of 1×10^5, and incubated at 37°C / 5% CO_2 for 24 hours in the presence or absence of 20 nM bafilomycin. HTS FluoroBlok™ inserts contain a 10 μm proprietary polyethylene terephthalate (PET) membrane impregnated with light absorbing dyes that will absorb visible light from 490-700nm. The inserts were subsequently visualized and images of the bottom and top of the insert obtained with a 20x objective and a Bio-Rad 1024 MRC confocal microscope (Bio-Rad, Hercules, CA) by exciting the fluorophore with the 488 nm line of a 15 mW krypton/argon laser and collecting emission with a photomultiplier tube utilizing the T1/T2 series filter blocks which contain a OG515 emission filter. Five images were obtained per insert of experiments done in triplicate. The images were subsequently analyzed and cells visually counted in defined areas. Percent invasion was corrected for proliferation and calculated by using the following equation:

$$\% \text{ Invasion } = \frac{\text{Total \# invading cells [lower well sample]} / \mu m^2}{\text{Total \# of cells seeded [upper well sample]} / \mu m^2} \times 100. \qquad \text{Equation [3.2]}$$

Data Analysis

The initial rate of recovery from an ammonium chloride induced acid load is measured as dpH/dt, as described previously (Roos and Boron, 1981). Briefly, to determine dpH/dt we looked at recovery of pH in the first five minutes following acid loading. The individual data points are subtracted from the zenith pH at five minutes and

plotted against time. These points where then used to construct a linear regression curve relating time and delta pH. The dpH/dt was expressed as the slope of the linear regression as described previously (Martínez-Zaguilán et al., 1993). The apparent buffering capacity (β_i) is given by (Roos and Boron, 1981):

$$\beta_{i\,(apparent)} = \frac{\Delta [NH_3]^i}{\Delta pH}, \qquad \text{Equation [3.3]}$$

where $\Delta[NH_3]^i$ is assumed to be equal to:

$$\Delta [NH_3]^i = [NH_3]^o \times \frac{10^{(pK - pH^{in})}}{1 + 10^{(pK - pH^{ex})}}, \qquad \text{Equation [3.4]}$$

and ΔpH is the change in pH^{in} from the plateau after the NH_4Cl load and the nadir pH^{in} after NH_4Cl removal. To quantify the pH^{in} recovery, we expressed the recoveries as proton fluxes (J_{H^+}) which is given by:

$$J_{H^+} = \beta_{i\,(apparent)} \times dpH/dt. \qquad \text{Equation [3.5]}$$

Statistical Analysis

Data are expressed as mean ± SE. Data were analyzed by a paired *t*-tests and *ANOVA* where indicated. Statistical significance was assigned at P values of < 0.05.

Results

Steady-state pH^{in} in BBn and BBd MCEC. The pH^{in} regulation in most cells is accomplished by the Na^+/H^+-exchanger and HCO_3 transport systems (Roos and Boron, 1981; Gillies et al., 1992). The relative contribution to overall pH^{in} regulation of these systems in MCE cells is unknown. We evaluated steady-state pH^{in}, which reflects the pH^{in} regulatory mechanisms in concert, by perfusing cells loaded with SNARF-1 at pH^{ex} = 7.15 in a HCO_3^--supplemented media. We determined that pH^{in} was 7.171 ± 0.053 (n = 6) and 7.243 ± 0.068 (n = 6) in BBn and BBd, respectively. To evaluate the contribution of HCO_3^- transport mechanisms in the regulation of pH^{in}, we repeated the experiments in a HCO_3^--free media and observed pH^{in} values of 7.156 ± 0.0187(n=6) and 7.138 ± 0.057 (n=6) in BBn and BBd, respectively. These data indicate that under steady-state condition pH^{in} these differences are not statistically significant between cell types regardless of the presence of HCO_3^- in the media. Because activation of HCO_3^- based H^+ transporting mechanisms may exhibit a pH optimum, we evaluated if the HCO_3^- contribution to steady-state pH^{in} regulation may occur at a particular pH optimum. We performed experiments at pH^{ex} values ranging from 6.5 to 7.4. For these experiments, cells were handled throughout the experiment in a buffer at the pH values being tested in either the presence or absence of HCO_3^-. Thus, cells were in the presence or absence of

HCO_3 for at least 75 minutes before the experiment. Previous studies from our laboratory have indicated that it takes ca. 30 minutes for cells to reach a new steady-state pH after HCO_3 removal/addition (Gillies and Martínez-Zaguilán; 1991). Thus, this period of time is sufficient for equilibration under these experimental conditions. We show that steady-state pH^{in} is not significantly different in the presence or absence of HCO_3 from pH^{ex} 6.5 to 7.4 (Fig. 3.2).

pH^{in} recoveries from acidification in are faster in BBn than in BBd cells. To characterize pH^{in} regulation in these cells, we proceeded with acid loading experiments utilizing the NH_4Cl pre-pulse technique (Roos and Boron, 1981). We employ media containing Na^+ and HCO_3^- to evaluate the contribution of all pH^{in} regulatory mechanisms. Cells loaded with SNARF-1 were perfused with CPB containing HCO_3, at pH^{ex} 7.4, until steady-state was achieved (typically 10 min). The cells were perfused with 25 mM NH_4Cl which causes a rapid intracellular alkalinization. This results from the dissociation of the NH_4Cl into the charged species NH_4^+, Cl^-, and a transient NH_3 species. The NH_3 is membrane-permeable and, once in the cell, rapidly scavenges H^+ causing intracellular alkalinization. The acute removal of NH_4Cl reverses the situation and results in intracellular acidification below baseline. This is followed by a subsequent pH^{in} recovery. The magnitude of the pH^{in} recovery was decreased in BBd compared to BBn (Figs. 3.3A, 3.3B, 3.4A). These cells did not exhibit statistically significant differences in β_i (Fig. 3.4B). Thus, after taking into account β_i, the rates of H^+ extrusion (J_H^+) are also significantly faster in BBn than in BBd (BBn = 1.2 ± 0.145; BBd = 0.48 ± 0.16; $p<0.05$;

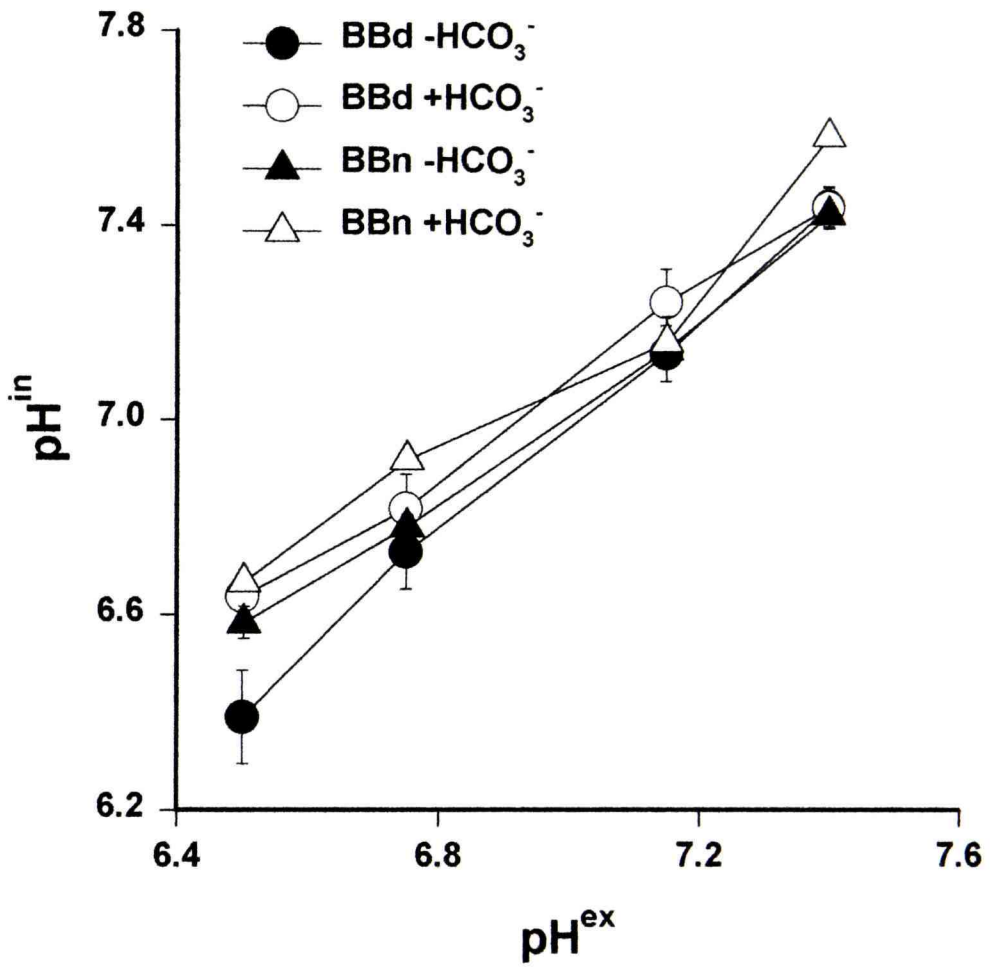

Figure 3.2 Steady-state pH is similar in normal and diabetic cells regardless of the presence or absence of HCO_3^-. BBn and BBd cells grown on cover slips were loaded with 7.5 μM SNARF in the presence (open triangles, BBn; open circles, BBd;) or absence (closed triangles,BBn; closed circles, BBd;) of HCO_3^- at the pH^{ex} being studied as described in "Materials and Methods". The fluorecence ratio values were converted to pH^{in} with equation [3.1]. Each data point is the S.E.M. of 3 to 6 experiments.

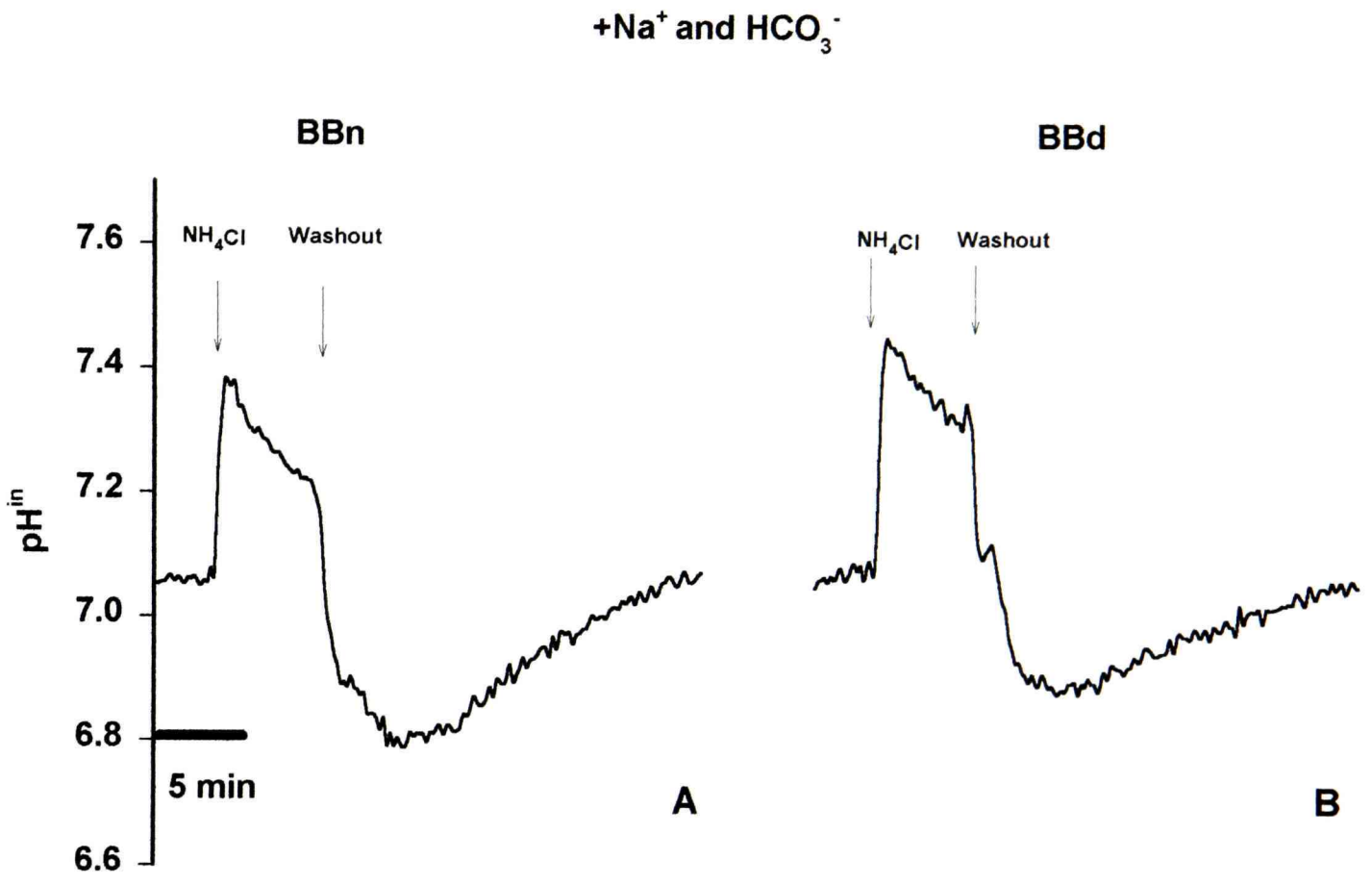

Figure 3.3 NH_4Cl experiments show that in the presence of Na^+ and HCO_3^- normal cells recover faster from an acid load. BBn and BBd cells grown on cover slips were loaded with 7.5 μM SNARF as described in "Materials and Methods". At the first arrow cells were perfused with NH_4Cl. At the time indicated by the second arrow NH_4Cl was removed with CSB containing HCO_3^-. (A) BBn (B) BBd.

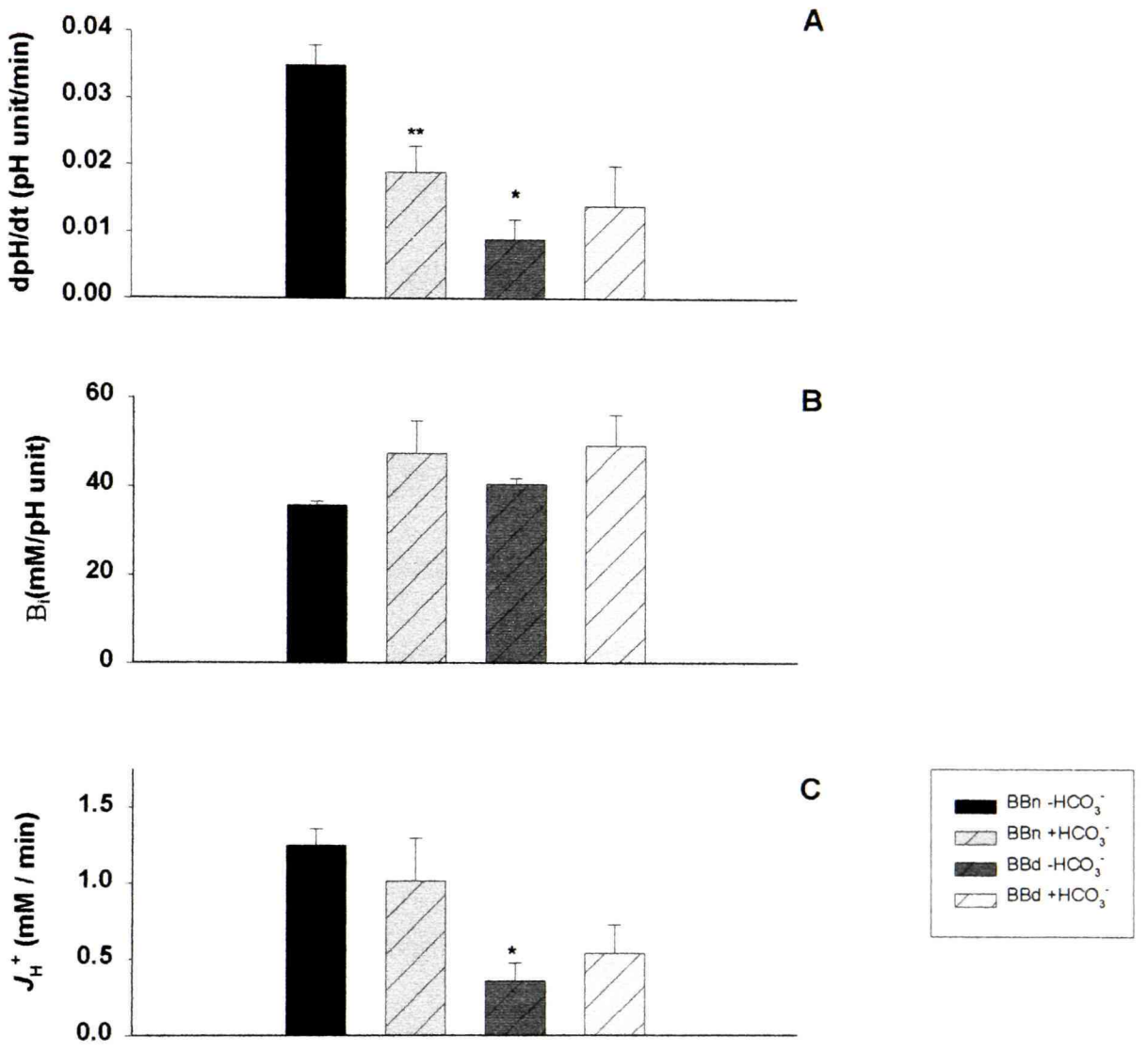

Figure 3.4 Buffering capcity is similar in normal and diabetic cells, yet proton fluxes are two-fold faster in normal cells. BBn and BBd cells grown on cover slips were loaded with 7.5 μM SNARF as described in Fig 3.3. (A) The difference between the zenith recovery at five minutes and each individual data point from the nadir acidification were plotted against time and the slope of that relationship was expressed as dpH/dt. (B) The intrinsic buffering capacity was calculated with equation [3.3]. (C) Proton fluxes were calculated with equation [3.5]. Data are expressed as SE.M. $P<0.05$ compared by pair-wise one-way *ANOVA*. *BBn versus BBd, **BBn + HCO_3^- versus BBn - HCO_3^-.

Fig. 3.5C). This recovery reflects the contribution of all pH^{in} regulatory mechanisms. This difference in J_H^+ in the presence of Na^+ and HCO_3^- could be due to either abnormalities in the Na^+/H^+-exchanger or HCO_3^- -transporting mechanisms. We proceeded with ion-substitution experiments on removal of NH_4Cl in an attempt to dissect out the contribution of these pH^{in} regulatory mechanisms to the observed differences in pH recovery. In the absence of HCO_3^- both the BBn and BBd exhibited a recovery (J_H^+) that was significantly faster in BBn than in BBd. However, these data are not significantly different than those observed in the presence of both Na^+ and HCO_3 (J_H^+: BBn = 1.25 ± 0.11; BBd = 0.36 ± 0.12), suggesting that the and HCO_3 transport mechanisms were not important for this recovery. To further demonstrate that Na^+/H^+ exchanger and HCO_3 transport mechanisms were not responsible for the recovery, we performed similar types of experiments with DIDS (a HCO_3 transport inhibitor) and amiloride (a Na^+/H^+- exchange inhibitor). Our data indicated that neither of these inhibitors alter the rates of H^+ extrusion observed in the presence of Na^+ and HCO_3, suggesting that neither Na^+/H^+-exchange nor HCO_3 transport systems are responsible for these pH^{in} recoveries (data not shown).

BBn exhibit a Na^+- and HCO_3^- - independent pH^{in} recovery. To determine if the recovery was attributed to the V-H^+-ATPase, we performed acid loading experiments in a Na^+- and HCO_3^--free buffer which resulted in recoveries that were faster in BBn than in BBd (J_H^+: BBn = 1.25 ± 0.11; BBd = 0.36 ± 0.12; Figs. 3.5A, 3.5B, 3.5C). We then evaluated the effect of bafilomycin on this Na^+- and HCO_3^- - independent pH^{in} recovery. The reported K_I for bafilomycin is 5 nM and we observed inhibition by preincubation in

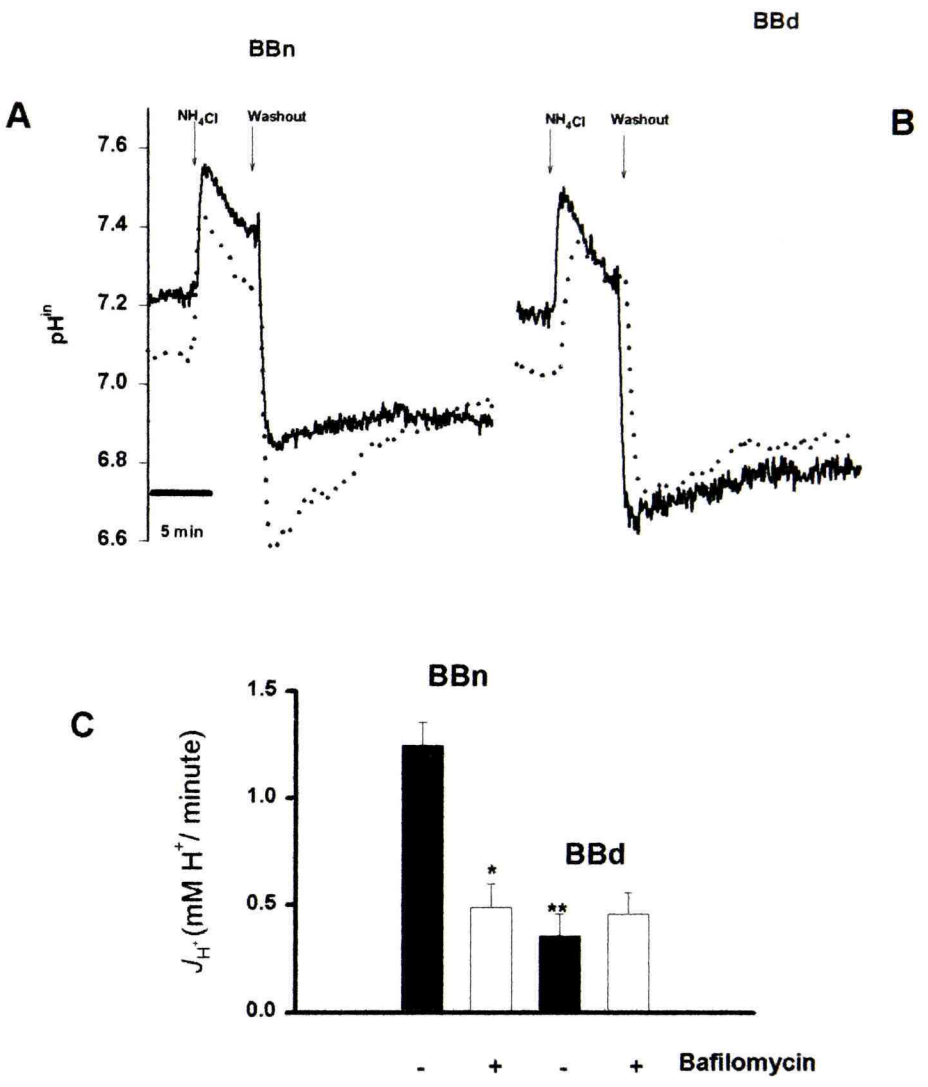

Figure 3.5 Normal microvascular endothelial cells exhibit a Na^+ and HCO_3^- -independent recovery from acid loads that is inhibited by bafilomycin. BBn and BBd cells loaded with 7.5 μM SNARF were pre-incubated and treated with 10 nM bafilomycin throughout experiment. At the second arrow NH_4Cl was removed with Na^+- and HCO_3^-- free CSB. (A) BBn + Bafilomycin (solid line), BBn control (dotted line) (B) BBd + Bafilomycin (solid line), BBd control (dotted line). (C) J_H^+ data derived from experiments similar to those performed in (A) & (B). Data are expressed as S.E.M. $P<0.05$ compared by pair-wise one-way *ANOVA*. * BBn control versus BBn treated with bafilomycin. ** BBn control versus BBd.

10 nM bafilomycin. These experiments resulted in acidification and suppresion of the recovery in BBn cells (J_H^+: BBn = 0.49 ± 0.11; BBd = 0.46 ± 0.10 (Figs. 3.5A. 3.5B, 3.5C). The use of P-type H^+-ATPase inhibitors at concentrations above the reported K_i for the H^+/K^+-ATPase inhibition had no effect on the observed recoveries (data not shown).

V-H^+-ATPase immunocytochemistry in BBn and BBd. V-H^+-ATPase activity responsible for pH^{in} recovery in the absence of Na^+ and HCO_3 is associated with plasma membrane distribution. We performed immunocytochemistry experiments on permeabilized MCE cells to determine if BBn expressed this distribution. Monoclonal antibodies for the 60 and 69 kDa subunits of the V-H^+-ATPase revealed a punctuated cytosolic distribution in BBn and BBd (Figs. 3.6A,3.6B). This is in agreement with the recognized distribution of H^+-ATPase in intracellular compartments (e.g., endosomes, lysosomes, ER, golgi). Using computer software to assess colocalization on a pixel by pixel basis it was observed that BBn exhibited pmV-ATPase (arrows). BBd only occasionaly show pmV-ATPase distribution (Figs. 3.6C, 3.6D) BBn cells treated cells: however note the colocalization at the plasma membrane (Fig. 3.6B, Arrows).

BBn display capillary-like structures in Matrigel® that are absent in BBd. It was observed that BBn readily form capillary-like structures in Matrigel®. In as little as two hours they begin to extend lamellipodia-like structures (data not shown) and in twelve

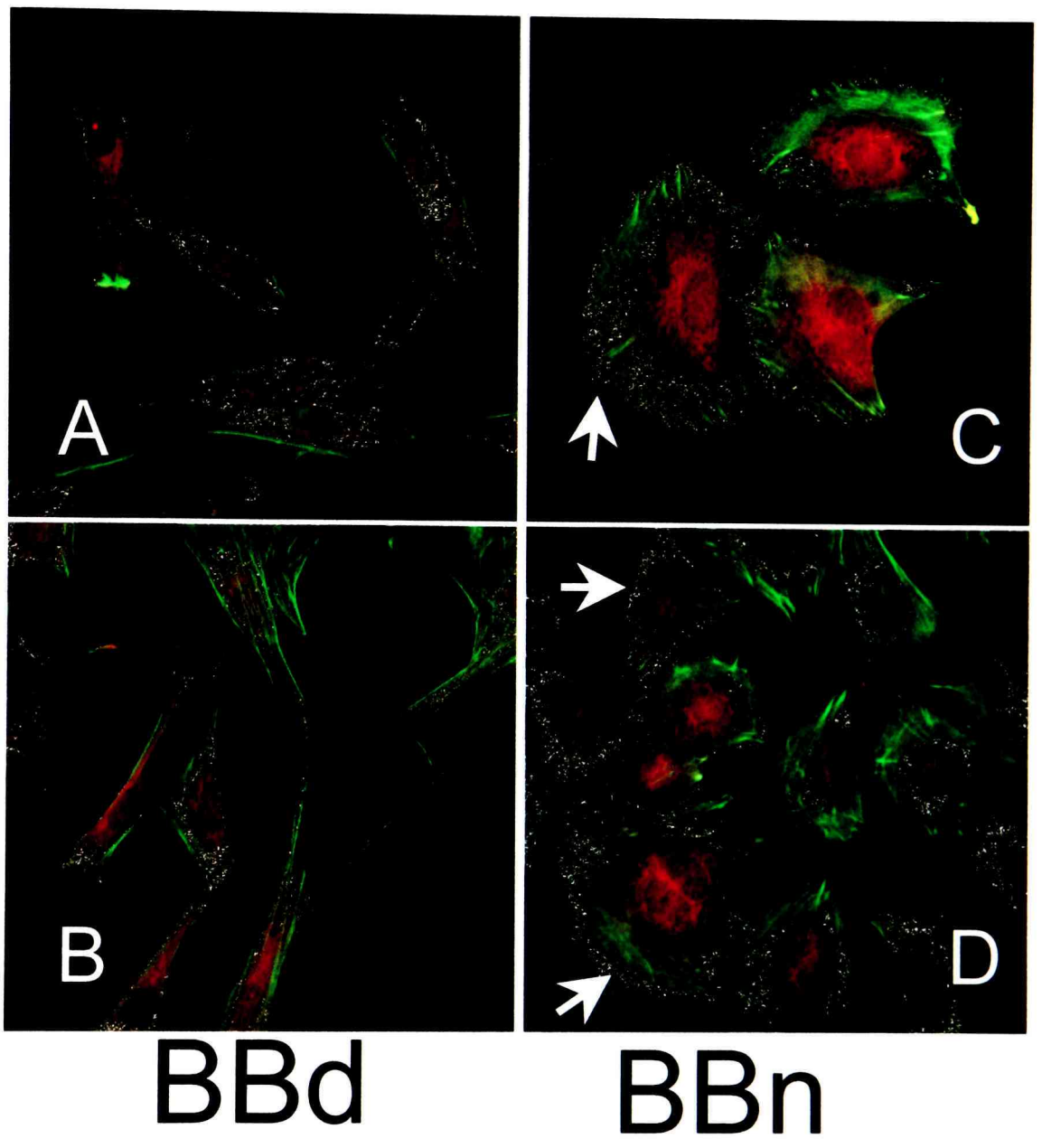

Figure 3.6 Immunocytochemistry reveals a plasma membrane distribution of V-ATPase in normal microvascular endothelial cells. BBn and BBd cells were grown of glass cover slips, subsequently fixed, permeabilized, and incubated with primary monoclonal antibodies for 60 or 69 kDa subunits of V-H^+-ATPase described in "Materials and Methods." Cytoskeleton is stained with FITC- phalloidin, shown in green. (A, B) BBd show cytoplasmic distribution. White dots indicate area of red and green colocalization. (C,D)BBn.

hours form networks of capillary-like structures (Fig. 3.7A). Interestingly, BBd for the most part remain rounded up and do not readily form these structures. Occasionally BBd will exhibit lamellipodia-like structures and invade (Fig. 3.7B)

BBn invasion of Matrigel® membranes is bafilomycin sensitive. In an effort to better quantify invasion we utilized Fluoroblok inserts coated with Matrigel® and assesed the invasion of endothelial cells after twenty-four hours. BBn readily invaded the membrane (Figs. 3.8A, 3.8B) while the BBd did not (Figs. 3.8C, 3.8D). The invasion by BBn could be completely inhibited by 20 nM bafilomycin (Figs. 3.8E, 3.8F).

Discussion

Long-term complications of diabetes include alterations in the process of angiogenesis as observed by conditions such as poor wound healing (Servold, 1991). Diabetes is a condition of altered glucose metabolism that can result in metabolic acidosis if untreated. It is unknown if this affects tissue pH chronically. Since the endothelial cells of the microvasculature are continually exposed to the acid load produced by surrounding tissue, it would be predicted that in diabetes these cells would have altered pH^{in} regulatory mechanisms. The pH^{in} regulation in most eucaryotic cells is believed to be

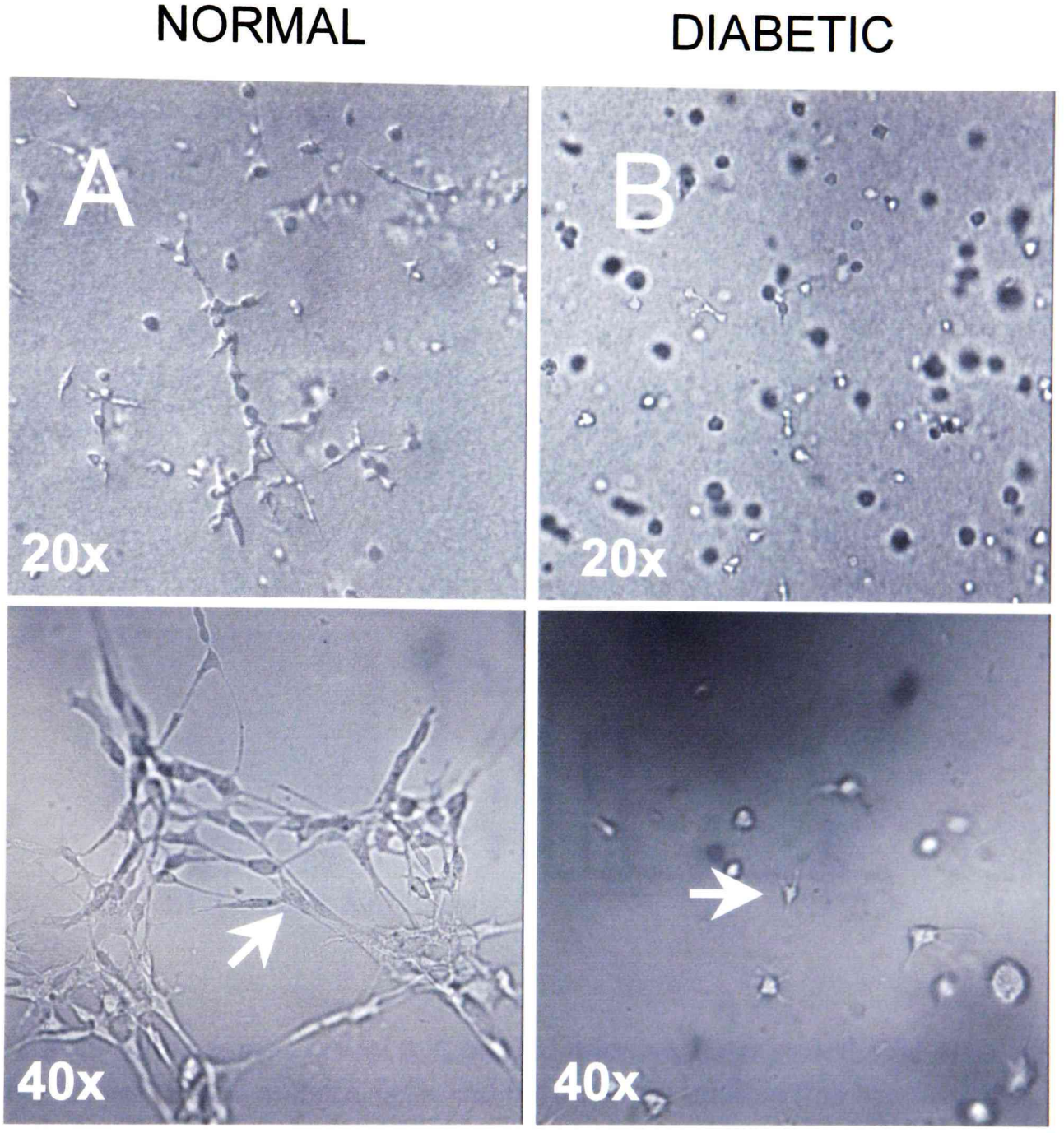

Figure 3.7 Microvascular endothelial cells from diabetic animals can not form capillary-like structures in an in vitro angiogenesis model. Microvascular endothelial cells were plated in 3-D gels of Matrigel® at densities of 1×10^5 and allowed to incubate at 37°C / 5% CO_2 for 24 hours. Images were obtained with phase contrast microscopy and collected with a CCD camera. (A) BBn; 20x top view; 40x bottom view; arrows show capillary-like structures. (B) BBd, note the absence of capillary-like structures; arrows show- few lamellipodia after 24 hours culture.

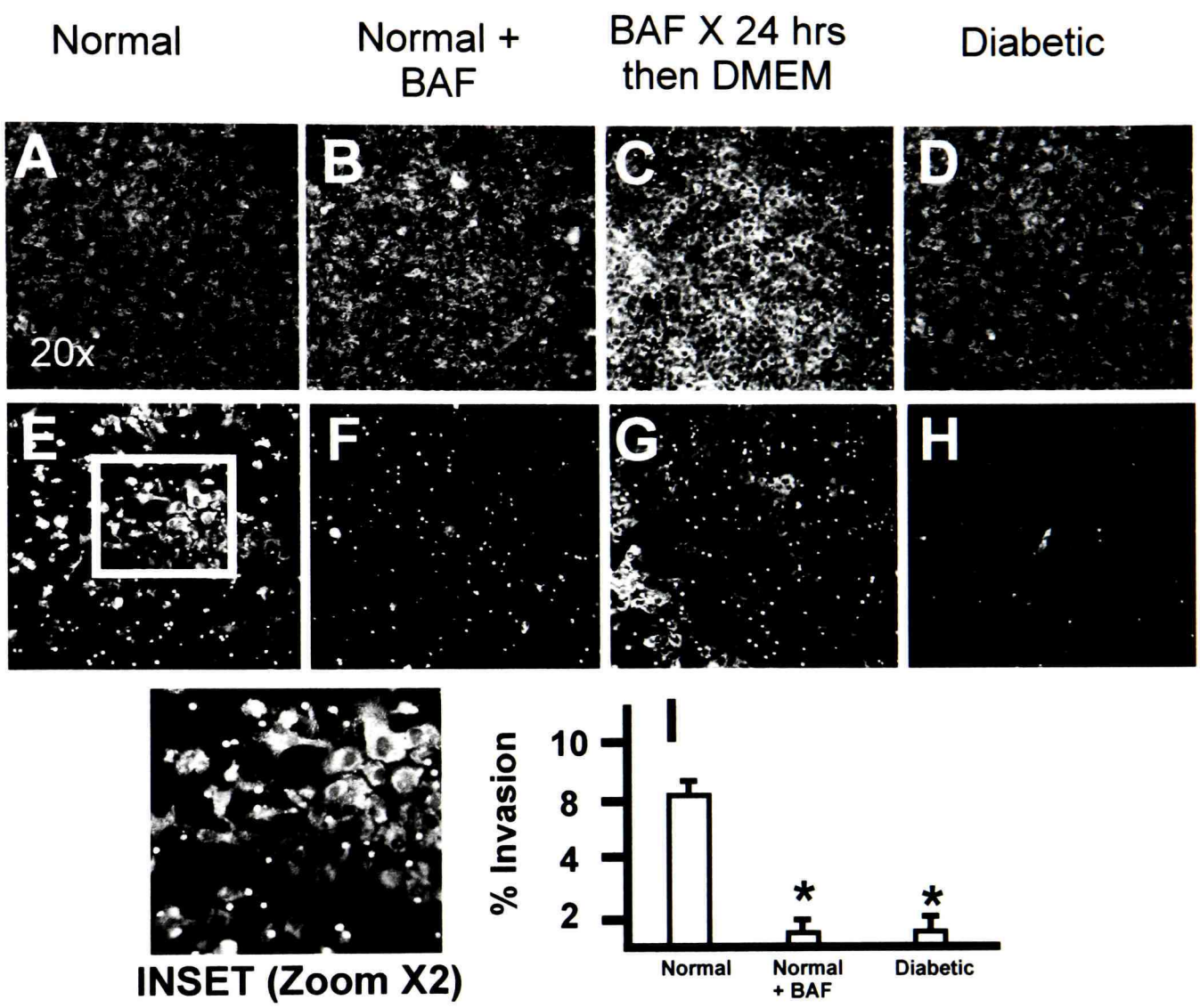

Figure 3.8 Invasion assays reveal that normal microvascular endothelial cells are four-fold more invasive than diabetic cells and bafilomycin inhibits this invasiveness. Cells were loaded with 5 μM Calcein-AM, plated onto 10 μm FluoroBlok™ inserts coated with Matrigel® and incubated for 24 hrs. Cells were visualized by confocal microscopy (20x; Ex = 488 nm; Em = 515 nm). The images were captured from either the top or the bottom of the insert. (A) BBn -top; untreated. (B) BBn -top; untreated. (C) BBn - top; treated for 24 hours in BAF and subsequently returned to DMEM for 24 hours. (D) BBd - top; untreated. (E) BBn - bottom; untreated (F) BBn bottom; treated. (G) BBn - bottom; treated as in (C). (H) BBd bottom; untreated. Inset in (E) magnified 2x. (I) Quantification of data obtained from experiments representative of those in A-H using Eqn 3.2. $P < 0.05$ compared by one-way *ANOVA* versus normal.

the result of the Na^+/H^+ exchanger and the various HCO_3^- -mechanisms (Roos and Boron, 1981; Gillies et al., 1992). Some specialized cells also utilize pm-V-H^+-ATPase as a pH regulatory mechanism. We have previously described pm V-H^+-ATPase activity in tumor cells and observed that this activity was related to increased invasiveness (Martínez-Zaguilán et al., 1993). The common theme of invasiveness in metastasis and the specialized function of macrophages, neutrophils, and osteoclasts suggest that pm V-H^+-ATPase activity is important for the acquisition of a more invasive phenotype. Because the process of angiogensis involves invasion of the adjacent extracellular matrix by microvascular endothelial cells we hypothesized that these cells would exhibit pm V-H^+-ATPase activity.

In this study we evaluated the pH^{in} regulatory mechanisms in microvascular endothelial cells from an animal model of spontaneous diabetes. It has been suggested that cellular ion transport is altered in diabetes, in particular the Na^+/H^+ exchanger (Salles et al., 1991; Koren et al., 1997; Ng et al., 1992; Davies et al., 1992) has been proposed to be affected. Studies of pH^{in} regulation in micro- and macrovascular endothelial cells from various species, and organs have indicated that they exhibit amiloride-sensitive Na^+/H^+ exchange (Kitazono et al., 1988; Escobales et al., 1990; Cutaia and Parks, 1994); Na^+-dependent HCO_3^-/Cl^- exchange (Hsu et al., 1996); Na^+-independent HCO_3^-/Cl^- exchange (Jentsch et al., 1988; Ziegelstein et al., 1992); and the electrogenic Na^+/HCO_3 symporter (Jentsch tet al., 1988). If our hypothesis were correct then microvascular endothelial cells from non-diabetic animals would express pm V-H^+-ATPase activity while those from diabetic animals would express decreased or no activity. To insure that

any differences we noted in fluorescence of our pH indicator were not attributed to distinct cytosolic differences in each cell type (e.g., viscosity) we performed in situ calibrations. These experiments revealed that there were no significant differences in the in situ calibration parameters used to estimate pH^{in} between BBn and BBd. It is generally accepted that the maintenance of pH^{in} is accomplished by the contribution of HCO_3^- transport and the Na^+/H^+-exchanger. Thus, if pH^{in} regulation were to be different between these cells it might be manifest by differences in steady-state pH^{in} in the presence or absence of Na^+ or HCO_3^-. At a pH^{ex} of 7.4 we did not observe differences in steady-state pH^{in} in the presence or absence of HCO_3^- (cf. Fig. 3.2). Since it has been suggested that the different pH^{in} regulatory mechanisms exhibit distinct pH optima (Ziegelstein et al., 1992), this observation did not conclusively prove that pH^{in} regulation in steady-state was not different. We then proceeded to evaluate pH^{in} in the presence and absence of HCO_3^- from pH^{ex} 6.5 to 7.4 (cf. Fig. 3.2). Again we observed no differences in steady-state pH^{in}. Although this suggested that the HCO_3^- -transporting mechanisms were not important in maintaining steady-state pH, it is possible that HCO_3^--transport is important in acute conditions of acid loading.

In order to determine if there were differences in response to acid loads, we compared the response of BBn and BBd to acid loads induced by NH_4Cl. The recovery from acid loads was evaluated in the presence of Na^+ and HCO_3^- and it was observed that the BBn exhibited a recovery that was two-fold greater than BBd (cf. Figs. 3.3, 3.4). Since this recovery was the result of all pH^{in} regulatory mechanisms, and it has been suggested that the Na^+/H^+-exchanger is altered in diabetes (Salles et al., 1991; Koren et

al., 1997; Ng et al., 1992; Davies et al., 1992), we decided to evaluate the recovery from an acid load in the absence of Na^+ and HCO_3^-. Our reasoning was that if the Na^+/H^+-exchanger or HCO_3^--transport were responsible for the differences in recovery, then ionic substitution should result in the BBn and BBd exhibiting similar responses to acid loads. We observed that in the absence of Na^+ and HCO_3^- the BBn and BBd exhibited recoveries similar to that in the presence of Na^+ and HCO_3^- that were still greater in the BBn (cf. Figs. 3.5A, 3.5B).

This Na^+ and HCO_3^-- independent recovery could be attributed to active transport, such as V- or P- type ATPases. These ATPases are distinguished by pharmacologic inhibition (Bowman et al., 1988; Mendlein and Sachs, 1990). P-type ATPases are inhibited by SCH 28080, at a reported K_i of 5 μM, which has no effect on V-type ATPases (Bowman et al., 1988; Mendlein and Sachs, 1990; Forgac, 1999). Similarly, V-type ATPases are inhibited by bafilomycin at a reported K_i of 5 nM, which has no effect on P-type ATPases (Bowman et al., 1988; Mendlein and Sachs, 1990; Forgac, 1999). We then repeated the acid loading experiments in the absence of Na^+ and HCO_3^- while pre-incubating the cells with 10 nM bafilomycin. This resulted in complete inhibition of the recovery in BBn (cf. Fig. 3.5A). Although the ion substitution experiments and the pharmacologic inhibition were conclusive in showing that the observed pH^{in} recovery was attributed to V-H^+-ATPase activity, they do not indicate that this activity is at the plasma membrane. To provide evidence for this, we performed immunocytochemistry. These experiments reveal that monoclonal antibodies to the 60 and 69 kDa subunits of the V-H^+-ATPase localized in a predicted cytosolic pattern in both BBd and BBn (cf. Figs.

3.6A, 3.6B, respectively). Importantly, there was a distinct plasma membrane distribution in the BBn that is not as evident in BBd (cf. Fig. 3.6D). To determine if the pmV-ATPase activity were related to invasiveness, BBn and BBd cells were plated in an in vitro model of angiogenesis. It was noted that BBn invaded their surrondings and readily formed capillary-like structures. Although, qualitatively there was a remarkable difference in the behavior of BBn and BBd it proved difficult to quantify the degree of invasion in each cell type. In order to quantify the invasiveness of BBn and BBd we employed Fluoroblok™ inserts coated with Matrigel®. We evaluated the degree of invasion as a percentage of cells that were able to invade to the bottom of the insert. By this approach BBn were three- to five-fold more invasive than BBd. Treatment of BBn with 20 nM bafilomycin had no cytotoxic effect on cells yet completely block their invasion. These data provide evidence that pm V-H^+-ATPase is decreased in BBd. The presence of pm V-H^+-ATPase in normal cells and its absence in diabetic cells demonstrates differences in invasiveness/angiogenic capability of these cells. Inhibition of pmV-ATPase renders BBn as non-invasive as BBd. Altogether this provides evidence that these differences could be responsible for some of the angiopathies seen in diabetes.

CHAPTER IV

PLASMALEMMAL V-H^+-ATPASES AS A NOVEL INTRACELLULAR pH REGULATOR IN HUMAN LUNG MICROVASCULAR ENDOTHELIAL CELLS[3]

We had shown pmV-ATPase activity in microvascular endothelial cells from coronary circulation and had suggested that the activity was important for invasion. In Chapter III, we show that microvascular cells from a spontaneous model of diabetes lack pmV-ATPase activity and are not invasive. This data supported our hypothesis that pmV-ATPase activity was important for invasion since a complication of diabetes is decreased wound healing and decreased angiogenesis. We reasoned that all vascular beds that undergo angiogenesis should express pmV-ATPase activity. Hsu et al. had done studies of pH^{in} regulation in microvascular endothelial cells from a porcine model but their data do not show Na^+ -andHCO_3^--independent recoveries. We were puzzled by this but felt that the discrepancy might be explained by species or tissue difference. Another possibility could be that the isolation of endothelial cells resulted in cells from larger vessels being harvested. Hsu et al. utilized cerebral cortex as a starting point and it would

---

[3]Forthcoming

[a]José D. Rojas, [a]Gloria M. Martínez, [a]Geraldine B. Tasby, [a,b]Donald E. Wesson, and [a,c]Raul Martínez-Zaguilán

Departments of [a]Physiology and [b]Internal Medicine Texas Tech University Health Sciences Center, and [c]Southwest Cancer Center, Lubbock, Texas, 79430.

be predicted that the vessels in this tissue would be mostly capillaries; however, the prep could have been contaminated with other cell types. It would be predicted that angiogenesis would readily occur in the cortex; however, it is possible that this tissue does not undergo much angiogenesis, however this did not seem likely since the source was newborn piglet. In an attempt to examine the tissue and species issue of pmV-ATPase actiivity, we evaluated pH^{in} regulation of human microvascular endothelial cells. The pulmonary microvasculature is known to undergo extensive vascular remodeling on exposure to hypoxia. This vasculature is also important in acid-base regulation and as such CO_2 is continually transported through this vascular bed, thus for these reasons we predicted that if our hypothesis were true this tissue would also exhibit pmV-ATPase as a dynamic pH^{in} regulatory mechanism.

Abstract

Continuous CO_2 transit that without adequate extrusion mechanisms subjects lung endothelium layer to a substantial acid load could be detrimental to cell function. The Na^+/H^+ exchanger and HCO_3^- -dependent mechanisms regulate intracellular pH (pH^{in}) in most cells, but those that must cope with such high acid loads might require additional primary energy-dependent mechanisms. We hypothesized that human lung microvascular endothelial (HLMVE) cells constitutively use a primary H^+-transporting mechanism in addition to Na^+/H^+ exchange and HCO_3^- mechanisms to maintain pH^{in} homeostasis. Acid loaded HLMVE cells exhibited proton fluxes in the absence of Na^+ and HCO_3^- that were forty percent lower than those observed in the presence of Na^+- and HCO_3 . This Na^+-

and HCO_3 -independent pH^{in} recovery was inhibited by bafilomycin A_1, a selective V-H^+-ATPase inhibitor. Immunocytochemical studies with antibodies against subunits of the V-H^+-ATPase revealed plasma membrane localization, in addition to the predicted distribution in vacuolar compartments. These studies show a Na^+ and HCO_3^- -independent pH^{in} regulatory mechanism in HLMVE cells that is mediated at least in part by plasma membrane V-H^+-ATPases (pm V-ATPases).

Introduction

The microvascular endothelium regulates many tissue functions including blood flow (Henrich, 1991; Mehta, 1995). Blood flow regulation is mediated in part by tissue metabolic demands (Belloni, 1979). This metabolism changes extracellular pH and CO_2, affecting microvascular endothelial cells and leading to generation/secretion of vaso-active substances (e.g., nitric oxide, endothelin) that modulate blood flow to meet metabolic demands (Henrich, 1991; Mehta, 1995). Lung microvasculature is exposed to high levels of CO_2 which pass through it before exiting through the alveoli (West, 1998). Increasing CO_2 increases cellular acid and challenges the cells' pH regulatory mechanisms (Roos and Boron, 1981). Since ventilatory regulation can change from minute to minute (West, 1998) and thus affect pH^{in} in microvascular endothelial cells, both hyper- and hypoventilation can result in an acid load to the microvascular endothelium. This can result from stasis of CO_2 in hypoventilation and from increased CO_2 flux through the endothelium in hyperventilation. It has been shown that pulmonary blood flow can be altered by hypo- and hypercapnia, although the mechanisms are

uncertain (Viles and Shephard, 1968; Shirai et al., 1986; Yamaguchi et al., 1998). Very little is known of the pH^{in} regulatory mechanisms in this microvascular endothelium. pH^{in} regulation in most endothelial cells is mediated by the Na^+/H^+ exchanger and HCO_3^- transporting mechanisms (Jentsch et al., 1988; Escobales et al., 1990; Ziegelstein et al., 1992; Cutaia and Parks, 1994; Hsu et al., 1996). In other cell types, studies support that the Na^+/H^+ exchanger is important in regulating pH^{in} below its reported set point of 7.2 and that HCO_3^--transporting mechanisms are the predominant pH^{in} regulatory mechanisms at pH values above 7.2 (Roos and Boron, 1981; Olsnes et al., 1986; Kurtz and Golchini, 1987; Gillies and Martínez-Zaguilán, 1991). The Na^+/H^+ exchanger utilizes the inwardly-directed Na^+ gradient to extrude protons leading to intracellular alkalinization (Roos and Boron, 1981; Jentsch et al., 1988; Escobales et al., 1990; Ziegelstein et al., 1992; Cutaia and Parks, 1994; Hsu et al., 1996; Gillies and Martínez-Zaguilán, 1991). This mechanism is pharmacologically inhibited by amiloride and its derivatives (Roos and Boron, 1981; Jentsch et al., 1988; Escobales et al., 1990; Ziegelstein et al., 1992; Cutaia and Parks, 1994; Hsu et al., 1996; Gillies and Martínez-Zaguilán, 1991). The various HCO_3 transport mechanisms include Na^+ -dependent and -independent Cl^-/HCO_3^- exchange, Cl^- -independent Na^+/HCO_3^- cotransport, and Cl^- channel mediated HCO_3^- transport (Roos and Boron, 1981; Olsnes et al., 1986; Kurtz and Golchini, 1987; Gillies and Martínez-Zaguilán, 1991). These mechanisms transport HCO_3^- by coupling its movement to other ions, in such a way to cause cellular acidification in some circumstances and alkalinization in others. All are inhibited by stilbene disulfonate derivatives (Roos and Boron, 1981; Olsnes et al., 1986; Kurtz and

Golchini, 1987; Gillies and Martínez-Zaguilán, 1991). All cells are sensitive to CO_2 because the CO_2 hydration/dehydration leads to changes in [HCO_3^-]. Because lung microvascular endothelium is exposed to ever changing CO_2 and thereby pH^{in} that might be detrimental to cell function, human lung microvascular endothelial (HLMVE) cells might exhibit CO_2 -independent pH^{in} regulatory mechanisms. We hypothesize that HLMVE cells utilize plasma membrane V-H^+-ATPases (pmV-ATPases) to contribute to pH^{in} regulation.

Methods

Cell Culture

HLMVE cells were obtained from Clonetics (San Diego, CA) proliferating in culture flasks at 4th passage and used through passage 10. HLMVE cells were cultured at 37°C under 5% CO_2 in endothelial cell growth medium (EGM® from Clonetics). After the cells reached confluency, they were passaged by trypsinization in Dulbeco's phosphate buffered saline containing 0.25% trypsin and 0.02% EDTA. For fluorescence experiments, cells were seeded at densities of 1×10^5 onto 60 mm Petri dishes containing 9× 22-mm cover slips and used at confluency.

Media, Buffers, and Chemicals

Cell perfusion buffer (CPB) consists of 110 mM NaCl, 1.3 mM $CaCl_2$, 1 mM $MgSO_4$, 5.4 mM KCl, 0.44 mM KH_2PO_4, 0.35 mM NaH_2PO_4, 5 mM glucose, 2 mM glutamine, and 25 mM HEPES and pH adjusted to 7.15, unless otherwise noted (16). Na^+-free CPB consists of all CPB ingredients, except those containing sodium. NaCl is substituted by 110 mM N-methyl-glucamine. CPB solutions containing HCO_3^- were bubbled with 5% CO_2 at 37°C for 45 minutes. The concentration of HCO_3^- was determined by the equation:

$$[HCO\ ] = (1.52\ mM) \times 10^{(pH - 6.24)}, \qquad \text{Equation [4.1]}$$

where 1.52 mM is the concentration of CO_2 in CPB at 37°C and 6.24 is the pK_a for the process of CO_2 hydration (Gillies et al., 1990). High K^+ buffer contains 146 mM KCl, 20 mM NaCl, 5 mM glucose, 2 mM glutamine, 10 mM HEPES, 10 mM MES, and 10 mM Bicine. The rationale for using these organic buffers is to allow for precise buffering across a wide pH range because they exhibit distinct pK_a at 37°C (MES = 6.0, HEPES = 7.4, Bicine = 8.0). The fluorescent dyes were obtained from Molecular Probes (Eugene, OR). Bafilomycin A_1 was purchased from Wako Chemicals (Richmond, VA). All other chemicals were obtained from Sigma Chemical (St. Louis, MO) unless otherwise stated.

Fluorescence Measurements

Intracellular pH was determined by the fluorescence of BCECF-AM (2′,7′-bis-(2-carboxyethyl)-5-(and-6)-carboxyfluorescein, acetoxymethyl ester) as described previously (Gillies et al., 1990). The dye is membrane permeable in the acetoxymethyl ester (AM) form, and once in the cell the dye is cleaved by cell esterases into the free acid form of the dye which is membrane impermeable. Two cover slips containing cells at confluency were placed into a 60 mm Petri dish with 3 ml CPB (pH^{ex} 7.15) and 2 μM BCECF-AM and incubated at 37°C in 5% CO_2 for 45 minutes. The cells were then washed with excess CPB, and further incubated in dye-free CPB at the pH being studied for 20 minutes at 37°C in 5% CO_2 to ensure complete ester hydrolysis and leakage of uncleaved dye. The two cover slips were placed back to back in a holder and perfused at a rate of 3 ml/min and the fluorescence of BCECF was monitored with a DMX-1000 spectrofluorometer (Spectronic Instruments, Rochester, NY) equipped with a thermostated cuvette holder. The sample temperature was maintained at 37°C by keeping both the water jacket and perfusion media at 37°C. All measurements were performed using 4 nm-bandpass slits and an external rhodamine standard as a reference. Fluorescence was monitored in continuous acquisition mode by using excitation wavelengths of 450 nm and 500 nm monitoring emissions at 529 nm as described elsewhere (Gillies et al., 1990). The excitation wavelength at 500 nm is pH sensitive and

increases with increasing pH, while the 450 nm wavelength is near the isoexcitation point and is relatively pH-insensitive, thus the ratio of emission intensity (500/450) at 529 nm increases with increasing pH, and was used to monitor pH changes. Fluorescence data were converted to ASCII format for manipulation and analysis.

Dye Calibration

In situ calibration curves were generated as described previously (Fig. 4.1; Gillies et al., 1990). Briefly, the cells attached to cover slips were perfused with a high K^+ buffer containing 2 μM valinomycin and 6.8 μM nigericin. The high K^+ is used to approximate intracellular K^+ and nigericin sets the H^+ gradient equal to the K^+ gradient, with valinomycin completing the collapse of the K^+ gradient without significant effects on cell volume (Gillies et al., 1990). The cells were then perfused with buffers ranging in pH^{ex} from 5.5 to 7.8. The pH of the buffers was determined using a Beckman pH meter with a glass electrode (Corning, Horsehead, NY) calibrated at 37°C with commercially available standard solutions (VWR Scientific, San Francisco, CA). Using the ratio (500/450) of BCECF we determined the R values at each pH^{ex} studied during in situ calibrations (cf. Fig. 22). The observed R values were fitted into the following equation:

$$pH = pK_a + \log\frac{(R_{obs} - R_{min})}{(R_{max} - R_{obs})}, \qquad \text{Equation [4.2]}$$

where R_{obs} is the ratio observed at any given pH, R_{min} is the ratio observed when the dye is fully protonated, and R_{max} represents the ratio of fluorescence obtained when the dye is

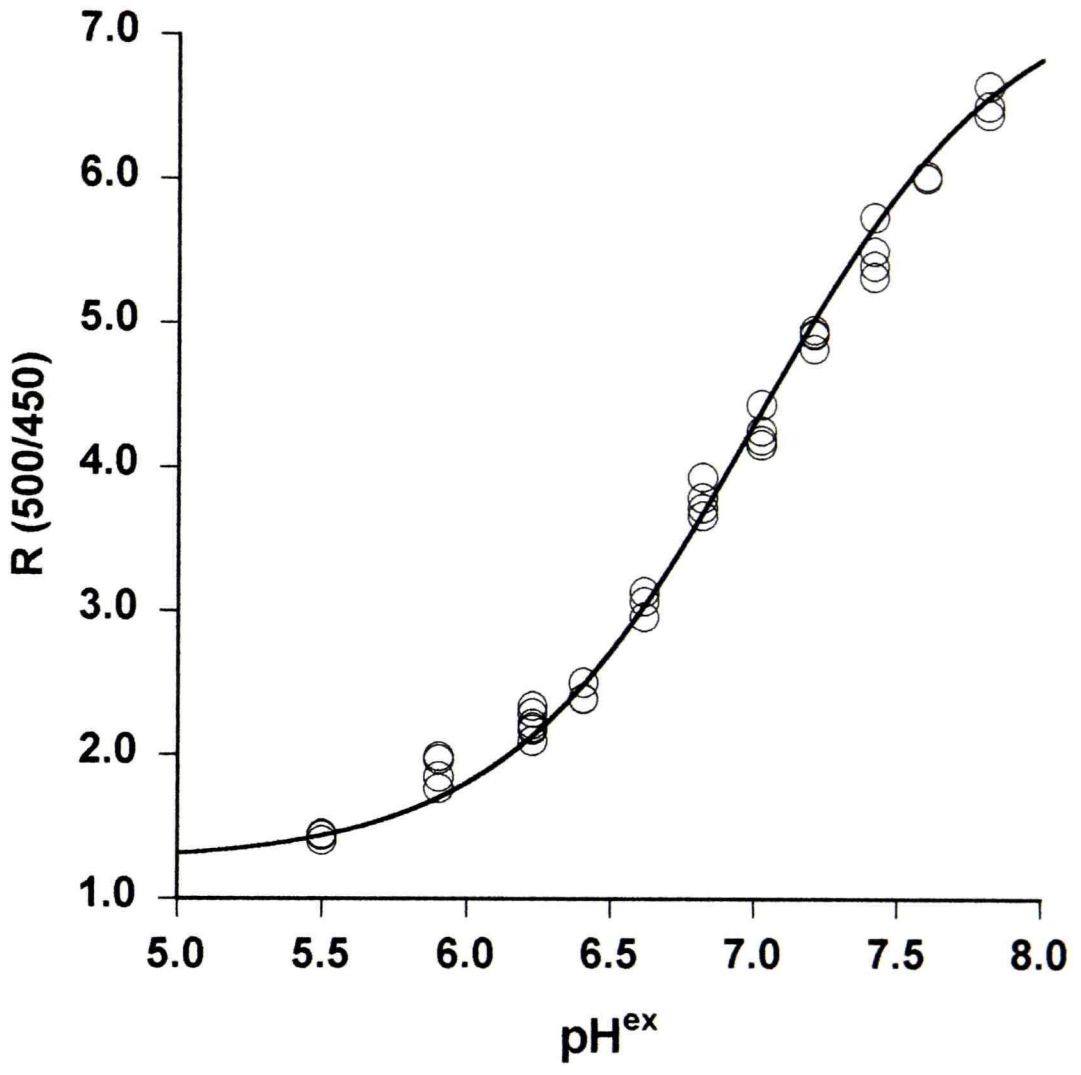

Figure 4.1 In situ calibration of BCECF in human lung microvascular endothelial cells. HLMVE cells grown on cover slips were loaded with 2 μM BCECF-AM as described in "Methods". Cells were then incubated in high K^+ buffer containing 2 μM valinomycin and 6.8 μM nigericin at pH^{ex} values from 5.5 to 7.8, setting $pH^{in} = pH^{ex}$. Fluorescence measurements were obtained with a SLM-8100/DMX spectrofluorometer to yield ratio values (500/450) at an emission of 529 nm. The solid line to fit the data was generated using equation [4.2] which was solved iteratively using nonlinear least squares analysis to yield pK_a, R_{min}, and R_{max} for BCECF in HMVEC-L. Ratio values at each pH^{ex} are the result of 3-6 experiments.

fully unprotonated. The equation is solved iteratively using nonlinear least squares analysis (MINSQ, MicroMath Scientific, Salt Lake City, UT) and yields the values of pK_a, R_{min}, and R_{max} for BCECF in these cells. From these in situ calibration curves, the following parameters were obtained for BCECF in HLMVE cells: $pK_a = 7.01 \pm 0.02$; $R_{min} = 1.26 \pm 0.02$; and $R_{max} = 7.45 \pm 0.05$. Intracellular pH values were then generated for each individual experiment by using equation [4.2] and the in situ calibration parameters with SigmaPlot 4.0 (Jandel Scientific, San Rafael, CA).

Immunocytochemistry

Monoclonal antibodies to 60 and 69 kDa subunits of the yeast V-H^+-ATPase (Molecular Probes, Eugene, OR) were utilized to identify the distribution of these proteins with immunocytochemistry, as described previously (Lynch et al., 1996). These antibodies have been reported to show cross-reactivity, across species, with the 60 and 69 kDa subunits of the V-H^+-ATPase (Kane et al., 1992). Cross-reactivity was also corroborated in our laboratory by Western blot analysis that yielded a single band, indicating monospecificity (data not shown). For immunocytochemistry, cells were grown at sub-confluence on 18-mm round coverslips, then incubated in 4% paraformaldehyde for 15 min. Fixation was terminated by removal of the paraformaldehyde and subsequent washes with 25 mM Glycine. Cells were then permeabilized by incubation with 0.1% Triton X-100. The cells were sequentially incubated with primary antibody and then with Texas Red-labeled secondary (anti-mouse immunoglobulin G) antibody. Cells were dual-labeled with FITC-phalloidin in a

subsequent incubation to label the cytoskeleton. Fluorescent images were obtained from five randomly selected fields per coverlip from five different experiments performed in triplicate. Simultaneous images of FITC and Texas Red fluorescence were obtained with a Bio-Rad 1024 MRC confocal microscope using the 488 and 568 nm lines of a krypton/argon laser and a trichroic filter for excitation, respectively. Images of fields were obtained with a 60x Olympus objective (N.A. 1.4) with green and red fluorescence being separated by using appropriate emission filters (522DF35 and 585LP). Images were subsequently analyzed for colocalization of dyes at or near the plasma membrane on a pixel by pixel basis using Lasersharp software (Bio-Rad, Hercules, CA).

Data Analyses

The initial rate of recovery from an ammonium chloride induced acid load is measured as dpH/dt and expressed as pH unit/minute. For this analysis we evaluated the first five minutes following acid loading. The dpH/dt was expressed as the slope of the linear regression of dpH plotted against time, as described previously (Martínez-Zaguilán et al., 1993). The apparent buffering capacity (β_i) expressed as mM $[NH_3]$/pH unit, is given by (Roos and Boron, 1981):

$$\beta_{i\,(aparent)} = \frac{\Delta\,[NH_3]^{in}}{\Delta\,pH}, \qquad \text{Equation [4.3]}$$

where $\Delta[NH_3]_i$ is assumed to be equal to:

$$\Delta[NH_3]^i = \frac{[NH_3]^o \times 10^{(pK - pH^{in})}}{1 + 10^{(pK \ pH^{ex})}}, \qquad \text{Equation [4.4]}$$

and ΔpH is the change in pH^{in} from the plateau after the NH_4Cl load and the nadir pH^{in} after NH_4Cl removal. To quantify the pH^{in} recovery, we expressed the recoveries as proton fluxes (J_{H^+}) in mM H^+/minute, which is given by:

$$J_{H^+} = \beta_i \times \text{dpH / dt.} \qquad \text{Equation [4.5]}$$

Statistical Analysis

Data are expressed as mean ± SE. Data were analyzed by a two-sample *t*-test and by one-way analysis of variance *(ANOVA)* where indicated. *P* values of < 0.05 were taken to indicate statistical significance.

Results

Antibodies of V-H^+-ATPase show a plasma membrane distribution in HLMVE cells. Immunocytochemical experiments on permeabilized cells utilizing monoclonal antibodies for the 60 kDa subunit of the V-H^+-ATPase show this transporter at the plasma membrane as well as the predicted cytosolic distribution in acidic compartments (Fig. 4.2). The plasma membrane was identified by co-staining the cytoskeleton with FITC-phalloidin to delineate the cell edge. The subcellular distribution observed with mAb to

the 69 kDa subunit was similar to that seen with the 60 kD subunit (data not shown). Confocal microscopy images of five randomly selected areas per coverslip from five independent experiments (performed in triplicate) were analyzed. Simultaneously acquired images of FITC (cytoskeleton) and Texas-Red (V-H^+-ATPase) revealed that ca. 60% of cells imaged displayed a plasma membrane distribution of V-H^+-ATPase as represented by Fig. 4.2 (arrows). Sectional images (XYZ series) were collected and each section was analyzed on a pixel by pixel basis utilizing Lasersharp software to assess colocalization of FITC and Texas red at the plasma membrane. Colocalization of V-H^+-ATPase and actin filaments is shown in white. Parallel experiments with secondary antibody only did not show any labeling in intracellular compartments or at the plasma membrane (data not shown). Altogether, these data show V-H^+-ATPase in the plasma membrane of HLMVE cells.

Steady-state pH^{in} HLMVE cells is similar in the presence and absence of HCO_3^-.

We evaluated steady-state pH^{in}, which reflects the pH^{in} regulatory mechanisms in concert, by perfusing cells loaded with BCECF at $pH^{ex} = 7.4$. pH^{in} was 6.970 ± 0.048 (n=5) in a HCO_3^--supplemented media and was 6.930 ± 0.028 (n=18) in a HCO_3^--free media. We then evaluated steady-state pH^{in} at pH^{ex} values ranging from 6.5 to 7.4. In these experiments, cells were exposed to buffer at the pH values being tested in either the presence or absence of HCO_3^- from beginning to the end of the experiment. Thus, cells were in the presence or absence of HCO_3^- for at least one hour before the experiment. There were no significant differences in steady-state pH^{in} in the presence or absence of

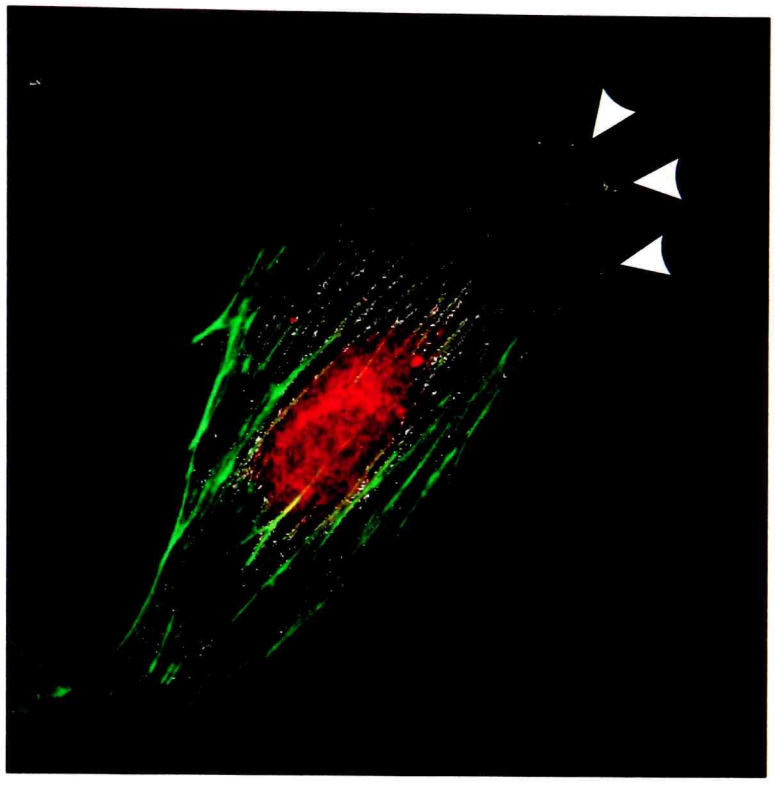

Figure 4.2 Immunocytochemistry reveals a plasma membrane distribution of V-ATPase in human lung microvascular endothelial cells. HLMVE cells were grown on glass cover slips and subsequently fixed, permeabilized, and incubated with primary antibodies as described in "Methods". Confocal microscopy image (60x oil objective; 1.4 N.A.) of cell labeled with antibodies to the 60 kDa subunit (red) and FITC-phalloidin (green). Co-localization of red/green was determined by computer analysis and is shown as white dots. Data are representative of 5 independent experiments performed in triplicate. For each experiment 50 cells were analyzed. The image is one of 20 sections in the Z plane taken at 0.4 μm intervals. The arrows indicate the regions of co-localization of V-H^+-ATPase at the plasma membrane.

HCO_3 from pH^{ex} 6.5 to 7.4 (Fig. 4.3). Previous studies from our laboratory show that about 30 minutes is required for cells to reach a new steady-state pH; therefore the loading and hydrolysis time should have been sufficient for equilibration (Gillies and Martínez-Zaguilán, 1991).

pH^{in} recoveries in HLMEV cells. To further understand the importance of HCO_3^- for pH^{in} regulation, we performed acid loading experiments utilizing the NH_4Cl pre-pulse technique (Roos and Boron, 1981). Cells loaded with BCECF were perfused with CPB at pH^{ex} 7.4. The cells were then perfused with 25 mM NH_4Cl, which causes a rapid intracellular alkalinization due to the dissociation of the NH_4Cl into the charged species NH_4^+, Cl^-, and a transient NH_3 species. The NH_3 is membrane-permeable and, once in the cell, rapidly scavenges H^+ causing intracellular alkalinization. Rapid NH_4Cl removal reverses the situation and leads to cellular acidification below baseline and subsequent recovery towards baseline. This pH^{in} recovery in the presence of Na^+ and HCO_3 represents the contribution of all pH^{in} regulatory mechanisms (Fig. 4.4A and summarized in Fig. 4.5). We used ion-substitution experiments to evaluate the contribution of other pH^{in} regulatory mechanisms to cellular recovery from an acid load.

When the contribution of HCO_3^- -transporting mechanisms was eliminated by incubating cells without HCO_3^- but with Na^+, recoveries were not significantly different than those in the presence of Na^+ and HCO_3^- (Figs. 4.4B, 4.5C). In the absence of both Na^+ and HCO_3^-, HLMVE cells' pH^{in} recovery were approximately 40% less than in the

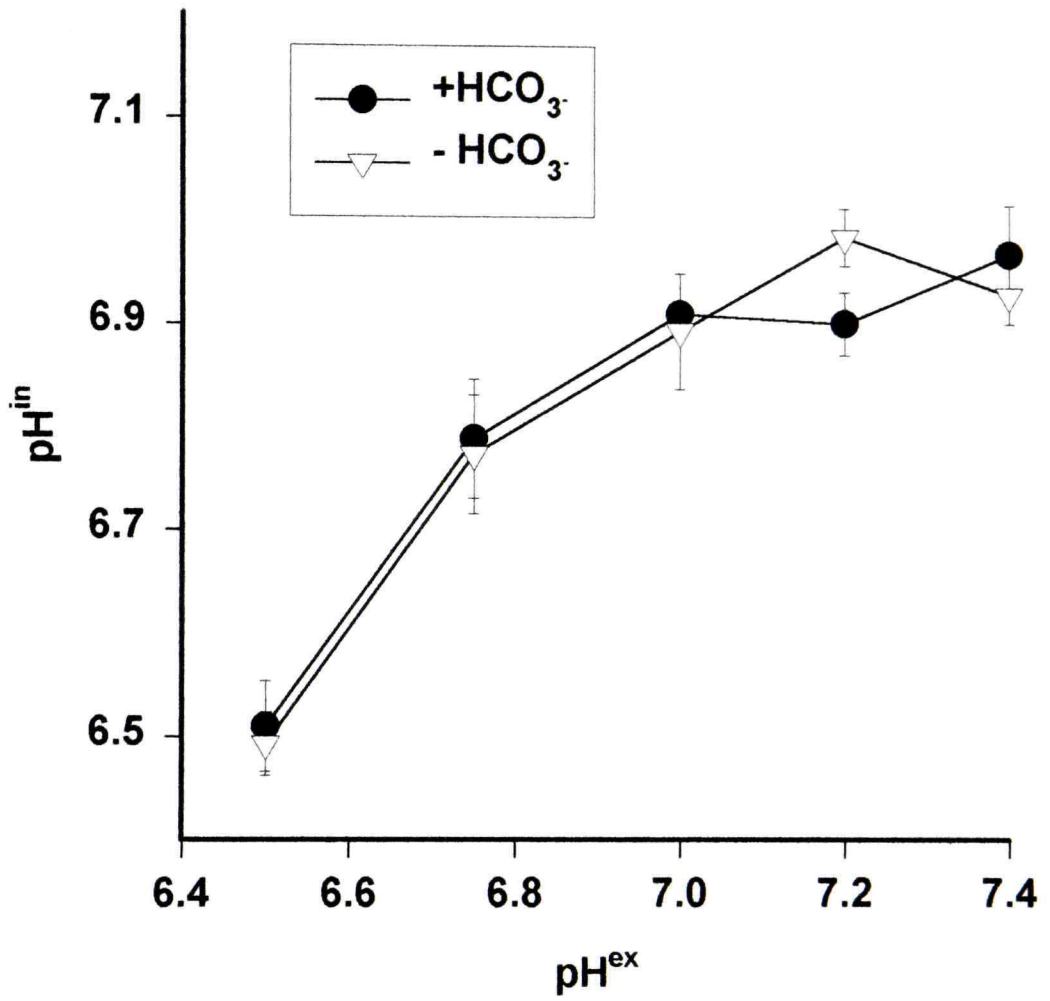

Figure 4.3 Steady-state pH^{in} is similar regardless of the presence or absence of HCO_3^-. HLMVE cells grown on cover slips were loaded with 2 μM BCECF-AM in the presence (closed circles) or absence (open triangles) of HCO_3^- at the indicated pH^{ex}. Cells were subsequently perfused with CPB in the presence or absence of HCO_3^- and fluorescence measurements converted to pH^{in} as described for Fig 4.1. Data are expressed as S.E.M. of 5 experiments per pH value. Differences in pH^{in} values in the presence and absence of HCO_3^- at each pH^{ex} are not statistically significant.

presence of Na^+ and HCO_3 (Figs. 4.4C, Fig 4.5C). Parallel experiments with media containing Na^+ and HCO_3 showed that the rates of pH^{in} recovery following NH_4Cl removal were not affected by 100 μM DIDS, an anion transport inhibitor (data not shown).

The Na^+- and HCO_3 -independent pH^{in} recoveries are inhibited by bafilomycin. We utilized a pharmacological approach to determine if the recovery was attributed to a primary H^+ transporting system. V-H^+-ATPases are present at the plasma membrane in some specialized cells and are inhibited bafilomycin A_1, (Martínez-Zaguilán et al., 1993; Mendlein and Sachs, 1990; Bowman et al., 1988). Thus, we performed acid loading experiments similar to those shown in Fig 25C. As shown in Fig. 4.6, pretreatment with 10 nM bafilomycin A_1, a V-H^+-ATPase inhibitor, suppresses the proton fluxes (J_H^+) compared to controls. In contrast, SCH 28080, an H^+/K^+-ATPase inhibitor, did not significantly alter J_H^+. In the absence of Na^+ and HCO_3^-, 100 μM DIDS decreases J_H^+ slightly (Fig. 4.7). Partial inhibition of J_H^+ by DIDS has been observed in other cell types (Martínez-Zaguilán et al., 1993).

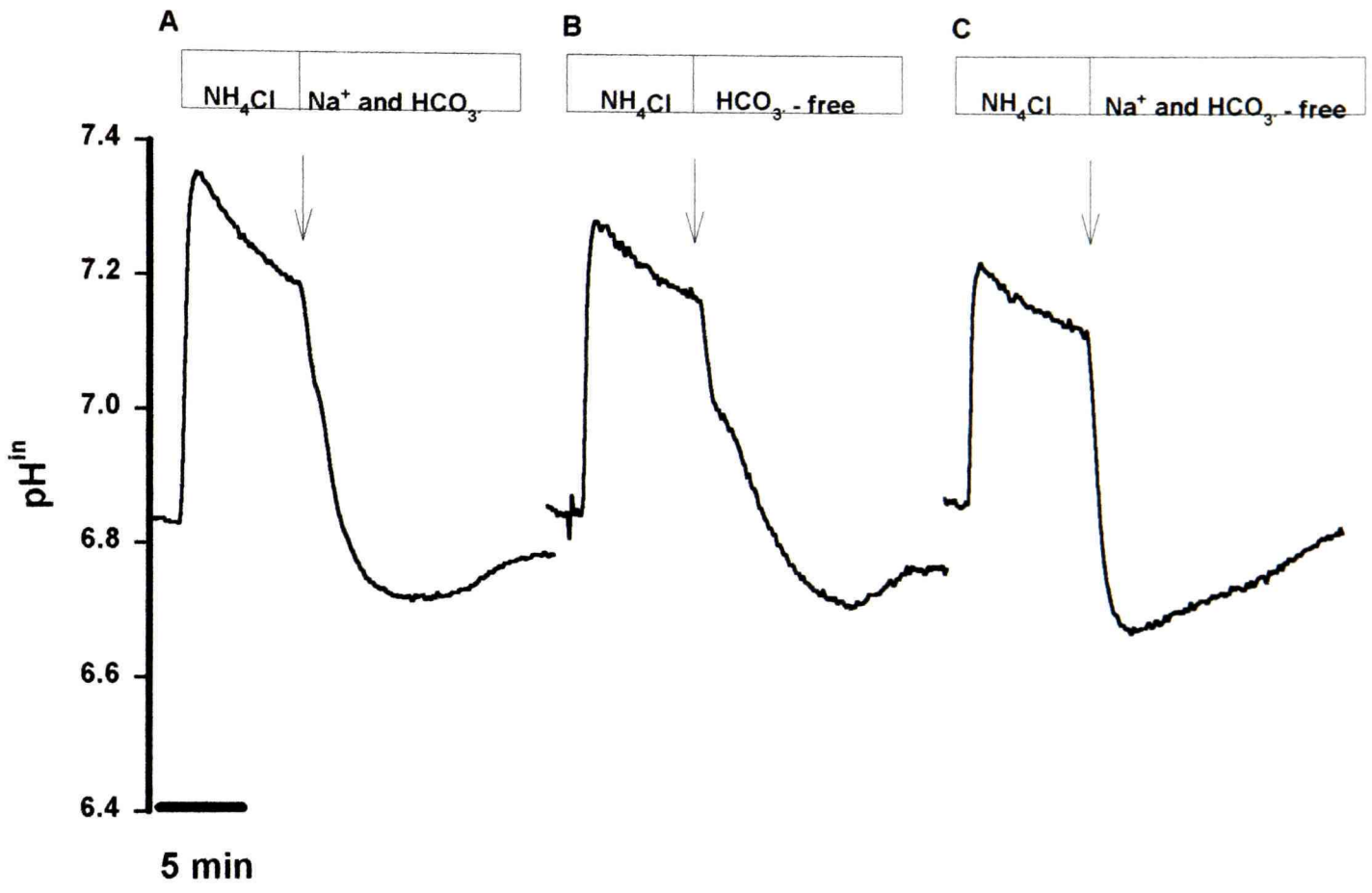

Figure 4.4 Human lung microvascular endothelial cells exhibit a Na^+ and HCO_3^- - independent pH^{in} regulatory mechanism. HLMVE cells grown on cover slips were handled as described for Figure 4.2. The cells were initially perfused with CPB in the presence (A) or absence (B, C) of HCO_3^- at a $pH^{ex} = 7.4$. Thereafter, NH_4Cl was applied for 5 minutes, as indicated above the tracings. At the arrow, NH_4Cl was removed to induce an acid load. Data are representative of 11 (A), 10 (B), and 21 (C) experiments. (A) the presence of Na^+ and HCO_3^-; (B) absence of HCO_3^-; (C) absence of Na^+ and HCO_3^-.

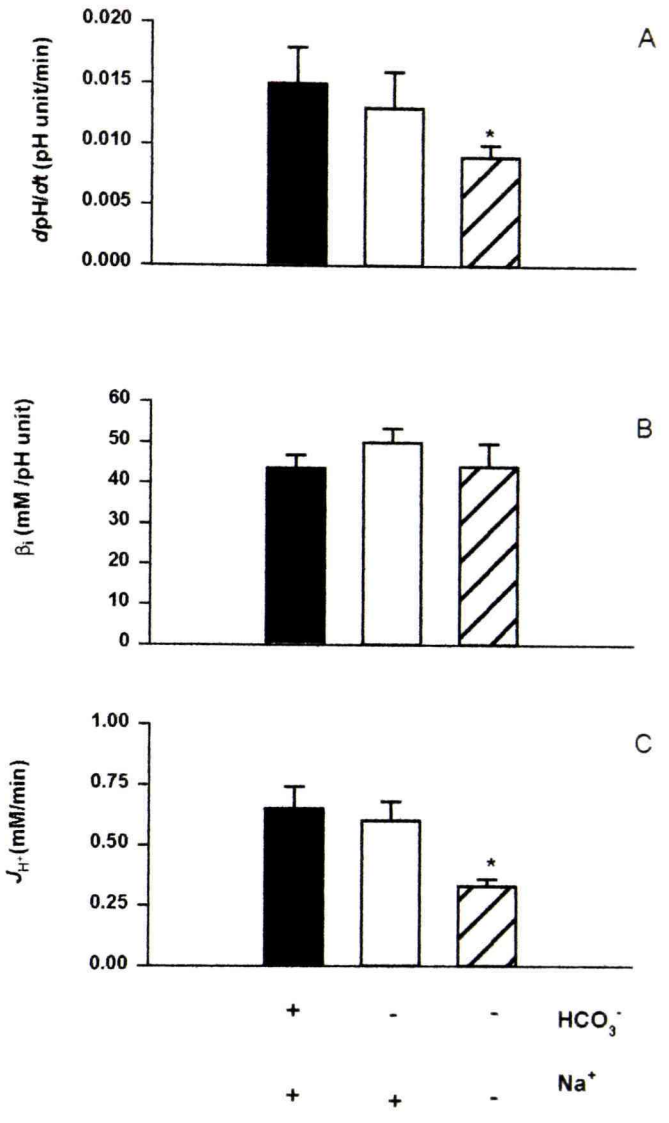

Figure 4.5 Human lung microvascular endothelial cells exhibit proton fluxes in the absence of Na^+ and HCO_3^- that are fifty-percent of that observed in the presence of Na^+ and HCO_3^- . HLMVE cells grown on cover slips were loaded with 2 μM BCECF-AM. Data are derived from experiments similar to those shown in Figure 4.4. (A) dpH was plotted against time and the slope of that relationship is shown. Black bar - in the presence of Na^+ and HCO_3^- (n =11). White bar - absence of HCO_3^- (n = 10). Hatched bar - absence of Na^+ and HCO_3^- (n = 30). (B) The intrinsic buffering capacity was calculated with equation [4.3]. (C) Proton fluxes were calculated with equation [4.4]. Data are expressed as S.E.M. $*P < 0.05$ compared by one-way *ANOVA* compared to media containing Na^+ and HCO_3^-, otherwise differences are not statistically significant.

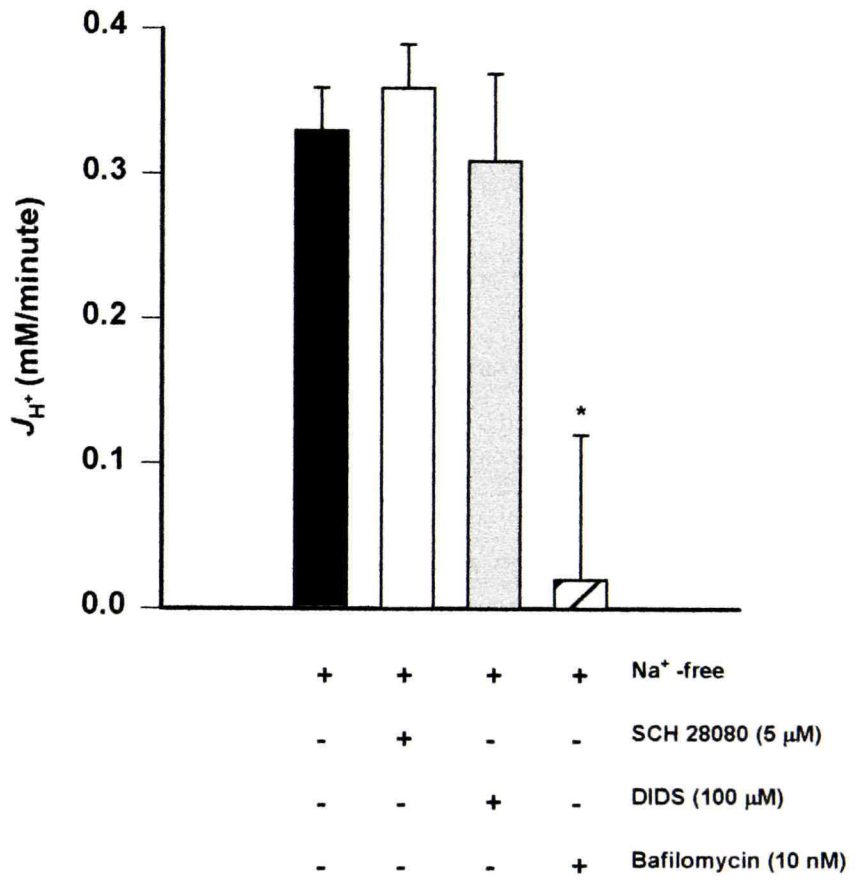

Figure 4.6 Bafilomycin inhibits the Na^+ and HCO_3^- -independent recoveries. HLMVE cells grown on cover slips were loaded with 2 μM BCECF-AM as described in "Methods". Cells were pre-incubated with 5 μM SCH 28080 (to inhibit H^+/K^+-ATPase), 100 μM DIDS (to inhibit anion transport), or 10 nM bafilomycin (to inhibit (V-H^+-ATPase). Experiments similar to those in Figure 4.4 were performed and the pH^{in} recoveries were evaluated in the absence of Na^+ and HCO_3^-. Proton fluxes were calculated with equation [4.4]. Black bar-control (absence of Na^+ and HCO_3^-; n = 30). White bar - SCH 28080 (n = 11). Gray bar - DIDS (n = 4). Hatched bar - bafilomycin (n = 4). Data represent S.E.M * $P<0.05$ as determined by *ANOVA* compared to absence of Na^+ and HCO_3^-.

Discussion

The Na^+/H^+ exchanger and HCO_3^- transport mechanisms are generally accepted as the main pH^{in} regulatory mechanisms in endothelial cells (Jentsch et al., 1988; Escobales et al., 1990; Ziegelstein et al., 1992; Cutaia and Parks, 1994; Hsu et al., 1996). Similarly, the effect of CO_2 on pH^{in} is well documented (Roos and Boron, 1981). In cells such as lung endothelial cells that express carbonic anhydrase (Effros et al., 1981; Sugai et al., 1981; Ryan et al., 1982; Tamai et al., 1996), CO_2 entry leads to H_2CO_3 formation that dissociates into H^+ and HCO_3^-, yielding an acid load (Roos and Boron, 1981). HLMVE cells might extrude the acid load imposed by CO_2 by over-expressing either or both the Na^+/H^+ exchanger and HCO_3^- transport mechanisms. Na^+-independent Cl^-/HCO_3^- exchange would not be a likely mechanism since it operates to acidify a cell. By contrast, the Na^+-HCO_3^- symporter and the Na^+-HCO_3^-/HCl exchanger could remove the acid load, using the inwardly-directed Na^+ gradient to bring HCO_3^- into the cell (Gillies and Martínez-Zaguilán, 1991). Since preventing excessive acid load is so important for survival, it seems reasonable to expect redundancy that would allow for acid removal without relying absolutely on the Na^+ gradient or limited proton flux at alkaline pH^{in}. We and others have observed pmV-H^+-ATPases as a dynamic pH^{in} regulatory mechanism in other cell types that are chronically exposed to acid loads (Martínez-Zaguilán et al., 1993; Lubman et al., 1989; Bidani and Brown, 1990; Vaananen et al., 1990; Goldstein et al., 1991; Nordstrom et al., 1995). We hypothesized that lung microvascular endothelial cells would also express pmV-ATPase.

If HCO_3^--transporting mechanisms were crucial for steady-state pH^{in} regulation in HLMVE cells, we reasoned that there would be differences in steady-state pH^{in} in the presence and absence of HCO_3 . In fact, our experiments revealed that there were no differences in steady-state pH^{in} in the presence or absence of HCO_3 across pH^{ex} values of 6.5 to 7.4. This reduced the possibility that HCO_3^--transport was not observed because of some physiologic pH^{ex} optimum (cf. Fig. 4.2). These experiments did not address the possibility that HCO_3^- transport was significant in conditions of acid loading, nor did they evaluate the role of the Na^+/H^+ exchanger in pH^{in} regulation. NH_4Cl experiments indicated that the rate of recovery from acidification in either the absence of HCO_3 or the presence of Na^+ and HCO_3^- were similar (cf. Fig. 4.3). If HCO_3^- transport mechanisms were important for pH^{in} recovery from acidification, HCO_3^- presence or absence should yield distinct pH^{in} recovery rates. Interestingly, experiments in the absence of Na^+ and HCO_3^- reveal that HLMVE cells' pH^{in} recovery was 40% lower than in the presence of Na^+ and HCO_3^- (cf. Fig. 4.4). These data support that other mechanisms besides Na^+/H^+ exchange and HCO_3^- transporting systems mediate pH^{in} regulation in HLMVE cells.

The presence of Na^+- and HCO_3^--independent pH^{in} recovery provided functional evidence for a primary H^+-transporting system. Possible candidates for this system are the H^+/K^+-ATPase and the V-H^+- ATPase. These ATPases are easily distinguished pharmacologically. The H^+/K^+-ATPase is inhibited by SCH 28080 (K_i of 5 μM) with no effect on V-H^+-ATPases (Mendlein and Sachs, 1990). Conversely, V-H^+-ATPases are inhibited by bafilomycin A_1 (K_i of 5 nM) with no effect on P-H^+-ATPases (Bowman et

al., 1988). Acid loading experiments in the absence of Na^+ and HCO_3^- indicated that bafilomycin A_1 completely inhibited the pH^{in} recoveries, while SCH 28080 had no effect (cf. Fig. 4.6). This provides pharmacologic evidence for the role of V-H^+-ATPases in the observed pH^{in} recovery but does not necessarily localize these ATPases at the plasma membrane. To address this issue, we performed immunofluorescence experiments with monoclonal antibodies to the 60 and 69 kDa subunits of the V-H^+- ATPase. This approach revealed a distinct plasma membrane localization of V-H^+-ATPase preferentially in lamellipodia (cf. Fig 4.2). The proton pump might be expressed in a polarized manner in the lung endothelium as has been observed in other tissues (Nordstrom et al., 1995; Al-Awqati, 1996). In this manner, the pmV-ATPase might be involved in acid-base regulation at the level of the lung endothelium as an acid extruding mechanism. If increased proton fluxes occur as would be predicted by conditions associated with hypercapnia and acidosis, the increased flux via pmV-ATPases could alter the extracellular matrix decreasing the stability of endothelial cell attachment and thereby result in the increased vascular permeability noted in lung failure (Ashbaugh et al., 1967; Sinclair et al., 1994). Alternatively since it has been reported that hypercapnia and hypocapnia alter pulmonary blood flow (Viles and Shephard, 1968; Shirai et al., 1986; Yamaguchi et al., 1998), it is tempting to speculate that a dysfunction of pmV-ATPase expression in lung endothelial cells may be associated with the altered secretion of vasoactive substances by endothelial cells (e.g., nitric oxide, endothelin, prostaglandin).

In summary, we demonstrate a novel primary active H^+ transport system that allows HLMVE cells to recover from acidosis in a Na^+- and HCO_3^- -independent manner. Ion substitution experiments, pharmacological inhibition of this system with bafilomycin A_1, and immunocytochemical location of V-H^+-ATPase at the plasma membrane show that this novel system is the pmV-ATPase.

CHAPTER V

CONCLUDING REMARKS

pmV-ATPase in Microcvascular Endothelial Cells

This study began with the hypothesis that pmV-ATPase was important/required for invasion due largely to the observation of this mechanism in highly invasive cells. Work done in our laboratory had previously shown a direct correlation between highly metastatic tumor cells and pmV-ATPase activity (Martínez-Zaguilán et al., 1993). We chose microvascular endothelial cells as an experimental paradigm to test this hypothesis because it is readily accepted that these cells are involved in the process of angiogenesis (Hudlická et al., 1998). Although there had been a considerable amount of work done on pH^{in} regulation in endothelial cells, our literature search found no mention of a Na^+- and HCO_3^- -independent pH^{in} regulatory mechanism (proton pumps) in endothelial cells. Several laboratories had used the common paradigm of exposing endothelial cells to Na^+ removal and had observed acidification and no subsequent recovery (Jentsch et al., 1988; Kitazono et al., 1988; Ziegelstein et al., 1992; Cutaia and Parks, 1994; Hsu et al., 1996). These observations would argue against the presence of proton pumps. We reasoned that proton pumps had not been identified because of the origin of endothelial cells. With the exception of Hsu et al., all other investigators had used endothelial cells of macrovascular origin. It is becoming more accepted that not only are there differences in morphology and growth characteristics (Kumar et al., 1987; McCarthy et al., 1991) in endothelial cells

from macro- and microvasculature; there have also recently been reported differences in $[Ca^{2+}]^{in}$ regulation (Stevens et al., 1997) and NO production (Geiger et al., 1997) depending on whether the cells are of macrovascular or microvascular origin. We reasoned that since angiogenesis is accepted to be a process that involves the microvasculature, the absence of proton pumps in macrovascular endothelial was consistent with the hypothesis. We set out to further characterize the invasive properties of microvascular (coronary) and macrovascular (aortic) endothelial cells. In our hands we found that microvascular endothelial cells were three-fold more invasive than macrovascular endothelial cells. In tumor cells that express pmV-ATPase activity it had been shown that conditioning these cells at acidic pH for a week enhanced their invasive profile and increases pmV-ATPase activity (Martínez-Zaguilán et al., 1996c). Conditioning microvascular endothelial cells at acidic pH resulted in an almost two-fold increase in the invasiveness of microvascular endothelial cells, yet did not increase the invasiveness of macrovascular endothelial cells. Moreover, we found that treating microvascular endothelial cells with nanomolar concentrations of bafilomycin blocked their invasiveness. The blocked invasiveness did not seem to be due to cytotoxic effects of bafilomycin since cells remained intact and attached to the membrane.

This was indirect evidence for the role of V-ATPase in invasion. We continued to examine the role of V-ATPase in invasion, because we could not rule that the inhibitory effect of bafilomycin was not related to changes in pH instead of just inhibition of the pump. Thus we decided to examine the invasiveness/migratory potential of endothelial cells employing wounded monolayers (Selden and Schwartz, 1979; Yoshida et al., 1996).

It is known that other cell types will still migrate at mildy acidic pH (Martínez-Zaguilán, 1996c); however, if the inhibition of migration was related to acutely acidic pH other inhibitors of pH regulation or acidic pH would block migration. Migration of wounded monolayers was unaffected by DIDS; HMA, or pH^{ex} of 6.8; however. nanomolar concentrations of bafilomycin did block migration. Thess data suggest that in microvascular endothelial cells V-ATPase are essential for migration/invasion.

To test for the presence of pmV-ATPase we employed commercially available monoclonal antibodies to the 60 and 69 kDa subunits of V-ATPase. By this approach we show the pump to be present in microvascular endothelial cells from two distinct vascular beds, coronary and pulmonary. The pump appears at the plasma membrane and in some instances appears to localize to the leading edge of cells or lamellipodia-like structures. We interpret this to be consistent with a role of pmV-ATPase in migration/invasion. We examined the functional role of pmV-ATPase in pH^{in} regulation at the population and single cell level. In populations, we show that pmV-ATPase is the major pH^{in} regulatory mechanism, given that J_H^+ is no different in the presence or absence of Na^+ or HCO_3. Furthermore, the J_H^+ can be completely blocked by bafilomycin. At the single cell level, again we confirmed the presence of a Na^+ - and HCO_3^- -independent pH^{in} regulatory mechanism. In polarized cells, we notice a tendency for this Na^+- and HCO_3 - independent mechanism to cause the leading edge of the cell to be more alkaline. We interpret this to be due to the pump being located/inserted at the leading edge. The fact that the mechanism is not always there could be explained by the dynamic nature of these cells. I would not predict that the cells are continually oriented in a single direction. In

experiments with wounded monolayers where images of the leading edge were captured during recovery at three minute intervals, it was common to observe forward movement followed by retraction. From experiments with wounded monolayers it was observed that if a 300 μm wound is inflicted, in 18 hours cells will migrate ca. 250 μm. If we assume the migration rate to be constant, this would result in a migration of ca. 0.2 μm /min. Thus in the course of our experiments (30 minutes), the cell could have changed direction multiple times and thus cause peristaltic type waves in pH^{in}. Indeed when our confocal experiments are analyzed, we see greater changes and oscillations in pH at the lagging edge. In this system we acquire at millisecond rates and typical experiments do not last longer than fifteen minutes. Thus the likelihood of the cell changing direction and observing that change are much less. However, the observed oscillations do seem to favor the existence of a dynamic pH^{in} environment and regulatory mechanism.

Altogether, we interpret these data to suggest pmV-ATPase to be present and a functional pH^{in} regulatory mechanism in microvascular endothelial cells. Furthermore, it seems to be important for the invasion/migration of these endothelial cells. Immunocytochemical data suggest that pmV-ATPase can and does localize in distinct areas of the cell. Studies of pH^{in} at the single cell level reveal pH^{in} gradients and oscillations that could a result of dynamic pH^{in} regulatory mechanisms (i.e., pmV-ATPase).

Angiogenesis and Diabetes

We have shown pmV-ATPase to be present in microvascular endothelial cells ando that it is involved in invasion. We had hypothesized that these cells would have this pH^{in} regulatory mechanism since they are responsible for angiogenesis. We sought to test this relationship in a model of diabetes since angiogenesis/healing are decreased in diabetes (Servold, 1991; Stehouwer and Schaper, 1996). Interestingly, we show that microvascular endothelial cells from diabetics do not express pmV-ATPase activity and exhibit decreased invasive and angiogenic potential. In this model it is easier to see that acidic pH does not enhance invasion/angiogenesis. The microvascular endothelial cells from diabetes are probably exposed to a more acidic environment constantly in vivo, yet they are unable to invade the extracellular matrix. Growing normal microvascular endothelial cells at acidic pH enhances invasiveness. This seems paradoxical, but as stated above, acidic pH enhances the pump's activity if it is present. Acidic pH in normal tissue could act as a signal that enhances the pump and stimulates angiogenesis/invasion.

Mechanism of pmV-ATPase in Invasion

There are several mechanism by which activation of the pump could be involved in invasion. Initially, I was entranced by the idea that the pump at the plasma membrane acidified the extracellular matrix. I imagined that this was required and served several purposes. First and foremost, in order for a cell to invade/migrate it must free itself from its tethered position (basement membrane). The basement membrane must be dissolved. It is known that matrix metalloprotienases (MMPs) are involved in this process

(Woessner, 1991). I had envisioned that these substances were either secreted as inactive precursor molecules and where attached to the extracllular matrix. If these MMPs are activated by acidic pH, then proton pumps could play a very important role in activation. However, it has been shown that most MMPs function at neutral pH therefore no pH regulatory mechanism need be invoked for activation (Ye and Henney, 1998). It is still possible that some MMPs could have enhanced function at an acidic pH. It is known that the extracellular matrix is kept in place by a delicate balance of MMPs and tissue inhibitors of metalloprotienases (TIMPs). TIMPs inactivate MMPs by stochiometrically binding to them and rendering them inactive (Ye and Henney, 1998). It is possible that acidic pH could destabilize TIMP/MMP binding and render TIMPS inactive thus increasing MMPs. An alternative is that all MMPs have an absolute requirement for Ca^{2+} and Zn^{+}. It is known that acidic pH decreases the K_d of calcium and zinc binding proteins, increasing the amount of free calcium. Activation of proton pumps could substantially raise available extracellular [Ca^{2+}], increase the activity of MMPs and dissolution of the extracellular matrix and enhance invasion. However, if this were to be the case acidifying the extracellular matrix would enhance invasion. If this were to be the case all tumors would be able to metastasize since they generate an acidic environment, but such is not the case. Furthermore, in diabetes the microvasculature should be more acidic and angiogenesis should be increased, but again such is not the case.

Proton pumps could be important for invasion not because of the acidification on the extracellular surface, but rather from point changes in pH on the intracellular surface that affect cytoskeletal restructuring. This would require an active process that could

readily be activated or inactivated and induce substantial changes in pH. I believe that the pumps importance is not in acidifying the exterior of the cell, but rather in alkalinizing the interior to alter cytoskeletal proteins. There are several experimental lines of evidence that support this. First, if we consider cancer cells, it has been observed that more metastatic cells exhibit a higher intracellular pH (Matrínez-Zaguilán et al., 1993) even in the presence of an acidic extracellular environment. On a common theme, small tumors are known to have acidic/necrotic cores yet are not invasive. If we examine the model of endocytosis we see that vesicles are budded off of the plasma membrane and they move into the interior of the cell. V-ATPase is known to be present in the membrane of these vesicles and it becomes activated as the vesicle moves interiorly and acidifies the compartment. Evidence for this is the differences in pH of early and late endosomes (pH is lower in late endosomes). Vesicles are usually considered to be moving along on motor proteins attached to the cytoskeleton. I imagine that as the pump is activated, the cytosol becomes alkaline as protons are pumped into the vesicle. These local changes in pH could favor cytoskeletal assembly/scaffolding that propels the vesicle forward akin to gaining forward velocity by pushing away from a solid surface. In added support of this mechanism staining of cytoskeletal proteins with phalloidin after collapsing the pH gradient across the cell and clamping pH^{in} at known values results in a dissolved cytoskeleton at acidic pH and organized structure at alkaline pH (Fig. 5.1). Along those same lines, if a cell were to activate proton pumps at the invading edge of a cell and shut them off at the lagging edge, a favorable pH gradient would be created that would organize cytoskeletal proteins in the advancing region of the cell and disorganize them in

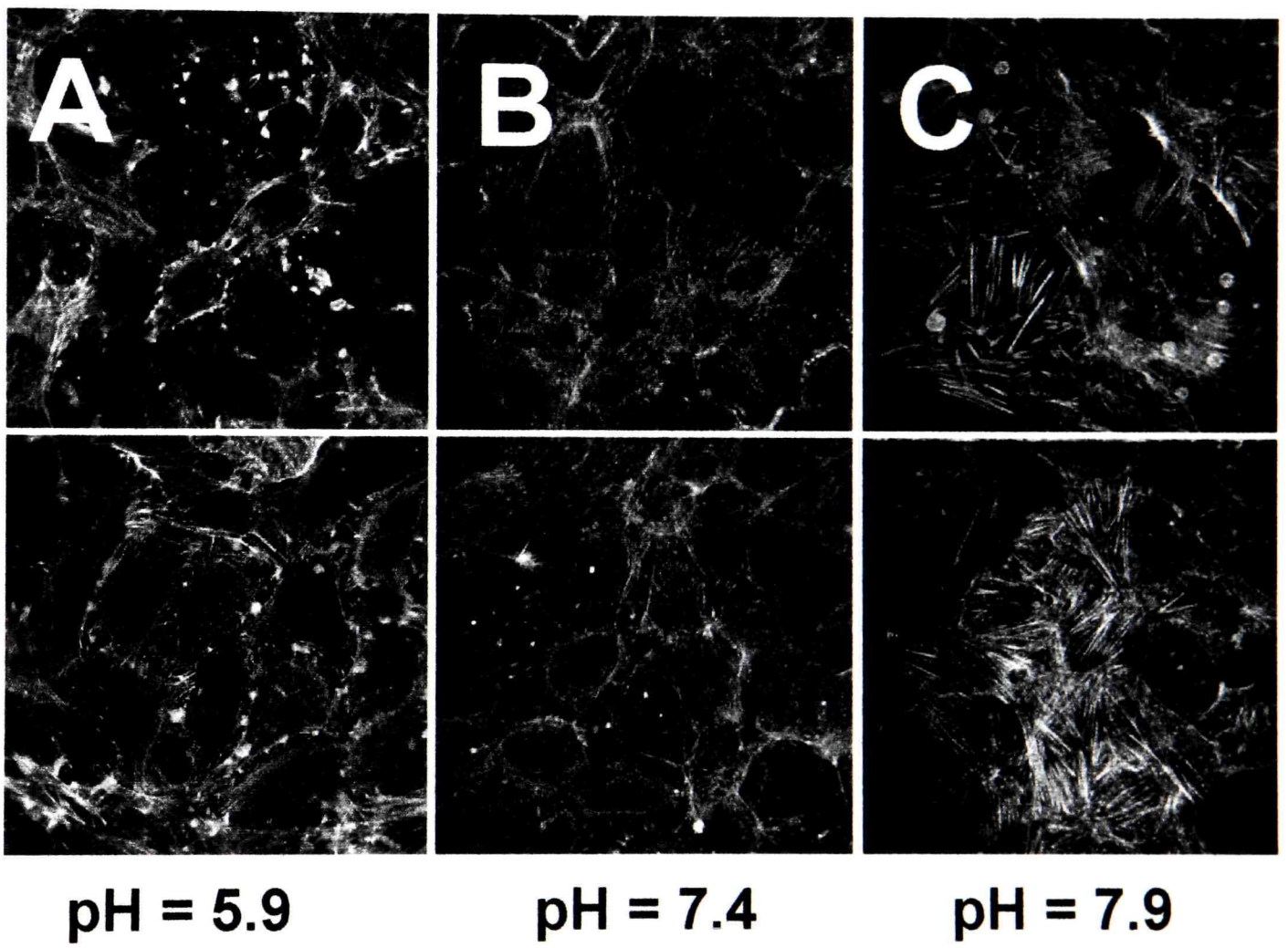

Figure 5.1 Cytoskeletal proteins exhibit a pH dependent assembly that is greater at alkaline pH. Microvascular endothelial cells were plated on round cover slips. Cells were incubated in High K^+ buffer containing 2 μM valinomycin and 6.8 μM nigericin at distinct $pH^{ex.}$ Cells were then fixed, permeabilized and incubated with FITC-phalloidin. (A) $pH^{in} = 5.9$ (B) $pH^{in} = 7.4$ (C) $pH^{in} = 7.9$.

the retracting portion of the cell. It is this mechanism that would generate gradients similar to what we have observed in single cells and would allow a cell to readily change direction. It is fairly well understood that cytochalasin stops migrtaion in wounded monolayers by dissolution of cytoskeletal proteins (Selden et al., 1981). An interesting approach to test this might be measure cell movement/restructuring in GFP-α-actin transfected cells. As a control, point addition of chemoattractant should demonstrate cytoskeletal restructuring in the direction of the chemoattactant and dissolution at a point opposite the restructuring. A single cell could be impaled with a micro-pipette containing buffer only and the chemoattract again added to verify that impaled cells will behave as non-impaled cells. Next a cell could be impaled with a pipette containing bafilomycin at a physiologic pH. After a period of equilibration, I would predict that adding chemoattractant should not result in cytoskeletal restructuring. If the experiment were to be done with bafilomycin and an alkaline pH, I would predict that there would be a diffuse cytoskeletal structure that would begin at the pipette and move in a diffusive pattern from the electrode.

In conclusion, we show that microvascular endothelial cells from two distinct vascular beds exhibit pmV-ATPase activity. In support of the hypothesis that pmV-ATPase is required for invasion/migration, microvascular endothelial cells that do not express this activity are non-invasive. Furthermore, inhibition of pmV-ATPase renders

invasive microvascular endothelial cells non-invasive. Single cell studies reveal the existence of pH gradients/oscillations in activated/migrating endothelial cells with the invading edge tending to be more alkaline than the non-invading edge. We interpret these gradients to be generated by pmV-ATPase and that they are essential for cytoskeletal remodeling associated with invasion/migration.

REFERENCES

Al-Awqati, Q. (1996). Plasticity in epithelial polarity of renal intercalated cells: targeting of the H(+)-ATPase and band 3. *Am J Physiol Cell Physiol.* 270: C1571-C1580.

Ashbaugh, D.G., Bigelow, D.B., Petty, T.L., & Levine, B.E. (1967). Acute respiratory distress in adults. *Lancet.* 2: 319-323.

Baatout, S. (1997). Endothelial differentiation using Matrigel. *Anticancer Res.* 17: 451-455.

Beisswenger, P.J., & Spiro, R.G. (1973). Studies on the human glomerular basement membrane. Composition, nature of the carbohydrate units and chemical changes in diabetes mellitus. *Diabetes.* 22: 180-93.

Belloni, F.L. (1979). The local control of coronary blood flow. *Cardiovasc Res.* 13: 63-85.

Bidani, A., Brown, S.E., Heming, T.A., Gurich, R., & Dubose, T.D.J. (1989). Cytoplasmic pH in pulmonary macrophages: recovery from acid load is Na+ independent and NEM sensitive. *Am J Physiol Cell Physiol.* 257: C65-C76.

Bidani, A., & Brown, S.E. (1990). ATP-dependent pHi recovery in lung macrophages: evidence for a plasma membrane H(+)-ATPase. *Am J Physiol Cell Physiol.* 259: C586-C598.

Bowman, E.J., Siebers, A., & Altendorf, K. (1988). Bafilomycins: a class of inhibitors of membrane ATPases from microorganisms, animal cells, and plant cells. *Proc Natl Acad Sci USA.* 85: 7972-7976.

Buss, F., Kendrick-Jones, J., Lionne, C., Knight, A.E., Cote, G.P., & Paul, L.J. (1998). The localization of myosin VI at the golgi complex and leading edge of fibroblasts and its phosphorylation and recruitment into membrane ruffles of A431 cells after growth factor stimulation. *J Cell Biol.* 143: 1535-1545.

Chu, S., Brownell, W.E., & Montrose, M.H.(1995). Quantitative confocal imaging along the crypt-to-surface axis of colonic crypts. *Am J Physiol Cell Physiol.* 269: C1557-C1564.

Cines, D.B., Pollak, E.S., Buck, C.A., et al. (1998). Endothelial cells in physiology and in the pathophysiology of vascular disorders. *Blood.* 91: 3527-3561.

Cutaia, M., & Parks, N. (1994). Oxidant stress decreases Na+/H+ antiport activity in bovine pulmonary artery endothelial cells. *Am J Physiol Lung Cell Mol Physiol.* 267: L649-L659.

Cutaia, M., Dawicki, D.D., Papazian, L.M., Parks, N., Clarke, E., & Rounds, S. (1997). Differences in nucleotide effects on intracellular pH, Na+/H+ antiport activity, and ATP-binding proteins in endothelial cells. *In Vitro Cell Dev Biol Anim.* 33: 608-614.

Davies, J.E., Ng, L.L., Kofoed-Enevoldsen, A., et al. (1992). Intracellular pH and Na+/H+ antiport acti.vity of cultured skin fibroblasts from diabetics. *Kidney Int.* 42: 1184-1190.

Effros, R.M., Mason, G., & Silverman, P. (1981). Asymmetric distribution of carbonic anhydrase in the alveolar-capillary barrier. *J Appl Physiol.* 51: 190-193.

Epstein, M., & Sowers, J.R. (1992). Diabetes mellitus and hypertension. *Hypertension.* 19: 403-418.

Escobales, N., Longo, E., Cragoe, E.J.J., Danthuluri, N.R., & Brock, T.A. (1990). Osmotic activation of Na(+)-H+ exchange in human endothelial cells. *Am J Physiol Cell Physiol.* 259: C640-C646.

Folkman, J., & Haudenschild, C. (1980). Angiogenesis in vitro. *Nature.* 288: 551-556.

Folkman, J. (1995). Angiogenesis in cancer, vascular, rheumatoid and other disease. *Nat Med.* 1: 27-31.

Folkman, J. (1997). Angiogenesis and angiogenesis inhibition: an overview. *EXS.* 79:1-8.

Forgac, M. (1989). Structure and function of vacuolar class of ATP-driven proton pumps. *Physiol Rev.* 69: 765-796.

Forgac, M. (1999). Structure and properties of the vacuolar (H+)-ATPases. *J Biol Chem.* 274: 12951-12954.

Furchgott, R.F., & Zawadzki, J.V. (1980). The obligatory role of endothelial cells in the relaxation of arterial smooth muscle by acetylcholine. *Nature.* 288: 373-376.

Garlanda, C., & Dejana, E. (1997). Heterogeneity of endothelial cells. Specific markers. *Arterioscler Thromb Vasc Biol.* 17: 1193-1202.

Geiger, M., Stone, A., Mason, S.N., Oldham, K.T., & Guice, K.S. (1997). Differential nitric oxide production by microvascular and macrovascular endothelial cells. *Am J Physiol Lung Cell Mol Physiol.* 273: L275-L281.

Gerritsen, M.E. (1996). Physiological and pathophysiological roles of eicosanoids in the microcirculation. *Cardiovasc Res.* 32: 720-732.

Gillies, R.J., Martínez-Zaguilán, R., Martinez, G.M., Serrano, R.. & Perona, R. (1990). Tumorigenic 3T3 cells maintain an alkaline intracellular pH under physiological conditions. *Proc Natl Acad Sci USA.* 87: 7414-7418.

Gillies, R.J. & Martínez-Zaguilán, R. (1991). Regulation of intracellular pH in BALB/c 3T3 cells. Bicarbonate raises pH via NaHCO3/HCl exchange and attenuates the activation of Na+/H+ exchange by serum. *J Biol Chem.* 266: 1551-1556.

Gillies, R.J., Martínez-Zaguilán, R., Peterson, E.P., & Perona, R. (1992). Role of intracellular pH in mammalian cell prolifereation. *Cell Physiol Biochem.* 2: 159-179.

Goldstein, D.J., Finbow, M.E., Andresson, T., et al. (1991). Bovine papillomavirus E5 oncoprotein binds to the 16K component of vacuolar H(+)-ATPases. *Nature.* 352: 347-349.

Grant, D.S., Kleinman, H.K., & Martin, G.R. (1990). The role of basement membranes in vascular development. *Ann NY Acad Sci.* 588:61-72.

Haugland, R. (1993). Intracellular ion indicators. In: Fluorescent and luminescent probes for biological activity. A practical guide to technology for quantitative real-time analysis. (ed. WT Mason), pp 34-43. Academic Press, San Diego.

Hendrix, M.J., Seftor, E.A., Seftor, R.E., & Fidler, I.J. (1987). A simple quantitative assay for studying the invasive potential of high and low human metastatic variants. *Cancer Lett.* 38: 137-147.

Henrich, W.L. (1991). The endothelium--a key regulator of vascular tone. *Am J Med Sci.* 302: 319-328.

Hsu, P., Haffner, J., Albuquerque, M.L., & Leffler, C.W. (1996). pHi in piglet cerebral microvascular endothelial cells: recovery from an acid load. *Proc Soc Exp Biol Med.* 212: 256-262.

Hudlicka, O., Brown, M.D., & Egginton, S. (1998). *An Introduction to Vascular Biology: from physiology to pathophysiology* (ed. A Halliday, BJ Hunt, L Poston, M Schachter), pp 3-19. Cambridge University Press, New York.

Jentsch, T.J., Korbmacher, C., Janicke, I., et al. (1988). Regulation of cytoplasmic pH of cultured bovine corneal endothelial cells in the absence and presence of bicarbonate. *J Membr Biol.* 103: 29-40.

Kalebic, T., Garbisa, S., Glaser, B., & Liotta, L.A. (1983). Basement membrane collagen: degradation by migrating endothelial cells. *Science.* 221: 281-283.

Kane, P.M., Kuehn, M.C., Howald-Stevenson, I., & Stevens, T.H. (1992). Assembly and targeting of peripheral and integral membrane subunits of the yeast vacuolar H(+)-ATPase. *J Biol Chem.* 267: 447-454.

Kitazono, T., Takeshige, K., Cragoe, E.J.J., & Minakami, S. (1988). Intracellular pH changes of cultured bovine aortic endothelial cells in response to ATP addition. *Biochem Biophys Res Commun.* 152: 1304-1309.

Koren, W., Koldanov, R., Pronin, V.S., et al. (1997). Amiloride-sensitive Na+/H+ exchange in erythrocytes of patients with NIDDM: a prospective study. *Diabetologia.* 40: 302-306.

Kumar, S., West, D.C., & Ager, A. (1987). Heterogeneity in endothelial cells from large vessels and microvessels. *Differentiation.* 36: 57-70.

Kurtz, I., & Golchini, K. (1987). Na+-independent Cl(-)-HCO-3- exchange in Madin-Darby canine kidney cells. Role in intracellular pH regulation. *J Biol Chem.* 262: 4516-4520.

Lubman, R.L., Danto, S.I., & Crandall, E.D. (1989). Evidence for active H+ secretion by rat alveolar epithelial cells. *Am J Physiol Lung Cell Mol Physiol.* 257: L438-L445.

Lüscher, T.F., Bock, H.A., Yang, Z.H., & Diederich, D. (1991). Endothelium-derived relaxing and contracting factors: perspectives in nephrology. *Kidney Int.* 39: 575-590.

Lynch, R.M., Carrington, W., Fogarty, K.E., & Fay, F.S. (1996). Metabolic modulation of hexokinase association with mitochondria in living smooth muscle cells. *Am J Physiol Cell Physiol.* 270: C488-C499.

Martínez-Zaguilán, R., Martinez, G.M., Lattanzio, F., & Gillies, R.J. (1991). Simultaneous measurement of intracellular pH and Ca2+ using the fluorescence of SNARF-1 and fura-2. *Am J Physiol Cell Physiol.* 260: C297-C307.

Martínez-Zaguilán, R. (1992). Measurement of Intracellular Ca2+ and pHin in cultured cells by fluorescence spectroscopy. In: *In Vitro Methods of Toxicology* (ed. R Watson), pp 217-236. CRC Press, Boca Raton, FL.

Martínez-Zaguilán, R., Lynch, R.M., Martinez, G.M., & Gillies, R.J. (1993). Vacuolar-type H(+)-ATPases are functionally expressed in plasma membranes of human tumor cells. *Am J Physiol Cell Physiol.* 265: C1015-C1029.

Martínez-Zaguilán, R., Gurule, M.W., & Lynch, R.M. (1996a). Simultaneous measurement of intracellular pH and Ca2+ in insulin- secreting cells by spectral imaging microscopy. *Am J Physiol Cell Physiol.* 270: C1438-C1446.

Martínez-Zaguilán, R., Parnami, G., & Lynch, R.M. (1996b). Selection of fluorescent ion indicators for simultaneous measurements of pH and Ca2+. *Cell Calcium.* 19: 337-349.

Martínez-Zaguilán, R., Seftor, E.A., Seftor, R.E., Chu, Y.W., Gillies, R.J., & Hendrix, M.J. (1996c). Acidic pH enhances the invasive behavior of human melanoma cells. *Clin Exp Metastasis.* 14: 176-186.

McCarthy, S.A., Kuzu, I., Gatter, K.C., & Bicknell, R. (1991). Heterogeneity of the endothelial cell and its role in organ preference of tumour metastasis. *Trends Pharmacol Sci.* 12: 462-467.

McCoy, C.L., McIntyre, D.J.O., Robinson, S.P., Aboagye, E.O., & Griffiths, J.R. (1996). Magnetic resonance spectroscopy and imaging methods for measuring tumour and tissue oxygenation. *Br J Cancer.* 74:S226-231.

Mehta, J.L. (1995). Endothelium, coronary vasodilation, and organic nitrates. *Am Heart J.* 129: 382-391.

Mendlein, J., & Sachs, G. (1990). Interaction of a K(+)-competitive inhibitor, a substituted imidazo[1,2a] pyridine, with the phospho- and dephosphoenzyme forms of H+, K(+)-ATPase. *J Biol Chem.* 265: 5030-5036.

Morahan, G., McClive, P., Huang, D., Little, P., & Baxter, A. (1994). Genetic and physiological association of diabetes susceptibility with raised Na+/H+ exchange activity. *Proc Natl Acad Sci USA.* 91: 5898-5902.

Moscatelli, D., Presta, M., & Rifkin, D.B. (1986). Purification of a factor from human placenta that stimulates capillary endothelial cell protease production, DNA synthesis, and migration. *Proc Natl Acad Sci USA.* 83: 2091-2095.

Nanda, A., Gukovskaya, A., Tseng, J., & Grinstein, S. (1992). Activation of vacuolar-type proton pumps by protein kinase C. Role in neutrophil pH regulation. *J Biol Chem.* 267: 22740-22746.

Nelson, N., & Klionsky, D.J. (1996). Vacuolar H(+)-ATPase: from mammals to yeast and back. *Experientia.* 52: 1101-10.

Ng, L.L., & Davies, J.E. (1992). Lipids and cellular Na+/H+ antiport activity in diabetic nephropathy. *Kidney Int.* 41: 872-876.

Nordstrom, T., Rotstein, O.D., Romanek, R., et al. (1995). Regulation of cytoplasmic pH in osteoclasts. Contribution of proton pumps and a proton-selective conductance. *J Biol Chem.* 270: 2203-2212.

Olsnes, S., Tonnessen, T.I., & Sandvig, K. (1986). pH-regulated anion antiport in nucleated mammalian cells. *J Cell Biol.* 102: 967-971.

Opas, M. (1997). Measurement of intracellular pH and pCa with a confocal microscope. *Trends Cell Biol.* 7: 75-80.

Roos, A., & Boron, W.F. (1981). Intracellular pH. *Physiol Rev.* 61: 296-434.

Ryan, U.S., Whitney, P.L., & Ryan, J.W. (1982). Localization of carbonic anhydrase on pulmonary artery endothelial cells in culture. *J Appl Physiol.* 53: 914-919.

Salles, J.P., Ser, N., Fauvel, J., et al. (1991). Platelet Na(+)-H+ exchange in juvenile diabetes mellitus. *J Hypertens Suppl.* 9: S222-S223.

Sanchez-Armass, S., Martínez-Zaguilán, R., Martinez, G.M., & Gillies, R.J. (1994). Regulation of pH in rat brain synaptosomes. I. Role of sodium, bicarbonate, and potassium. *J Neurophysiol.* 71: 2236-2248.

Schmid, A., Scholz, W., Lang, H.J., & Popp, R. (1992). Na+/H+ exchange in porcine cerebral capillary endothelial cells is inhibited by a benzoylguanidine derivative. *Biochem Biophys Res Commun.* 184: 112-117.

Selden, S.C., & Schwartz, S.M. (1979). Cytochalasin B inhibition of endothelial proliferation at wound edges in vitro. *J Cell Biol.* 81: 348-354.

Selden, S.C., Rabinovitch, P.S., & Schwartz, S.M. (1981). Effects of cytoskeletal disrupting agents on replication of bovine endothelium. *J Cell Physiol.* 108: 195-211.

Servold, S.A. (1991). Growth factor impact on wound healing. *Clin Podiatr Med Surg.* 8: 937-953.

Sheng, S., Carey, J., Seftor, E.A., Dias, L., Hendrix, M.J., & Sager, R. (1996). Maspin acts at the cell membrane to inhibit invasion and motility of mammary and prostatic cancer cells. *Proc Natl Acad Sci USA.* 93: 11669-11674.

Shirai, M., Sada, K., & Ninomiya, I. (1986). Effects of regional alveolar hypoxia and hypercapnia on small pulmonary vessels in cats. *J Appl Physiol.* 61: 440-448.

Sinclair, D.G., Braude, S., Haslam, P.L., & Evans, T.W. (1994). Pulmonary endothelial permeability in patients with severe lung injury. Clinical correlates and natural history. *Chest.* 106: 535-539.

Stehouwer, C.D., & Schaper, N.C. (1996). The pathogenesis of vascular complications of diabetes mellitus: one voice or many? *Eur J Clin Invest.* 26: 535-543.

Stevens, T., Fouty, B., Hepler, L., et al. (1997). Cytosolic Ca2+ and adenylyl cyclase responses in phenotypically distinct pulmonary endothelial cells. *Am J Physiol Lung Cell Mol Physiol.* 272: L51-L59.

Sugai, N., Ninomiya, Y., & Oosaki, T. (1981). Localization of carbonic anhydrase in the rat lung. *Histochemistry.* 72: 415-424.

Swallow, C.J., Grinstein, S., & Rotstein, O.D. (1990). A vacuolar type H(+)-ATPase regulates cytoplasmic pH in murine macrophages. *J Biol Chem.* 265: 7645-7654.

Tamai, S., Waheed, A., Cody, L.B., & Sly, W.S. (1996). Gly-63-->Gln substitution adjacent to His-64 in rodent carbonic anhydrase IVs largely explains their reduced activity. *Proc Natl Acad Sci USA.* 93: 13647-13652.

Vaananen, H.K., Karhukorpi, E.K., Sundquist, K., et al. (1990). Evidence for the presence of a proton pump of the vacuolar H(+)-ATPase type in the ruffled borders of osteoclasts. *J Cell Biol.* 111: 1305-1311.

Vaupel, P. (1996). Is there a critical tissue oxygen tension for bioenergetic status and cellular pH regulation in solid tumors? *Experentia.* 52: 464-468.

Viles, P.H., & Shepherd, J.T. (1968). Relationship between pH, Po2, and Pco2 on the pulmonary vascular bed of the cat. *Am J Physiol.* 215: 1170-1176.

West, J.B. (1998). *Respiratory Physiology: The essentials.* pp. 1-10. Wilkins and Wilkins, Baltimore.

Woessner, J.F. (1991). Matrix metalloproteinases and their inhibitors in connective tissue remodeling. *FASEB J.* 5: 2145-2154.

Wu, G. & Meininger, C.J. (1995). Impaired arginine metabolism and NO synthesis in coronary endothelial cells of the spontaneously diabetic BB rat. *Am J Physiol Heart Circ Physiol.* 269: H1312-H1318.

Yamaguchi, K., Suzuki, K., Naoki, K., et al. (1998). Response of intra-acinar pulmonary microvessels to hypoxia, hypercapnic acidosis, and isocapnic acidosis. *Circ Res.* 82: 722-728.

Ye, S., & Henney, M. (1998). Vascular matrix proteins and their remodeling in atherosclerosis. In: *An introduction to vascular biology: from physiology to pathophysiology* (ed. A Halliday, BJ Hunt, L Poston, M Schachter), pp 131-148. Cambridge University Press, New York.

Yoshida, A., Anand-Apte, B., & Zetter, BR. (1996). Differential endothelial migration and proliferation to basic fibroblast growth factor and vascular endothelial growth factor. *Growth Factors*. 13: 57-64.

Zannini, G. (1974). Diabetic arteriopathy. *J Cardiovasc Surg*. 15: 68-71.

Ziegelstein, R.C., Cheng, L., & Capogrossi, M.C. (1992). Flow-dependent cytosolic acidification of vascular endothelial cells. *Science*. 258: 656-659.